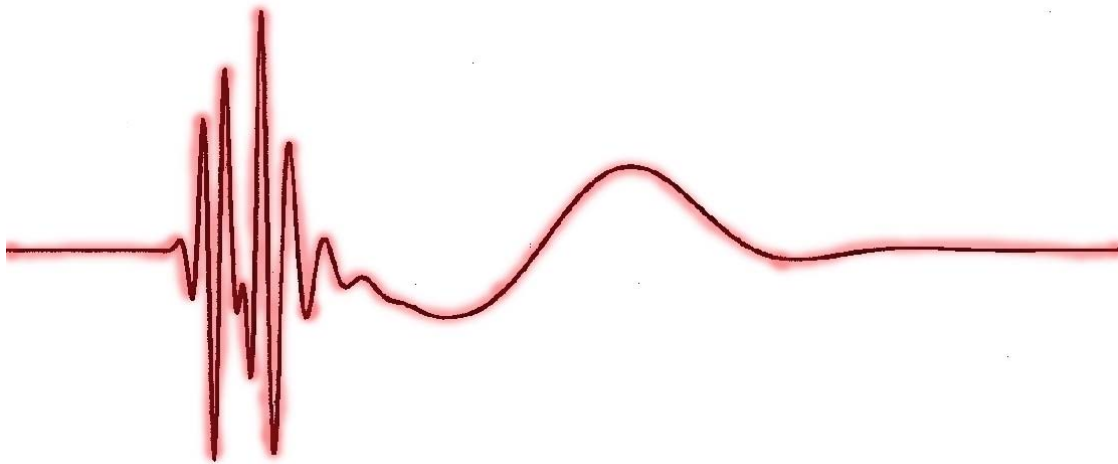


On the Myth of Superluminality in Dispersive Pulse Propagation



Kurt Edmund Oughstun
College of Engineering & Mathematics
University of Vermont

*Research supported by the United States Air
Force Office of Scientific Research (Grant #
USAF 49620-01-1-0306).*

*Quantum Optics Workshop
University of California at Santa Barbara
July 2002*

Collaborators

University of Rochester (Thesis Committee)

George C. Sherman (“retired” to Southern California)

Emil Wolf

Carlos Stroud

University of Wisconsin-Madison

Shioupyn Shen – multiple resonance Lorentz model dielectrics

University of Vermont

Judith Laurens – Debye (Rocard-Powles) + Lorentz model dielectrics

Paul Smith – Evolved Heat & Energy Loss in Lossy Materials

Costas Balitsis – Generalized Asymptotic Description of Gaussian Pulse Propagation in Lorentz model dielectrics

Hong Xiao – Failure of the Group Velocity Approximation

Natalie Cartwright – Pulse Velocity Measures

Universitet i Bergen

Jakob Stamnes & Jostein Solhaug – Transitional Asymptotic Expansions & Ultrashort Pulse Focusing in Lorentz model dielectrics

Armstrong Laboratory, Brooks AFB

Dr. Richard Albanese – Ultrawideband Electromagnetic Pulse Effects in Biological Systems (Health & Safety) & Remote Material Identification

Classical theory due to Sommerfeld* & Brillouin⁺ provided the first proof that an *electromagnetic signal could not propagate faster than the vacuum speed of light c in a causal dielectric (the Lorentz model).*

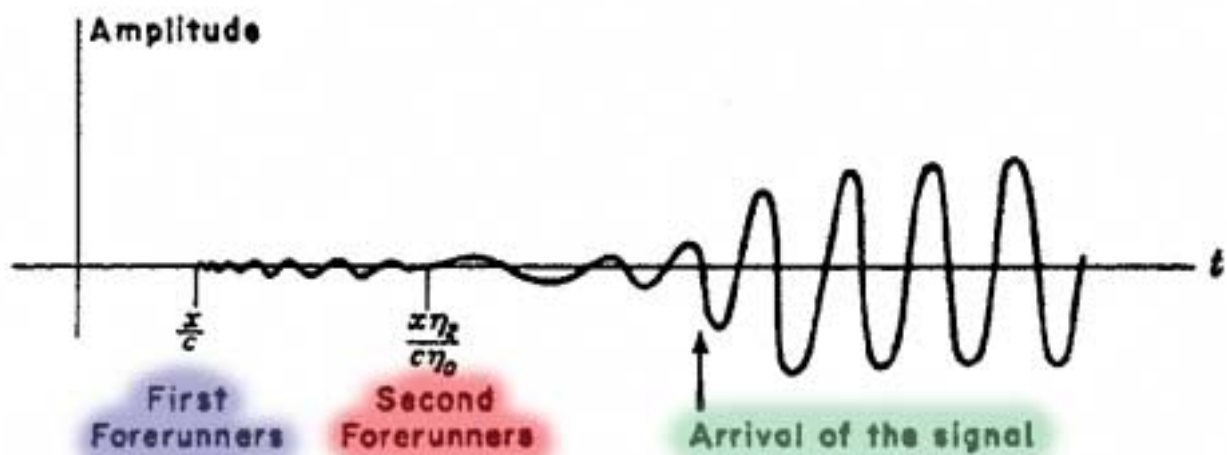
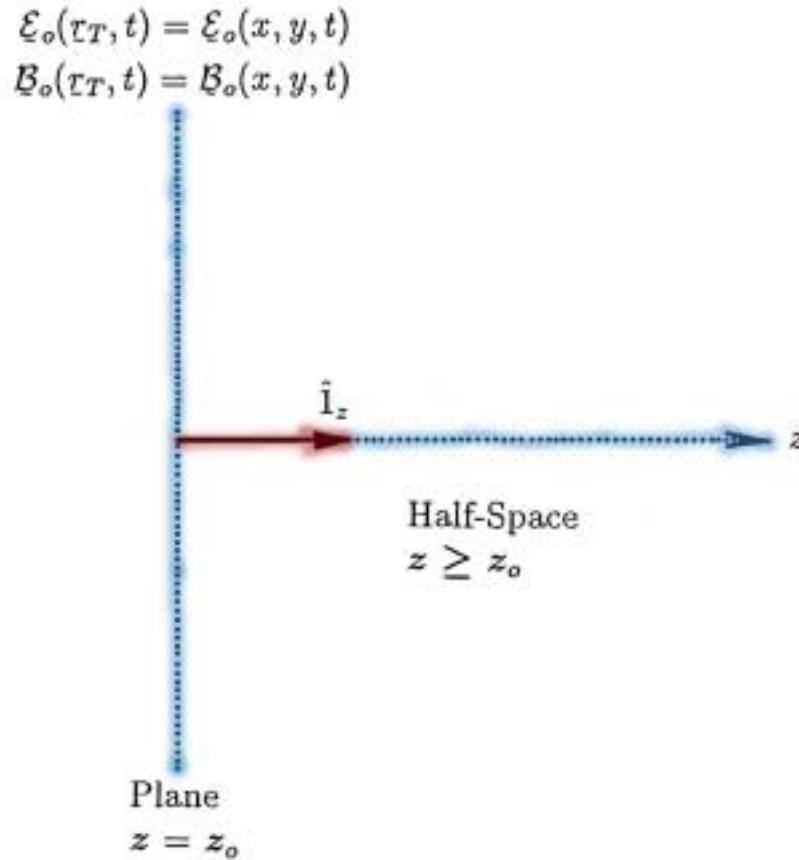


FIG. 20.

*A. Sommerfeld, *Ann. Phys., Lpz.* **44**, 177-202 (1914).

⁺L. Brillouin, *Ann. Phys., Lpz.* **44**, 203-240 (1914).

Sommerfeld's Relativistic Causality Theorem:
 [A. Sommerfeld, *Ann. Phys. Lpz.* 44, 177-202 (1914)]



$$\left(\nabla^2 + \tilde{k}^2(\omega)\right)\tilde{A}(z, \omega) = 0 ; \quad \tilde{k}(\omega) = (\omega/c)n(\omega)$$

$$\tilde{A}(z, \omega) = \int_{-\infty}^{\infty} A(z, t) \exp(i\omega t) dt ; \quad A(0, t) = f(t)$$

$$\begin{aligned}
 A(z, t) &= \frac{1}{2\pi} \int_C \tilde{f}(\omega) \exp\left[i\left(\tilde{k}(\omega)\Delta z - \omega t\right)\right] d\omega \\
 &= \frac{1}{2\pi} \int_C \tilde{f}(\omega) \exp\left[(\Delta z/c)\phi(\omega, \theta)\right] d\omega
 \end{aligned}$$

where

$$\phi(\omega, \theta) = i(c/\Delta z) [\tilde{k}(\omega)\Delta z - \omega t] = i\omega[n(\omega) - \theta]$$

Sommerfeld's Theorem: If $f(t) = 0$ for all $t < 0$ and if $\Re\{i\omega[n(\omega) - \theta]\} \rightarrow -\infty$ as $|\omega| \rightarrow \infty$; $\omega'' > 0$ for all $\theta < 1$, where $\theta = ct/\Delta z$, then $A(z, t) = 0$ for all $\Delta z > 0$ when $\theta < 1$.

[Oughstun & Sherman, J. Opt. Soc. Am. B 5, 817-849 (1988)]

This luminal arrival of the signal front tells you that any information that may be present in the signal will follow at some later space-time point $\theta > 1$.

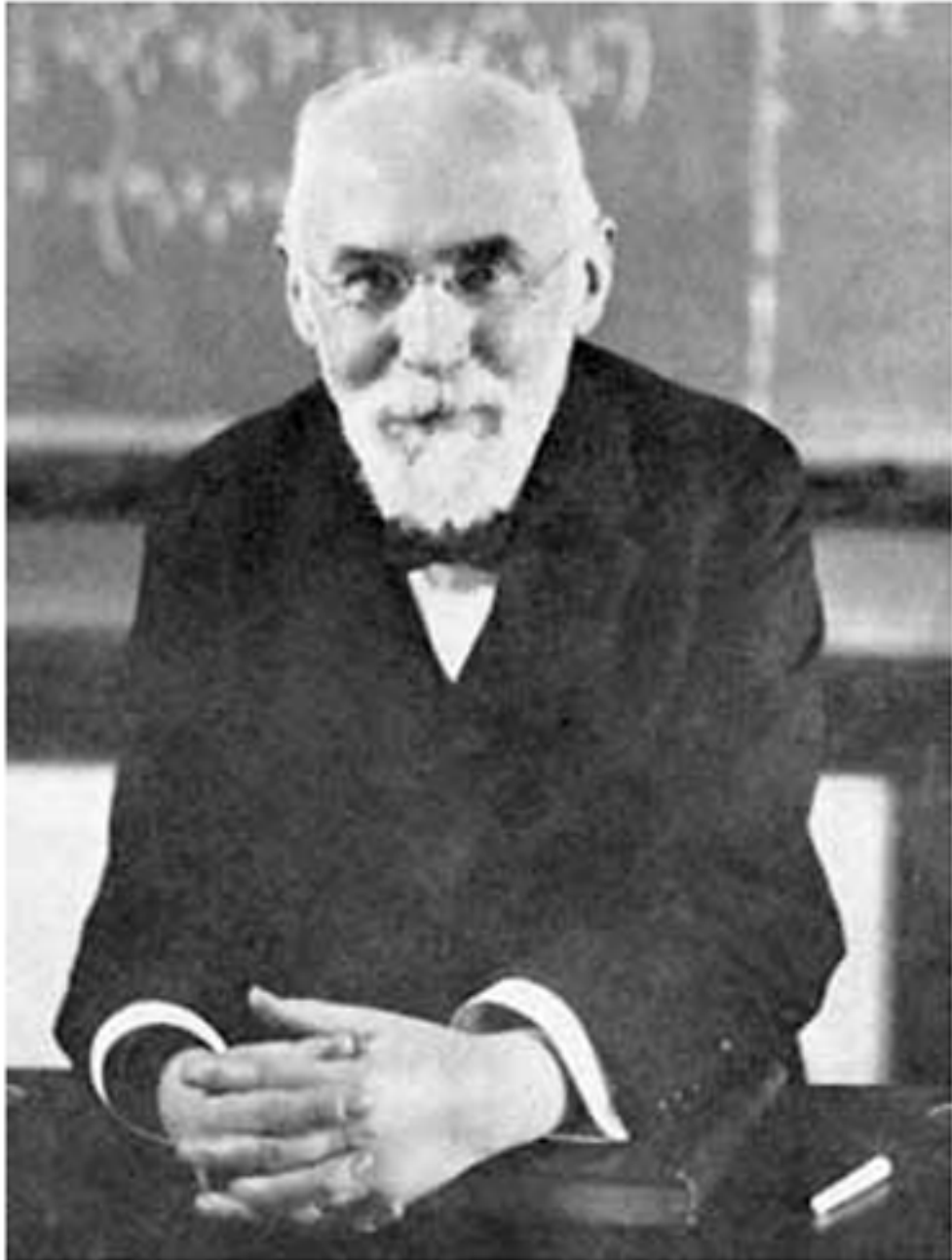
Arnold Sommerfeld
(1868 – 1951)



Leon Brillouin
(1889 – 1969)



Hendrik A. Lorentz
(1853 – 1928)



Phase Velocity [Lord Rayleigh, *Proc. London Math. Soc.* **IX**, 21-26, (1877)]:

The phase velocity describes the rate at which the phase fronts of the wave propagate through the dispersive medium.

Group Velocity [W. R. Hamilton, *Proc. Royal Irish Academy* **1**, 341-349 (1839)]:

The group velocity describes the rate at which a group of waves propagates as a whole through the dispersive medium [M. Born and E. Wolf, *Principles of Optics*, 7th expanded edition, (Cambridge U. Press, Cambridge, 1999) §1.3.4].

Signal Velocity [L. Brillouin, *Ann. Phys. Lpz.* **44**, 204-240 (1914); L. Brillouin, *Wave Propagation and Group Velocity* (Academic, New York, 1960)]:

A group of waves has originally been defined by Rayleigh “as moving beats...following each other in a regular pattern. A signal is a short isolated succession of wavelets, with the system at rest before the signal arrived and also after it has passed...In general, the signal velocity will differ from the group velocity, especially if the phase velocity is strongly frequency dependent and if the absorption cannot be ignored.”

Brillouin defined the signal velocity for a unit step function signal as the space-time point at which the path of steepest descent (passing through all of the relevant saddle points) crosses the simple pole singularity at the carrier frequency of the signal.

A Simple Wave Group

[M. Born & E. Wolf, *Principles of Optics*, 7th expanded edition (Cambridge U. Press, Cambridge, 1999)]

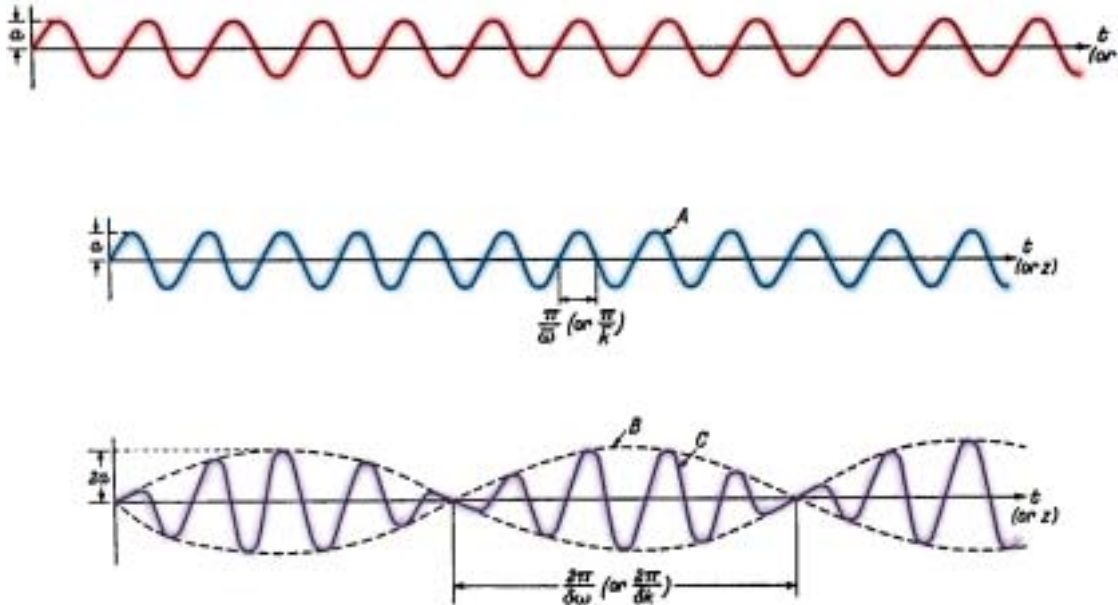


Fig. 1.5. A simple wave group.

- (A) The wave $a \cos(\bar{\omega}t - \bar{k}z)$.
- (B) The wave $2a \cos[\frac{1}{2}(t\delta\omega - z\delta k)]$.
- (C) The wave group $2a \cos[\frac{1}{2}(t\delta\omega - z\delta k)] \cos(\bar{\omega}t - \bar{k}z)$.

The ordinate represents one of the two independent variables (t or z) whilst the other is kept constant.

$$\begin{aligned}
 u(z, t) &= a \exp[i(kz - \omega t)] + a \exp[i((k + \delta k)z - (\omega + \delta\omega)t)] \\
 &= 2a \cos\left[\frac{1}{2}(z\delta k - t\delta\omega)\right] \exp[i(\bar{k}z - \bar{\omega}t)]
 \end{aligned}$$

where $\bar{k} = k + \frac{1}{2}\delta k$ & $\bar{\omega} = \omega + \frac{1}{2}\delta\omega$. The wave group then travels with the group velocity $v_g = \delta\omega/\delta k$.

The *Group Velocity* is a physically valid velocity measure when it is used in connection with the original structure for which it was introduced: a *Wave Group*.

In that situation, the group velocity describes the velocity of a point (e.g. the peak amplitude point, or the zero amplitude point, etc.) in the infinite wave group. *This can then take on any value since it does not describe either energy or information transfer.*

Profound difficulties arise whenever one attempts to extend this concept of the group velocity to a single ultrashort pulse (*superluminal pulse velocities, negative pulse velocities, complex pulse velocities*).

In order to overcome these difficulties, Brillouin introduced the concept of the *Signal Velocity*.

Deformed Contour of Integration taken along the Paths of Steepest Descent through all of the Relevant Saddle Points

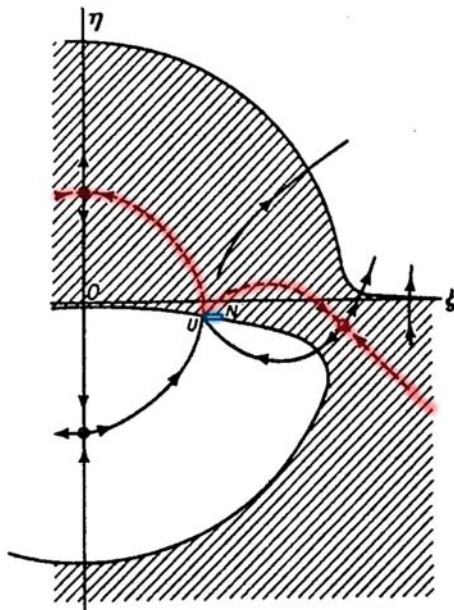


FIG. 10. Key: - - - - , path of integration.

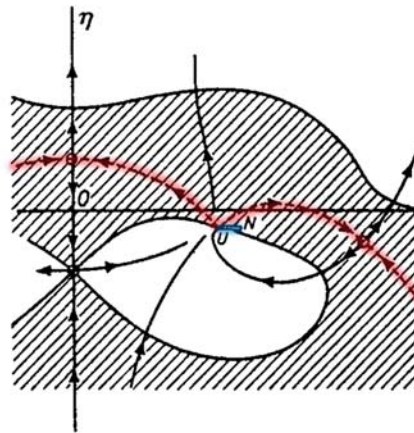


FIG. 11.

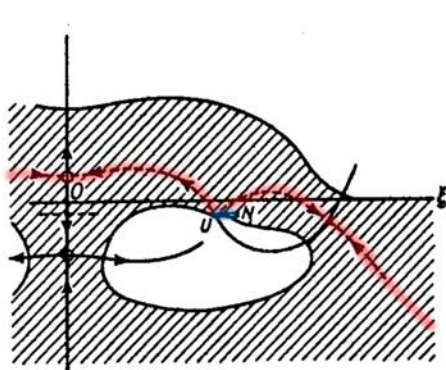


FIG. 12.

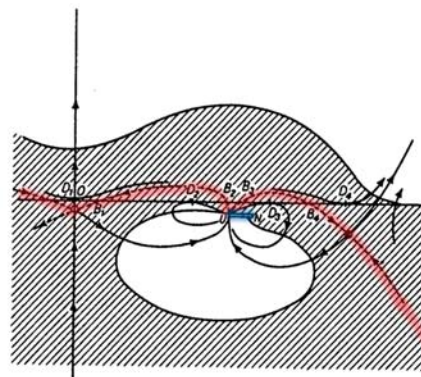


FIG. 13.

L. Brillouin, *Ann. Phys. Lpz.* **44**, 203-240 (1914).
 P. Debye, *Math. Ann.* **67**, 535-558 (1909).

Comparison of the (Inverse) Relative *Phase*, *Group*, & *Signal Velocities* in a single resonance Lorentz model dielectric. Notice that Brillouin's signal velocity peaks to c near the material resonance frequency.

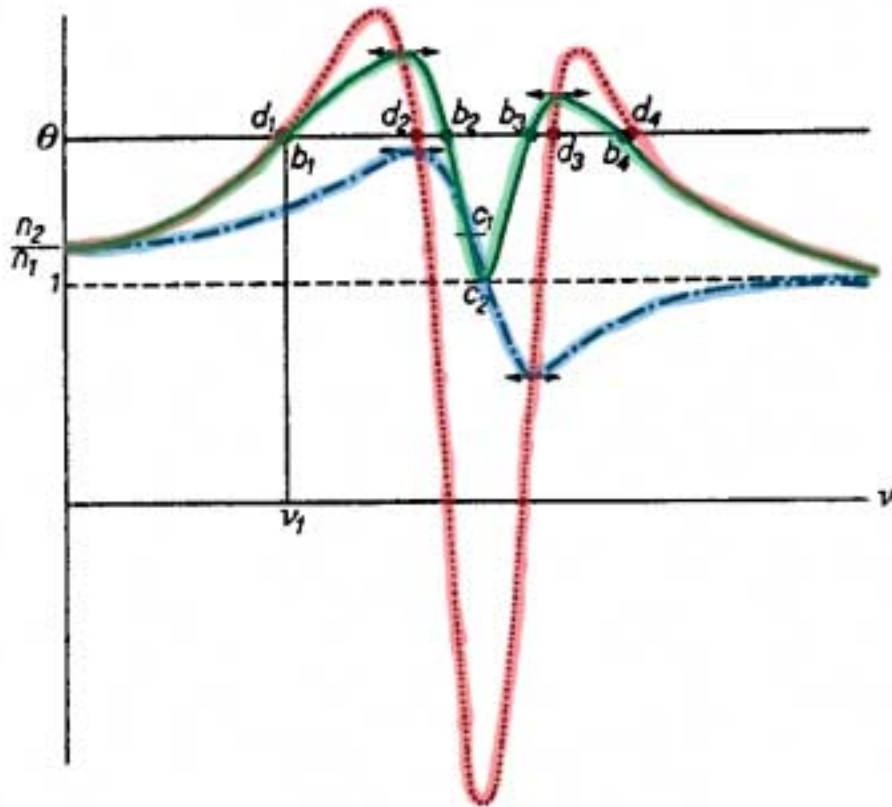
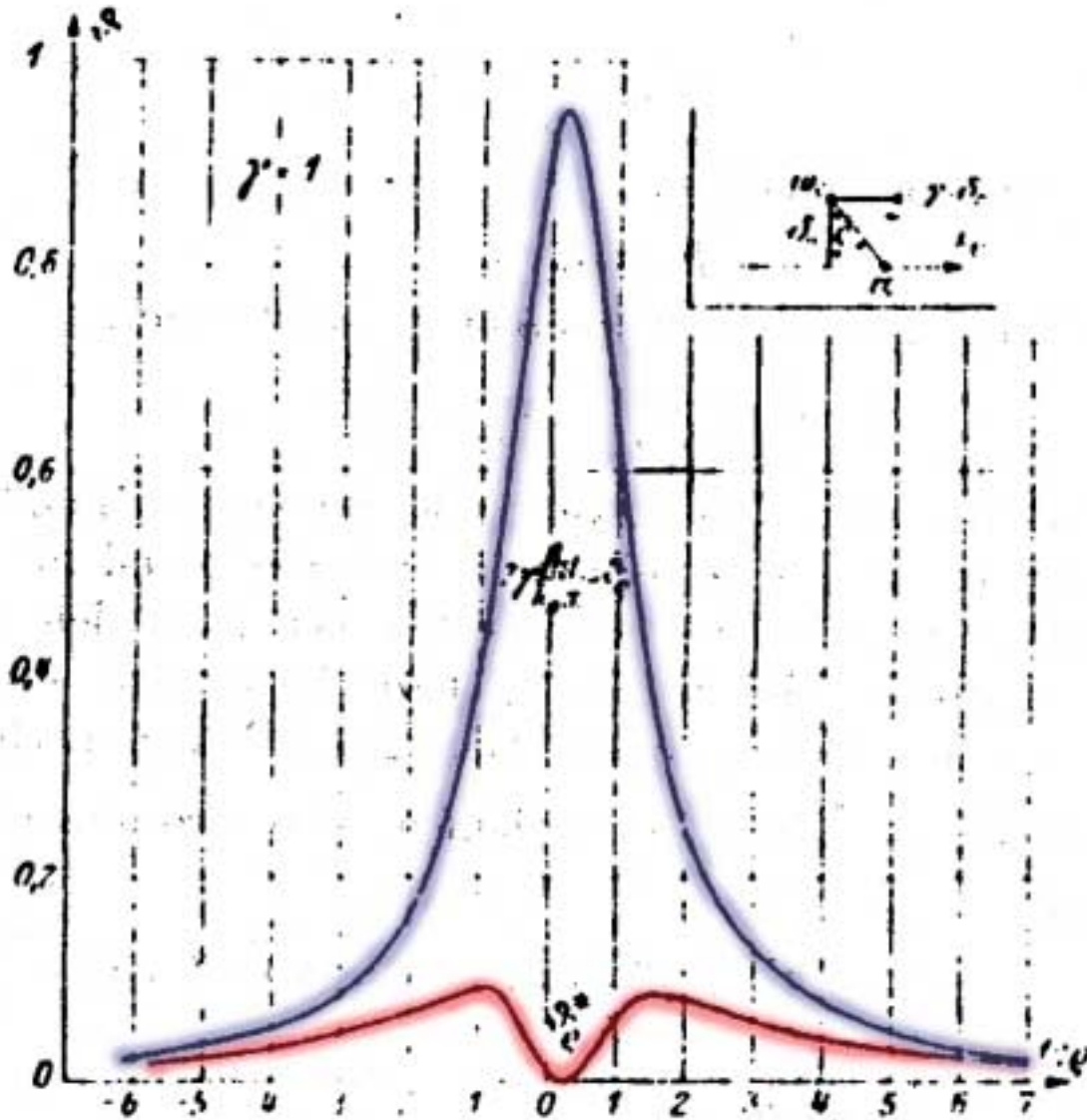


FIG. 19. Key: — · — ·, $c/\text{phase velocity} = c/W$; · · · ·, $c/\text{group velocity} = c/U$; —, $c/\text{signal velocity} = c/S$.

L. Brillouin, Ann. Phys., Lpz. 44, 203-240 (1914).

Modified *Signal Velocity* due to Baerwald*.



Brillouinische unterkritische und asymptotische überkritische Signalzeit in einem Gebiet selektiver Absorption bei $\gamma = 1$

Fig. 10

*H. Baerwald, *Ann. Phys.* 7, 731-760 (1930).

Poynting's Theorem: Energy Density & Evolved Heat in a Dispersive, Absorptive Medium

[Yu. S. Barash & V. L. Ginzburg, *Usp. Fiz. Nauk.* **118**, 523-530 (1976); *Sov. Phys. Usp.* **19**, 263-270 (1976)]

Poynting's Theorem [J. H. Poynting, *Phil. Trans.* **175**, 343 (1884)]

$$-\nabla \cdot \mathbf{S} = \left\| \frac{1}{4\pi} \right\| \left(\mathbf{E} \cdot \frac{\partial \mathbf{D}}{\partial t} + \mathbf{H} \cdot \frac{\partial \mathbf{B}}{\partial t} \right) + \mathbf{J} \cdot \mathbf{E}$$

where

$$\mathbf{S} \equiv \left\| \frac{c}{4\pi} \right\| \mathbf{E} \times \mathbf{H}$$

is the Poynting vector, and where $\mathbf{J} = \mathbf{J}_c + \mathbf{J}_{ext}$ is the total current density. In general, one may define the scalar quantities U'_e and U'_m associated with the electric and magnetic fields, respectively, by the relations

$$\frac{\partial U'_e}{\partial t} \equiv \left\| \frac{1}{4\pi} \right\| \mathbf{E} \cdot \frac{\partial \mathbf{D}}{\partial t} ; \quad \frac{\partial U'_m}{\partial t} \equiv \left\| \frac{1}{4\pi} \right\| \mathbf{H} \cdot \frac{\partial \mathbf{B}}{\partial t}$$

with sum $U' = U'_e + U'_m$, which have the dimensions of *energy per unit volume*.

Differential Form of Poynting's Theorem

$$\nabla \cdot \mathbf{S} = -\frac{\partial U'}{\partial t} - \mathbf{J} \cdot \mathbf{E}$$

Which is interpreted as a statement of the conservation of energy in the electromagnetic system.

“A theory is not an absolute truth but a self-consistent analytical formulation of the relations governing a group of natural phenomena.” *J. A. Stratton, Electromagnetic Theory (McGraw-Hill, New York, 1941) §2.19.*

In the simplest case of a *nonmagnetic and nondispersive medium*, the constitutive relations are $\mathbf{D} = \epsilon\mathbf{E}$, $\mathbf{B} = \mu\mathbf{H}$, $\mathbf{J}_c = \sigma\mathbf{E}$, where ϵ , μ , σ are scalar constants, then

$$U'_e \rightarrow U_e = \left\| \frac{1}{4\pi} \right\| \frac{1}{2} \mathbf{E} \cdot \mathbf{D}, \quad U'_m \rightarrow U_m = \left\| \frac{1}{4\pi} \right\| \frac{1}{2} \mathbf{H} \cdot \mathbf{B}$$

which are identified as the electric and magnetic energy densities. The total electromagnetic energy density is then given by

$$U = U_e + U_m = \left\| \frac{1}{4\pi} \right\| \frac{1}{2} (\epsilon|\mathbf{E}|^2 + \mu|\mathbf{H}|^2)$$

For isotropic, locally linear, temporally dispersive media one has the multipole expansion [J. D. Jackson, *Classical Electrodynamics*, 2nd ed. (Wiley, New York, 1975) §6.7]

$$\mathbf{D}(\mathbf{r}, t) = \varepsilon_0 \mathbf{E}(\mathbf{r}, t) + \frac{1}{4\pi} \nabla \cdot \mathbf{P}(\mathbf{r}, t) - \frac{1}{4\pi} \nabla \times \mathbf{Q}(\mathbf{r}, t) + \dots$$

The electric energy density of the coupled field-medium system is then given by

$$U'_e = \frac{1}{2} \varepsilon_0 \mathbf{E} \cdot \mathbf{E} + \int \mathbf{E} \cdot \frac{\partial \mathbf{P}}{\partial t} dt - \int \mathbf{E} \cdot \frac{\partial \nabla \cdot \mathbf{Q}}{\partial t} dt + \dots$$

so that a portion of the electric field energy resides in the dispersive medium where it is either reactively stored or dissipated.

For a nonmagnetic medium with frequency dependent dielectric permittivity $\varepsilon(\omega) = \varepsilon_r(\omega) + i\varepsilon_i(\omega)$ and electrical conductivity $\sigma(\omega) = \sigma_r(\omega) + i\sigma_i(\omega)$, the relation

$$\frac{\partial U'_e}{\partial t} \equiv \frac{1}{4\pi} \mathbf{E} \cdot \frac{\partial \mathbf{D}}{\partial t}$$

is replaced by

$$\frac{\partial U_e}{\partial t} + Q = \frac{1}{4\pi} \mathbf{E} \cdot \frac{\partial \mathbf{D}}{\partial t} + \mathbf{J}_c \cdot \mathbf{E}$$

where U_e now represents just the *electric energy density both in the field and reactively stored in the dispersive medium* and where Q represents the *evolved heat or dissipation in the medium*. Comparison of these two relations shows that

$$\frac{\partial U_e}{\partial t} + Q = \frac{\partial U'_e}{\partial t} + \mathbf{J}_c \cdot \mathbf{E}$$

from which it follows that $U_e = U'_e$ only in the absence of all loss mechanisms. With this separation, Poynting's theorem becomes

$$\frac{\partial}{\partial t}(U_e + U_m) + Q = -\nabla \cdot \mathbf{S} - \mathbf{J}_{ext} \cdot \mathbf{E}$$

All that now remains is to obtain separate expressions for U_e and Q .

In general, the electric displacement vector and the conduction current in an isotropic, locally linear, temporally dispersive media may be represented by the series expansions

$$\mathbf{D}(\mathbf{r}, t) = \sum_{n=0}^{\infty} \epsilon^{(n)} \frac{\partial^n \mathbf{E}(\mathbf{r}, t)}{\partial t^n}, \quad \mathbf{J}_c(\mathbf{r}, t) = \sum_{n=0}^{\infty} \sigma^{(n)} \frac{\partial^n \mathbf{E}(\mathbf{r}, t)}{\partial t^n}$$

where

$$\epsilon^{(n)} = \frac{(-1)^n}{n!} \int_0^\infty \hat{\epsilon}(\tau) \tau^n d\tau, \quad \sigma^{(n)} = \frac{(-1)^n}{n!} \int_0^\infty \hat{\sigma}(\tau) \tau^n d\tau$$

are proportional to the n^{th} order moments of the dielectric permittivity and electric conductivity functions, respectively, where

$$\mathbf{D}(\mathbf{r}, t) = \int_{-\infty}^t \hat{\epsilon}(t - t') \mathbf{E}(\mathbf{r}, t') dt', \quad \mathbf{J}_c(\mathbf{r}, t) = \int_{-\infty}^t \hat{\sigma}(t - t') \mathbf{E}(\mathbf{r}, t') dt'$$

Substitution of these two expressions then yields

$$\frac{\partial U_e}{\partial t} + Q = \left\| \frac{1}{4\pi} \right\| \mathbf{E} \cdot \frac{\partial \mathbf{D}}{\partial t} + \mathbf{J}_c \cdot \mathbf{E}$$



$$\frac{\partial U_e}{\partial t} + Q = \left\| \frac{1}{4\pi} \right\| \mathbf{E} \cdot \frac{\partial}{\partial t} \sum_{n=0}^{\infty} \epsilon^{(n)} \frac{\partial^n \mathbf{E}}{\partial t^n} + \mathbf{E} \cdot \frac{\partial}{\partial t} \sum_{n=0}^{\infty} \sigma^{(n)} \frac{\partial^n \mathbf{E}}{\partial t^n}$$



$$\begin{aligned}
\frac{\partial U_e}{\partial t} + Q &= \sigma^{(0)} \mathbf{E}^2 + \frac{1}{2} \left(\left\| \frac{1}{4\pi} \right\| \varepsilon^{(0)} + \sigma^{(1)} \right) \frac{\partial \mathbf{E}^2}{\partial t} \\
&+ \frac{1}{2} \left(\left\| \frac{1}{4\pi} \right\| \varepsilon^{(1)} + \sigma^{(2)} \right) \frac{\partial^2 \mathbf{E}^2}{\partial t^2} \\
&- \left(\left\| \frac{1}{4\pi} \right\| \varepsilon^{(1)} + \sigma^{(2)} \right) \left(\frac{\partial \mathbf{E}^2}{\partial t} \right)^2 + \dots
\end{aligned}$$

In general, one then has that

$$\begin{aligned}
U_e(\mathbf{r}, t) &= \frac{1}{2} \left\| \frac{1}{4\pi} \right\| \alpha_1 \mathbf{E}^2(\mathbf{r}, t) + \dots \\
Q(\mathbf{r}, t) &= \sigma^{(0)} \mathbf{E}^2(\mathbf{r}, t) + \frac{1}{2} \left\| \frac{1}{4\pi} \right\| \beta_1 \frac{\partial \mathbf{E}^2(\mathbf{r}, t)}{\partial t} + \dots
\end{aligned}$$

with

$$\alpha_1 + \beta_1 = \varepsilon^{(0)} + \left\| 4\pi \right\| \sigma^{(1)}$$

and so on for higher-order coefficients.

As a consequence, *one cannot, in general, express the electric energy density U_e and the dissipation (evolved heat) Q separately in terms of the dielectric permittivity and electric conductivity of a dispersive medium.*

In order to unambiguously determine these quantities, it is necessary to employ a specific physical model of the dispersive medium, e.g., the equation of motion at the microscope level.

For example, for a *multiple resonance Lorentz model dielectric* the equation of motion for each electronic resonance is

$$m_e \frac{d^2 \mathbf{r}_j}{dt^2} + 2\delta_j \frac{d\mathbf{r}_j}{dt} + \omega_j^2 \mathbf{r}_j = -q_e \mathbf{E}$$

With the macroscopic polarization vector given by

$$\mathbf{P} = -\sum_j N_j q_e \mathbf{r}_j$$

one obtains

$$\mathbf{E} \cdot \frac{\partial \mathbf{P}}{\partial t} = \sum_j N_j m_e \left[\frac{1}{2} \frac{d}{dt} \left(\frac{d\mathbf{r}_j}{dt} \right)^2 + 2\delta_j \left(\frac{d\mathbf{r}_j}{dt} \right)^2 + \frac{1}{2} \omega_j^2 \frac{d}{dt} (\mathbf{r}_j)^2 \right]$$

The last term appearing on the right-hand side of Poynting's theorem

$$\nabla \cdot \mathbf{S} = -\left\| \frac{1}{4\pi} \right\| \left(\mu_0 \mathbf{H} \cdot \frac{\partial \mathbf{H}}{\partial t} + \varepsilon_0 \mathbf{E} \cdot \frac{\partial \mathbf{E}}{\partial t} + \left\| 4\pi \right\| \mathbf{E} \cdot \frac{\partial \mathbf{P}}{\partial t} \right)$$

is then seen to be the sum of a perfect time-differential and the term in δ_j which corresponds to the dissipation mechanism. The total energy density is then given by the sum

$$U = U_f + U_{osc}$$

where

$$U_f \equiv \left\| \frac{1}{4\pi} \right\| \frac{1}{2} (\epsilon_0 |\mathbf{E}|^2 + \mu_0 |\mathbf{H}|^2)$$

is the *energy density stored in the field alone*, and where

$$U_{osc} \equiv \frac{1}{2} \sum_j N_j m_e \left[\left(\frac{d\mathbf{r}_j}{dt} \right)^2 + \omega_j^2 (\mathbf{r}_j)^2 \right]$$

is the *energy density stored in the multiple-resonance Lorentz medium*.

With these identifications, the differential form of Poynting's theorem becomes

$$\nabla \cdot \mathbf{S} + 2 \sum_j N_j m_e \delta_j \left(\frac{d\mathbf{r}_j}{dt} \right)^2 = - \frac{dU}{dt}$$

Integration over a closed region V with surface ∂V followed by application of the divergence theorem then yields the integral form of Poynting's theorem for a Lorentz model dielectric

$$\underbrace{\oint_{\partial V} \mathbf{S} \cdot \hat{\mathbf{n}} da + 2 \sum_j \iiint_V N_j m_e \delta_j \left(\frac{d\mathbf{r}_j}{dt} \right)^2 d^3 r}_{\text{Rate of Energy Loss in } V \text{ by Leakage across } \partial V \text{ and by Dissipation in the Medium contained in } V}$$

Rate of Energy Loss in V by Leakage across ∂V and by Dissipation in the Medium contained in V

$$= - \frac{d}{dt} \underbrace{\iiint_V U d^3 r}_{\text{Rate of Change of the Total Electromagnetic Energy stored in } V}$$

Rate of Change of the Total Electromagnetic Energy stored in V

Energy Transport Velocity

L. Brillouin, Wave Propagation & Group Velocity (Academic Press, New York, 1960).

*R. Loudon, J. Phys. A **3**, 233-245 (1970).*

*K. Oughstun & S. Shen, J. Opt. Soc. Am. B **5**, 2395-2398 (1988).*

For a time-harmonic field with angular frequency ω travelling in a multiple resonance Lorentz model dielectric, the phasor solution of the equation of motion for the j^{th} harmonically bound electron is

$$\mathbf{r}_j = \frac{q_e/m_e}{\omega^2 - \omega_j^2 + 2i\delta_j\omega} \mathbf{E}_{loc}$$

The time-average electromagnetic energy density stored in the multiple resonance Lorentz medium is then given by (with the replacement $\mathbf{E}_{loc} \rightarrow \mathbf{E}$)

$$\langle U_{osc} \rangle = \left\| \frac{1}{4\pi} \right\| \frac{\epsilon_0}{4} |\mathbf{E}|^2 \sum_j \frac{b_j^2 (\omega^2 + \omega_j^2)}{(\omega^2 - \omega_j^2)^2 + 4\delta_j^2 \omega^2}$$

where $b_j^2 \equiv (\|4\pi\|/\epsilon_0) N_j q_e^2/m_e$ is the square of the plasma frequency for the j^{th} resonance structure with number density N_j .

The time-average energy density stored in the monochromatic plane wave electromagnetic field is given by

$$\langle U_f \rangle = \left\| \frac{1}{4\pi} \right\| \frac{\epsilon_0}{4} [n_r^2(\omega) + n_i^2(\omega) + 1] |\mathbf{E}|^2$$

With use of the identity

$$n_r^2(\omega) - n_i^2(\omega) = \frac{\epsilon_r(\omega)}{\epsilon_0} = 1 - \sum_j \frac{b_j^2 (\omega^2 - \omega_j^2)}{(\omega^2 - \omega_j^2)^2 + 4\delta_j^2 \omega^2}$$

the total time-average electromagnetic energy density stored in both the field and the medium is found to be given by

$$\begin{aligned} \langle U \rangle &= \langle U_f \rangle + \langle U_{osc} \rangle \\ &= \left\| \frac{1}{4\pi} \right\| \frac{\epsilon_0}{2} |\mathbf{E}|^2 \left\{ n_r^2(\omega) + \sum_j \frac{b_j^2 \omega^2}{(\omega^2 - \omega_j^2)^2 + 4\delta_j^2 \omega^2} \right\} \end{aligned}$$

where the summation extends over all the medium resonance frequencies.

The time-average value of the magnitude of the Poynting vector for the monochromatic plane wave field is given by

$$\langle |\mathbf{S}| \rangle = \left\| \frac{c^2}{4\pi} \right\| \frac{1}{2\mu_0 c} n_r(\omega) |\mathbf{E}|^2$$

The time-average *velocity of energy transport* for a monochromatic plane wave propagating through a multiple resonance Lorentz model dielectric is then given by the ratio of these two time-averaged quantities

$$v_E \equiv \frac{\langle |\mathbf{S}| \rangle}{\langle U \rangle} = \frac{c}{n_r(\omega) + \frac{1}{n_r(\omega)} \sum_j \frac{b_j^2 \omega^2}{(\omega^2 - \omega_j^2)^2 + 4\delta_j^2 \omega^2}}$$

In the case of a single resonance Lorentz model dielectric, this expression reduces to Loudon's result

$$v_E = \frac{c}{n_r(\omega) + \omega n_i(\omega) / \delta_0}$$

Both of these expressions yield relativistically causal results, i.e. $0 < v_E \leq c$.

Energy Transport Velocity in a Double Resonance Lorentz Model Dielectric

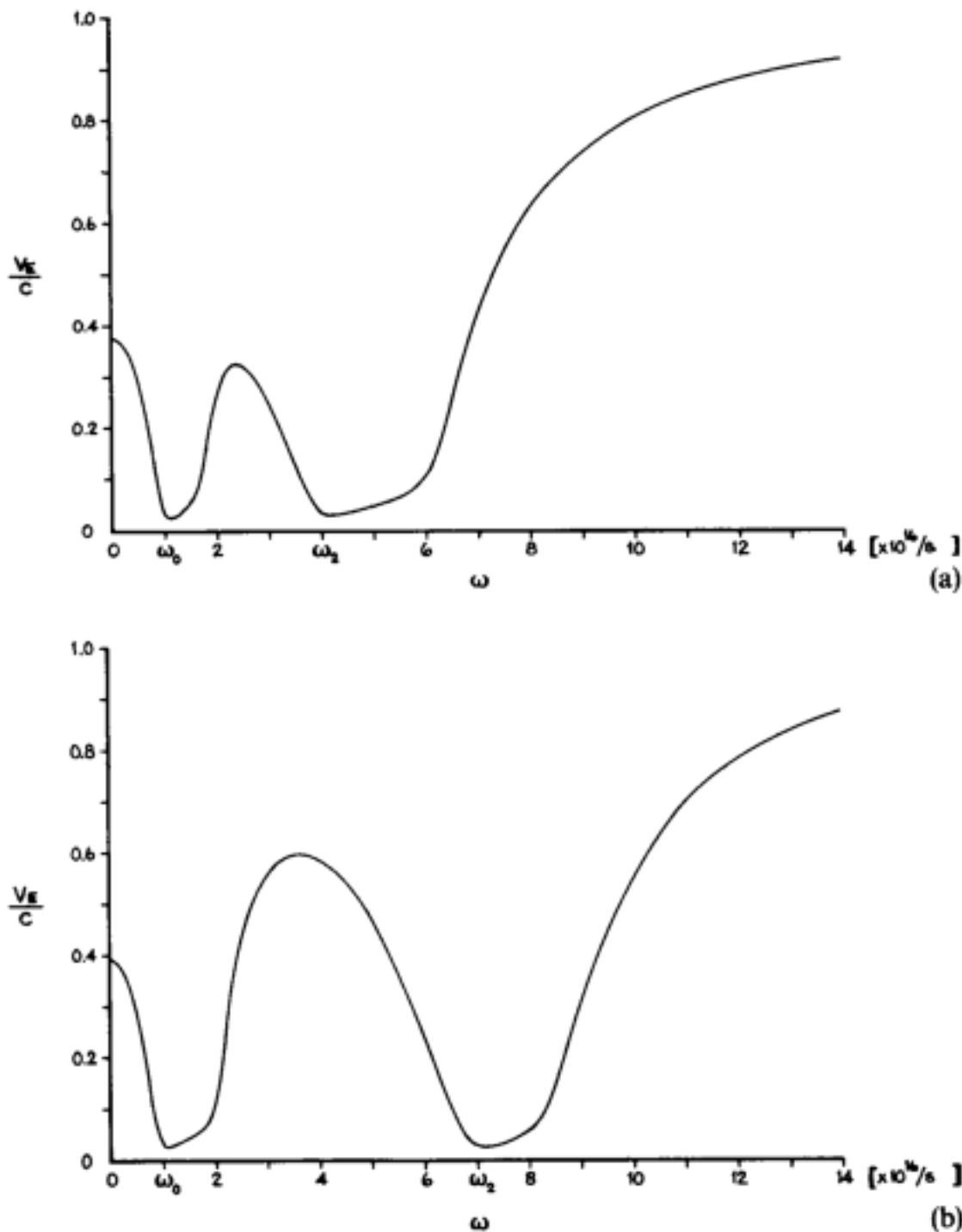


Fig. 2.2a, b. Frequency dispersion of the relative time-average energy-transport velocity v_E/c in a double-resonance Lorentz medium. The medium parameters in part (a) are: $\omega_0 = 1 \times 10^{16}/s$, $b_0^2 = 5 \times 10^{32}/s^2$, $\delta_0 = 0.1 \times 10^{16}/s$, $\omega_2 = 4 \times 10^{16}/s$, $b_2^2 = 20 \times 10^{32}/s^2$, $\delta_2 = 0.28 \times 10^{16}/s$. The medium parameters in part (b) are the same except that $\omega_2 = 7 \times 10^{16}/s$.

Fourier-Laplace Integral Representation of the Propagated Plane Wave Pulse ($z \geq 0$)

$$A(z, t) = \frac{1}{2\pi} \Re \left\{ i \exp(-i\psi) \int_C \tilde{u}(\omega - \omega_c) \exp \left[i \left(\tilde{k}(\omega) z - \omega t \right) \right] d\omega \right\}$$

Temporal Spectrum of $A(z, t)$ satisfies the Helmholtz Equation

$$\left(\nabla^2 + \tilde{k}^2(\omega) \right) \tilde{A}(z, \omega) = 0$$

Initial/Boundary Value at the Plane $z = 0$

$$A(0, t) = u(t) \sin(\omega_c t + \psi)$$

where $\psi = \{0, \pi/2\}$ for sine (cosine) wave carrier.

Initial Pulse Envelope Spectrum

$$\tilde{u}(\omega) = \int_{-\infty}^{\infty} u(t) \exp(i\omega t) dt$$

Complex Wavenumber

$$\tilde{k}(\omega) = (\omega/c)n(\omega)$$

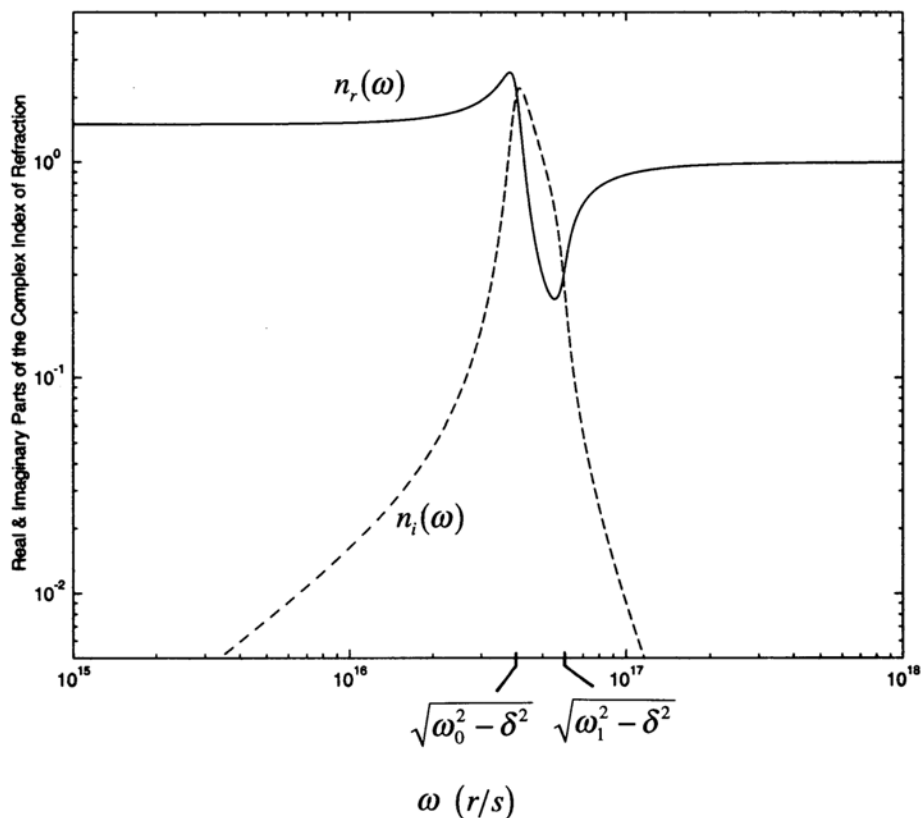
Single Resonance Lorentz Model Dielectric

$$n(\omega) = \left(1 - \frac{b_0^2}{\omega^2 - \omega_0^2 + 2i\delta_0\omega} \right)^{1/2}$$

Undamped Resonance Frequency ω_0

Phenomenological Damping Constant δ_0

Plasma Frequency $b_0 = \left((4\pi N q_e^2 / m_e) \right)^{1/2}$ is a function of the material density

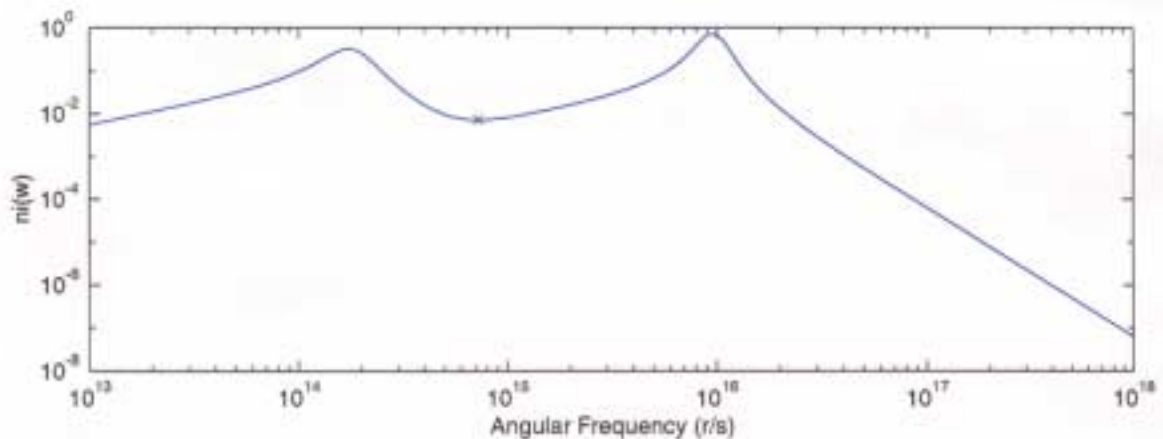
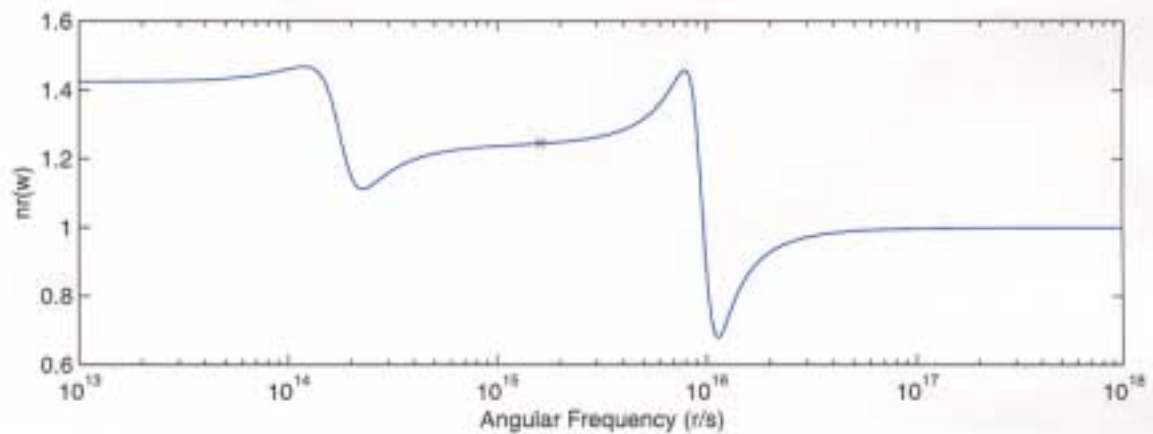


Double Resonance Lorentz Model Dielectric

$$\epsilon(\omega)/\epsilon_0 = 1 - \frac{b_0^2}{\omega^2 - \omega_0^2 + 2i\delta_0\omega} - \frac{b_2^2}{\omega^2 - \omega_2^2 + 2i\delta_2\omega}$$

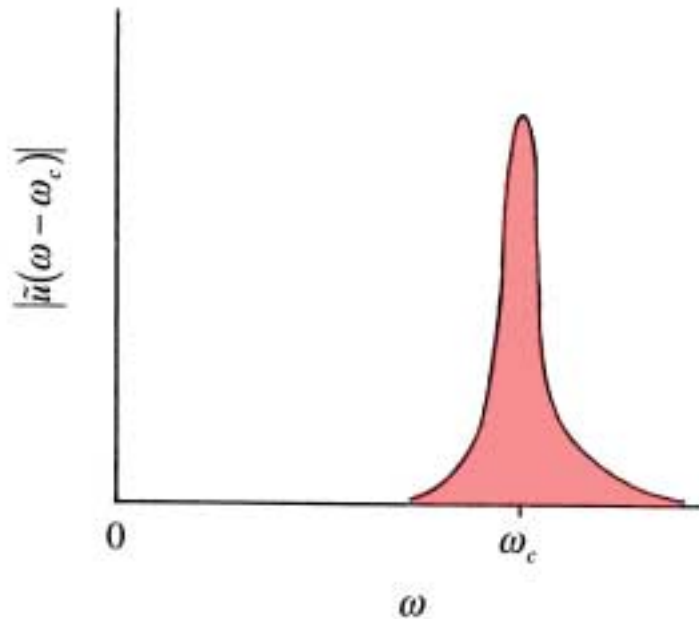
Complex Index of refraction ($\mu/\mu_0 = 1$)

$$n(\omega) = \left(1 - \frac{b_0^2}{\omega^2 - \omega_0^2 + 2i\delta_0\omega} - \frac{b_2^2}{\omega^2 - \omega_2^2 + 2i\delta_2\omega} \right)^{1/2}$$



Group Velocity Description

Quasimonochromatic or Slowly - Varying Envelope Approximation: *Introduced by Born & Wolf in the context of Partial Coherence Theory. Initial Pulse Envelope Spectrum $\tilde{u}(\omega - \omega_c)$ is Sharply peaked about the Pulse Carrier Frequency.*



Taylor Series Expansion of the Complex Wavenumber about the Carrier Frequency

$$\tilde{k}(\omega) = \sum_{j=0}^{\infty} \frac{1}{j!} \tilde{k}^{(j)}(\omega_c) (\omega - \omega_c)^j$$

Linear Dispersion Approximation

Complex Wavenumber

$$\tilde{k}(\omega) \approx \tilde{k}(\omega_c) + \tilde{k}'(\omega_c)(\omega - \omega_c)$$

Propagated Pulse

$$A(z, t) \approx \Re \left\{ i u \left(t - \tilde{k}'(\omega_c) z \right) \exp \left[i \left(\tilde{k}(\omega_c) z - \omega_c t \right) \right] \right\}$$

Pulse Phase Propagates with the Phase Velocity

$$v_p = \frac{\omega_c}{\tilde{k}(\omega_c)} \rightarrow \frac{\omega_c}{\beta(\omega_c)}$$

Pulse Envelope Propagates undistorted in shape with the Group Velocity

$$v_g = \frac{1}{\tilde{k}'(\omega_c)} \rightarrow \frac{1}{\beta'(\omega_c)}$$

where $\beta(\omega) = \Re \{ \tilde{k}(\omega) \}$ is the Plane Wave Propagation Factor.

Quadratic Dispersion Approximation

Complex Wavenumber

$$\tilde{k}(\omega) \approx \tilde{k}(\omega_c) + \underbrace{\tilde{k}'(\omega_c)}_{\text{Group Velocity}}(\omega - \omega_c) + \frac{1}{2} \underbrace{\tilde{k}''(\omega_c)}_{\text{Group Velocity Dispersion (GVD)}} (\omega - \omega_c)^2$$

Propagated Pulse

$$A(z, t) \approx \Re \left\{ \frac{1}{[2\pi\tilde{k}''(\omega_c)z]^{1/2}} \exp\left[i(\tilde{k}(\omega_c)z - \omega_c t + 3\pi/4)\right] \cdot \int_{-\infty}^{\infty} u(t') \exp\left[-i \frac{(\tilde{k}'(\omega_c)z + t' - t)^2}{2\tilde{k}''(\omega_c)z}\right] dt' \right\}$$

Pulse Envelope Propagates distorted in shape at the Group Velocity. Propagated Pulse Structure depends upon the parameter $T_F \equiv |2\pi\tilde{k}''(\omega_c)z|^{1/2}$ which corresponds to the Principal Fresnel Zone in the Analogous Slit Diffraction Problem.*

**J. Jones, Am. J. Phys. 42, 43-46 (1974).*

Complex Wavenumber

$$\tilde{k}(\omega) \equiv \beta(\omega) + i\alpha(\omega) = \frac{\omega}{c}n(\omega)$$

Linear Dispersion Approximation

$$\beta^{(1)}(\omega) = \beta(\omega_c) + \beta'(\omega_c)(\omega - \omega_c)$$

Pulse Phase Propagates at the *Phase Velocity*

$$v_p(\omega) = \frac{\omega}{\beta(\omega)}$$

while the Pulse Envelope Shape Propagates Undistorted at the *Group Velocity*

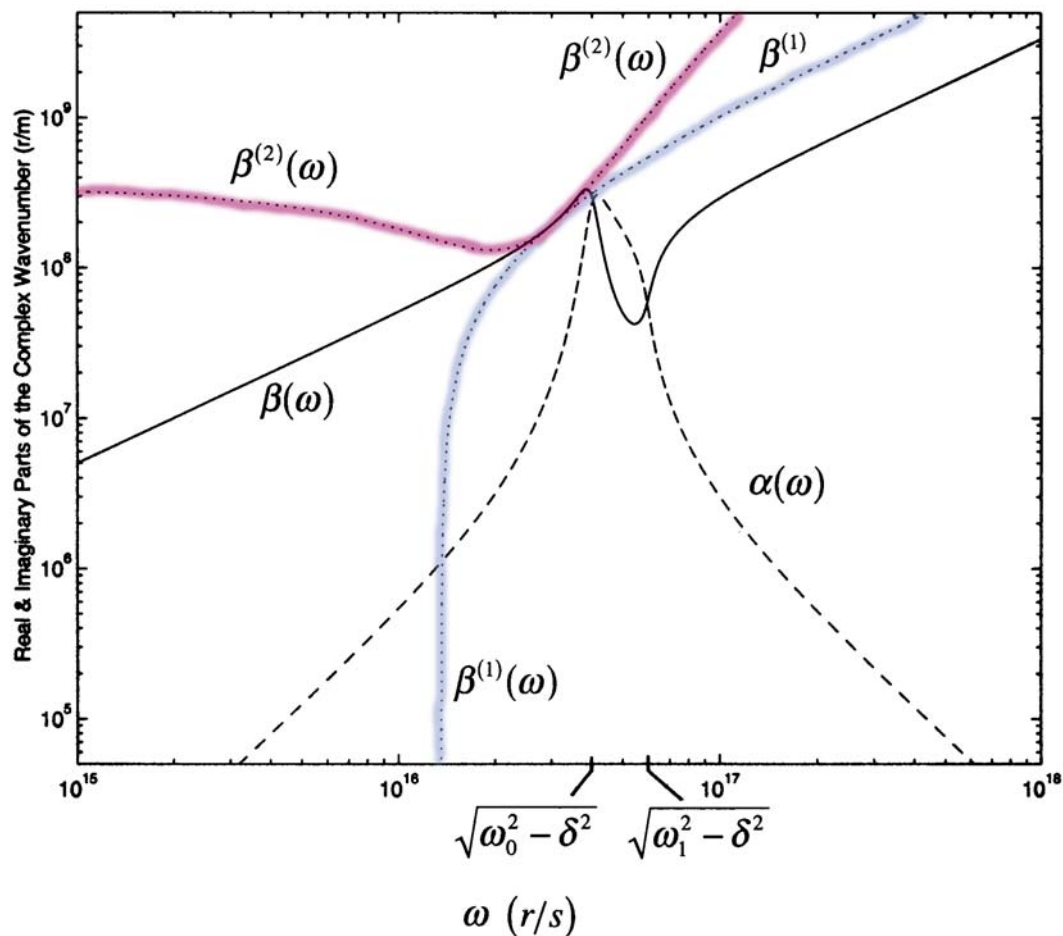
$$v_g(\omega) = \frac{1}{\partial\beta(\omega)/\partial\omega}$$

Quadratic Dispersion Approximation

$$\beta^{(2)}(\omega) = \underbrace{\beta(\omega_c)}_{\text{Phase Velocity}} + \underbrace{\beta'(\omega_c)}_{\text{Group Velocity}} (\omega - \omega_c) + \frac{1}{2} \underbrace{\beta''(\omega_c)}_{\substack{\text{Group Velocity} \\ \text{Dispersion}}} (\omega - \omega_c)^2$$

Pulse Propagates with the Group Velocity with Shape Proportional to the Fresnel Transform of the Initial Pulse Shape. Dependent upon the size of the Initial Pulse

Width T in comparison to the “Temporal Fresnel Zone” size $T_F \equiv |2\pi\beta''(\omega_c)\Delta z|^{1/2}$ (J. Jones, *Am. J. Phys.* **42**, 43-46, 1974).

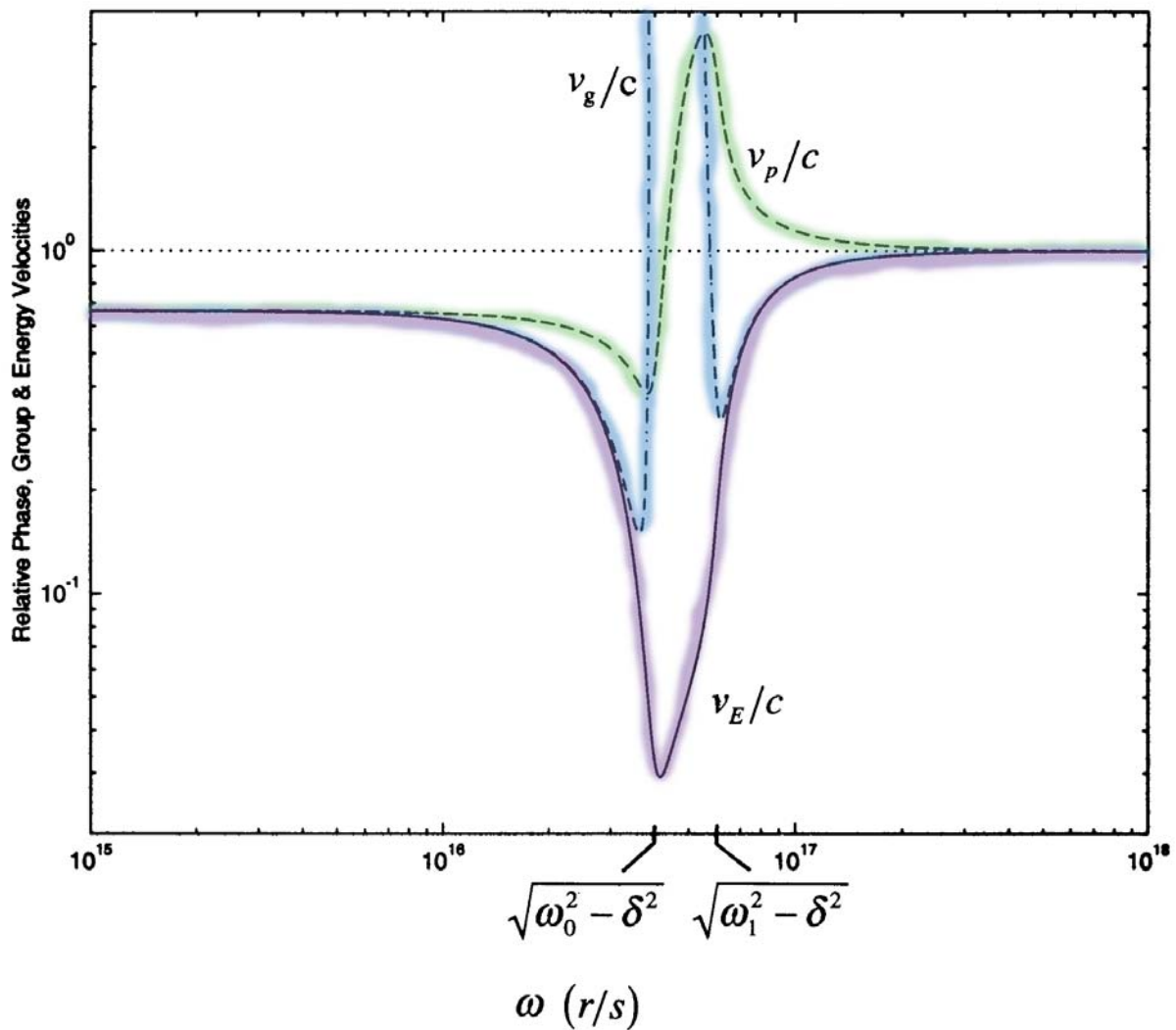


Quite unfortunately, this Taylor series approximation of the wavenumber does not improve with the inclusion of higher-order terms (Xiao & Oughstun, *J. Opt. Soc. Am. B* **16**, 1773-1785, 1999).

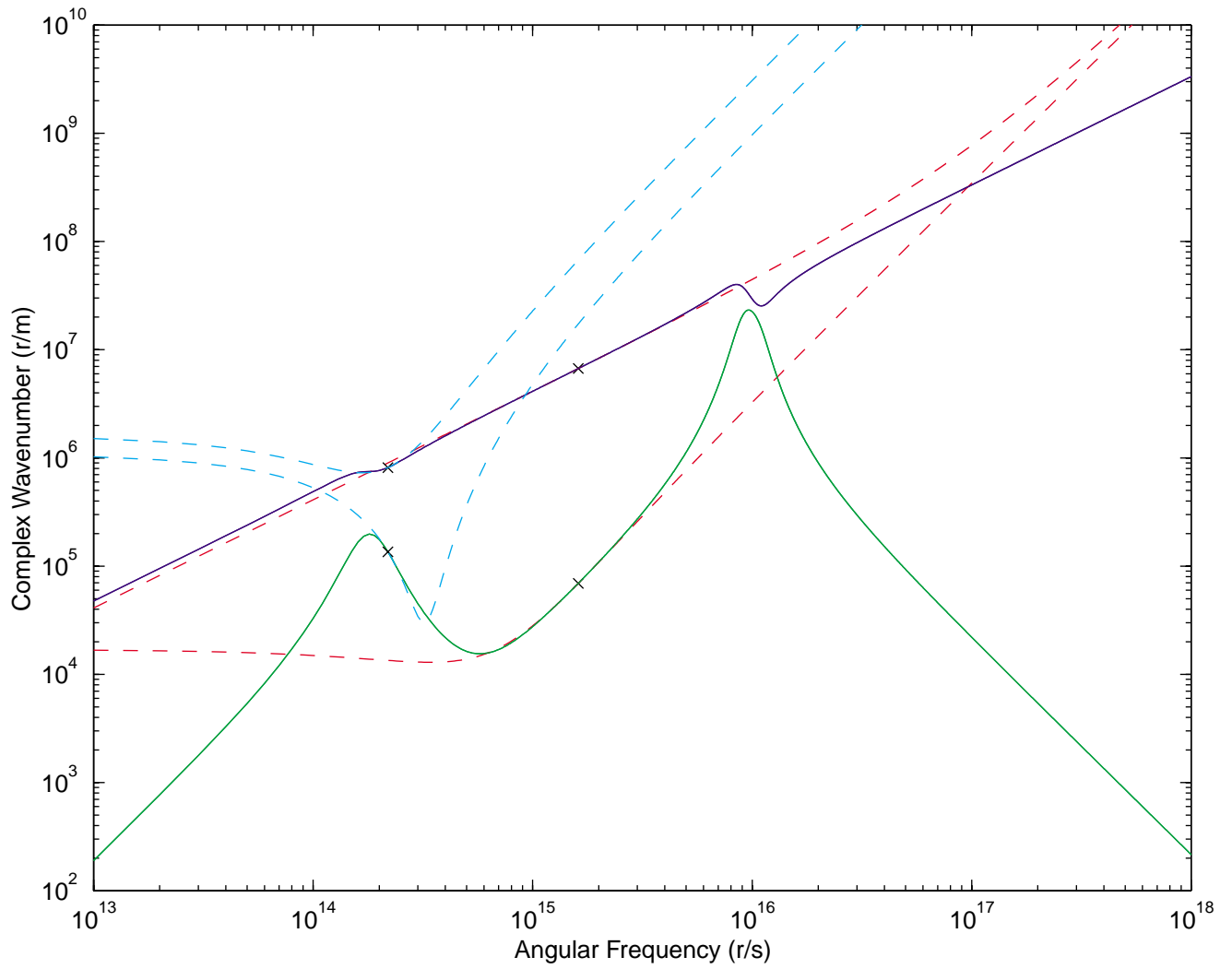
Energy Transport Velocity (R. Loudon, *J. Phys. A*, **3**, 233-245 1970)

$$v_E(\omega) \equiv \frac{\langle |S| \rangle}{\langle U \rangle} = \frac{c}{n_r(\omega) + \omega n_i(\omega)/\delta_0}$$

Phase, Group & Energy Velocities

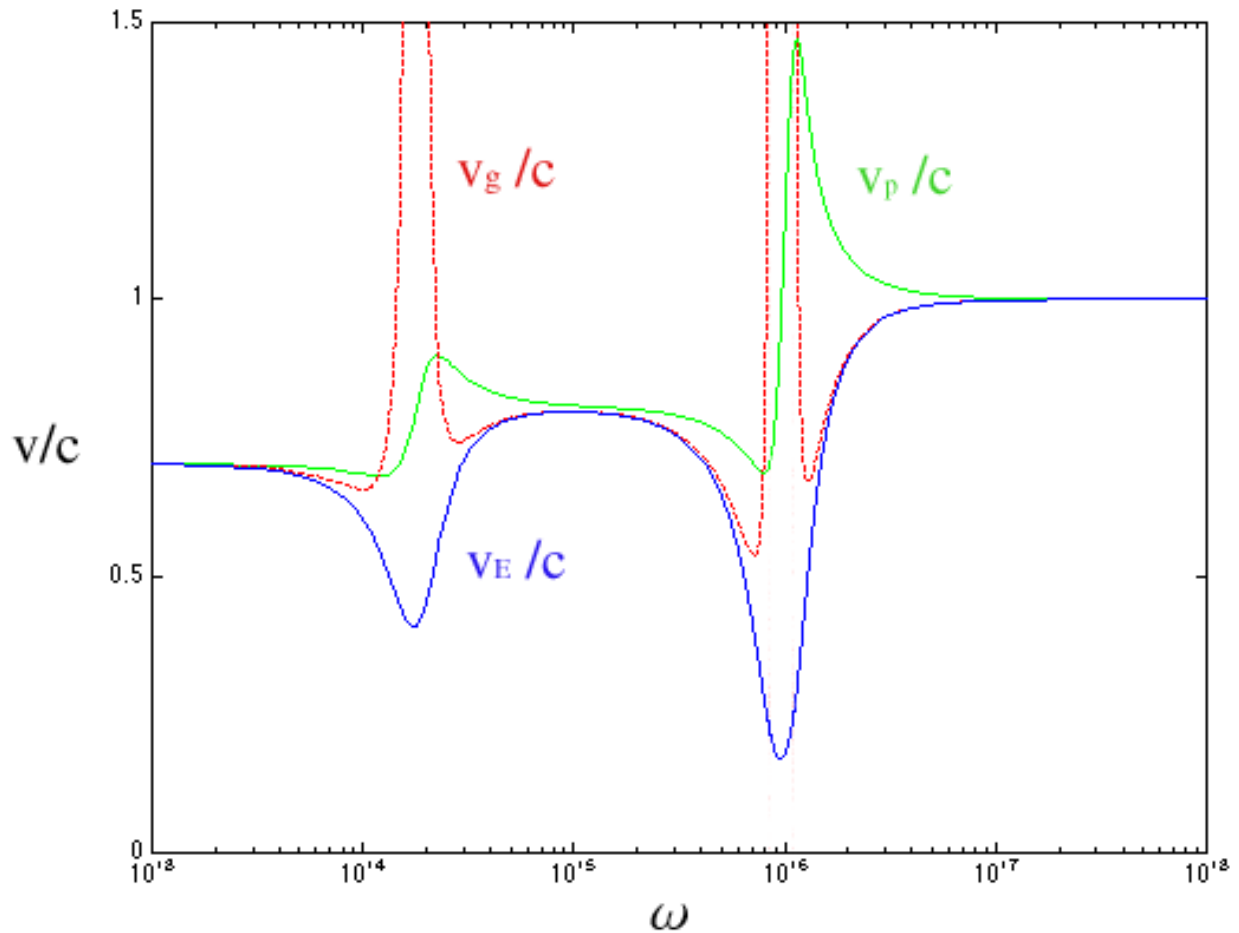


Quadratic Dispersion Approximation of the Complex Wavenumber



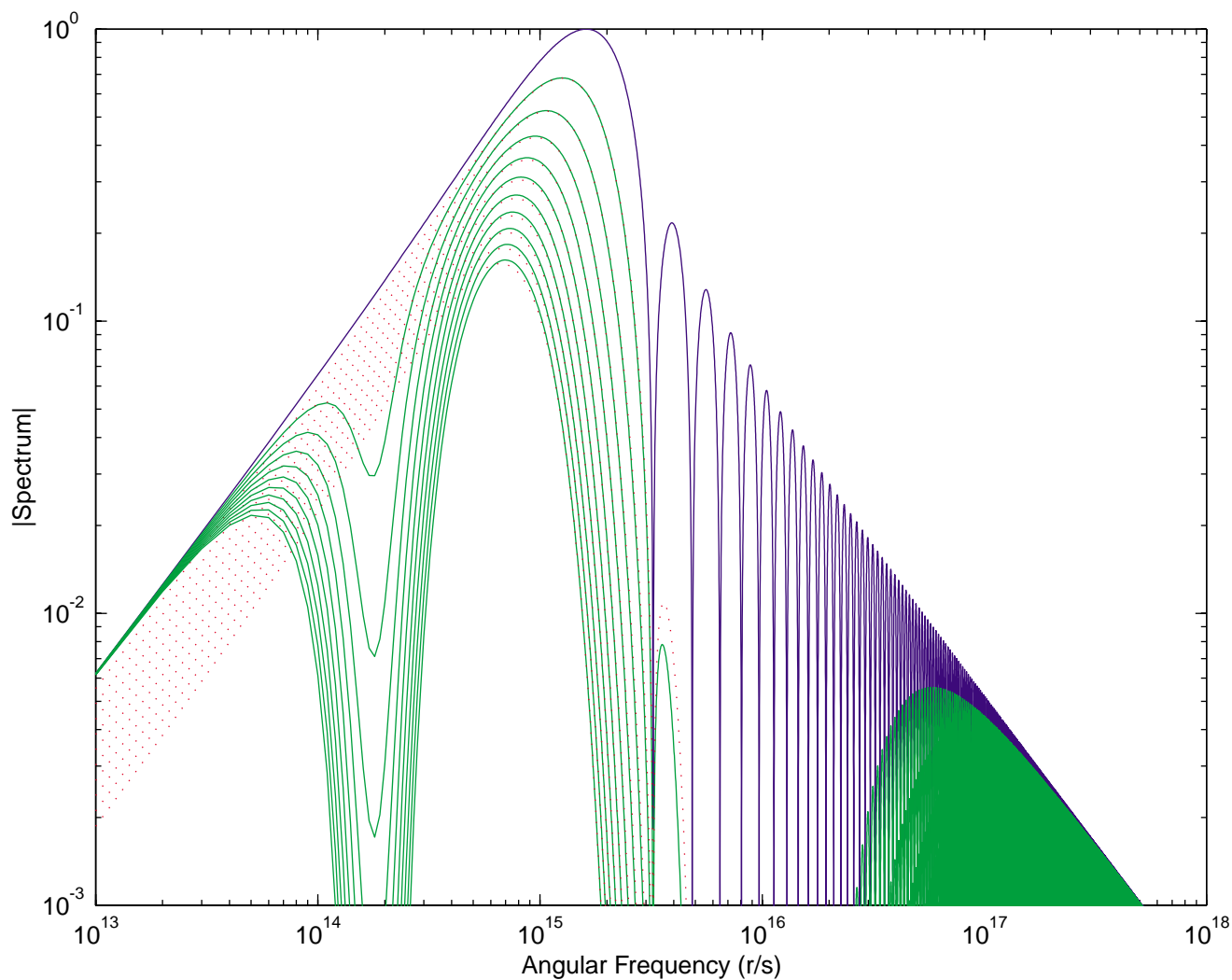
Phase, Group, & Energy* Velocities In a Multiple Resonance Lorentz Medium

$$v_E = \frac{\langle |S| \rangle}{\langle U \rangle} = \frac{c}{\left\{ n_r(\omega) + \frac{1}{n_r(\omega)} \sum_j \frac{b_j^2 \omega^2}{(\omega^2 - \omega_j^2)^2 + 4\delta_j^2 \omega^2} \right\}}$$



*Oughstun & Shen, *J. Opt. Soc. Am. B* 5, 2395-2398 (1988).

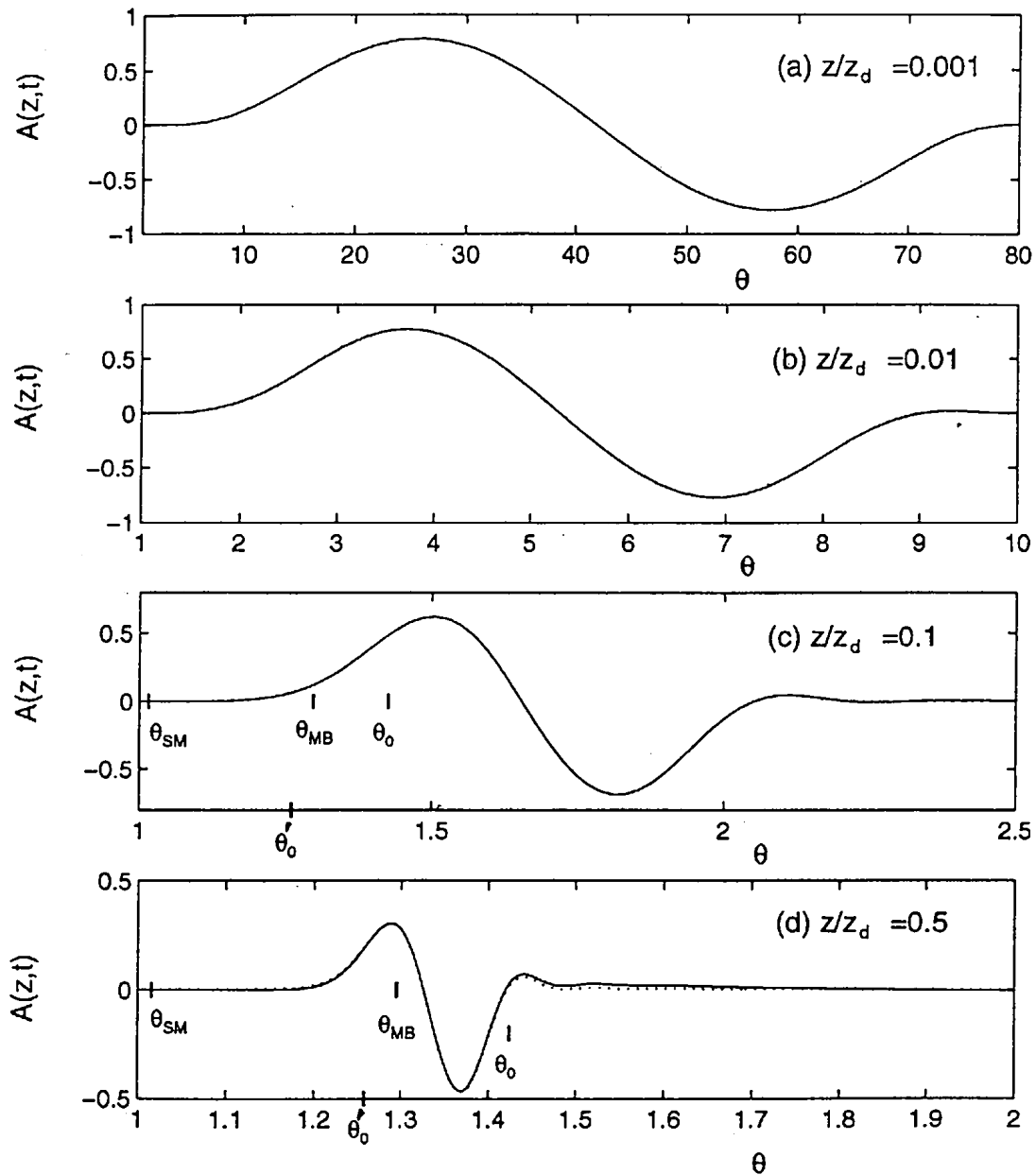
Initial & Propagated Pulse Spectra
Input Single Cycle Rectangular Envelope Pulse
 $T = 3.89fs$



$$z/d = 0, 0.5, 1.0, \dots, 5.0$$

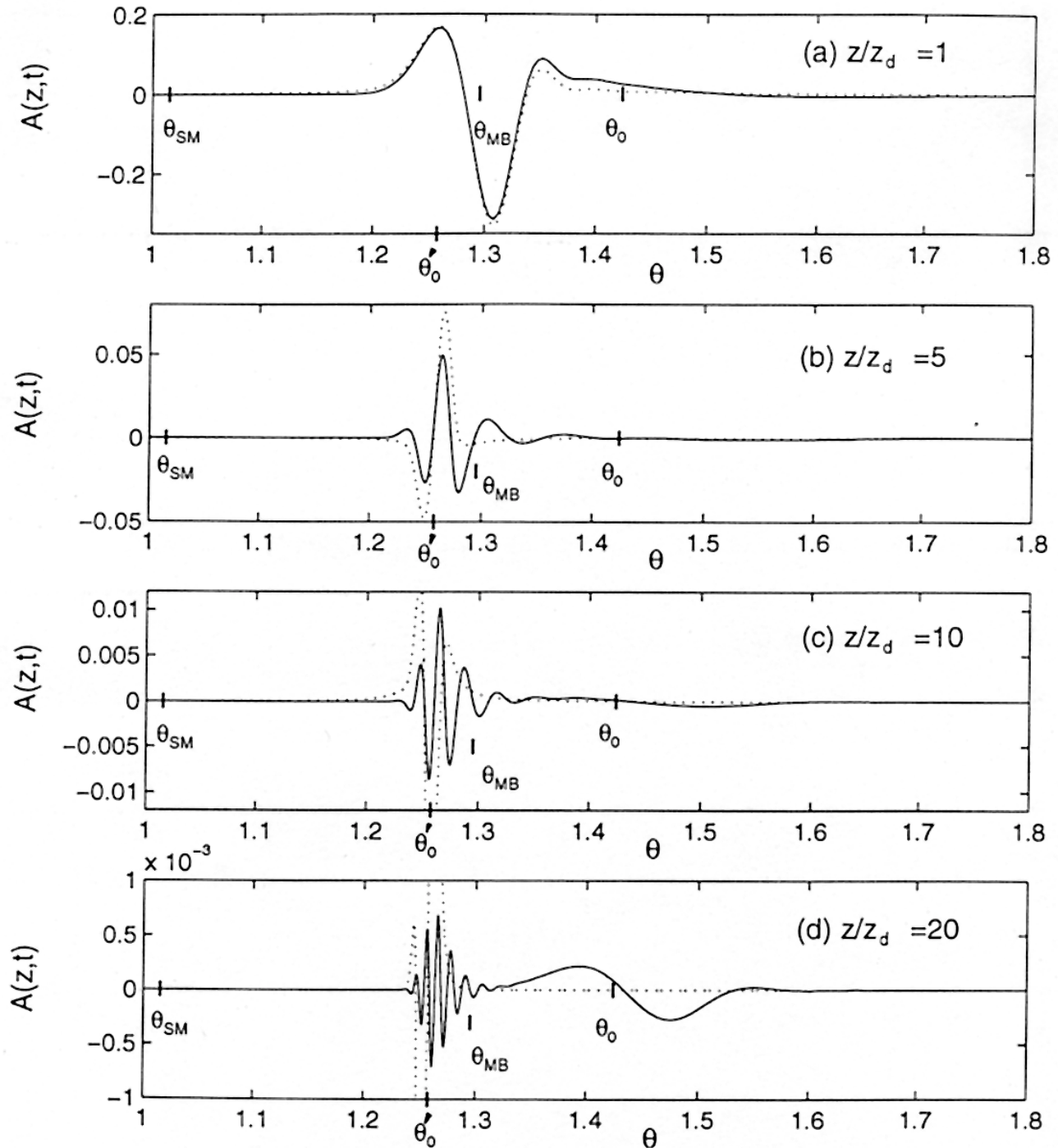
Propagated Single Cycle Pulse

$$0 < z/z_d < 1.0$$



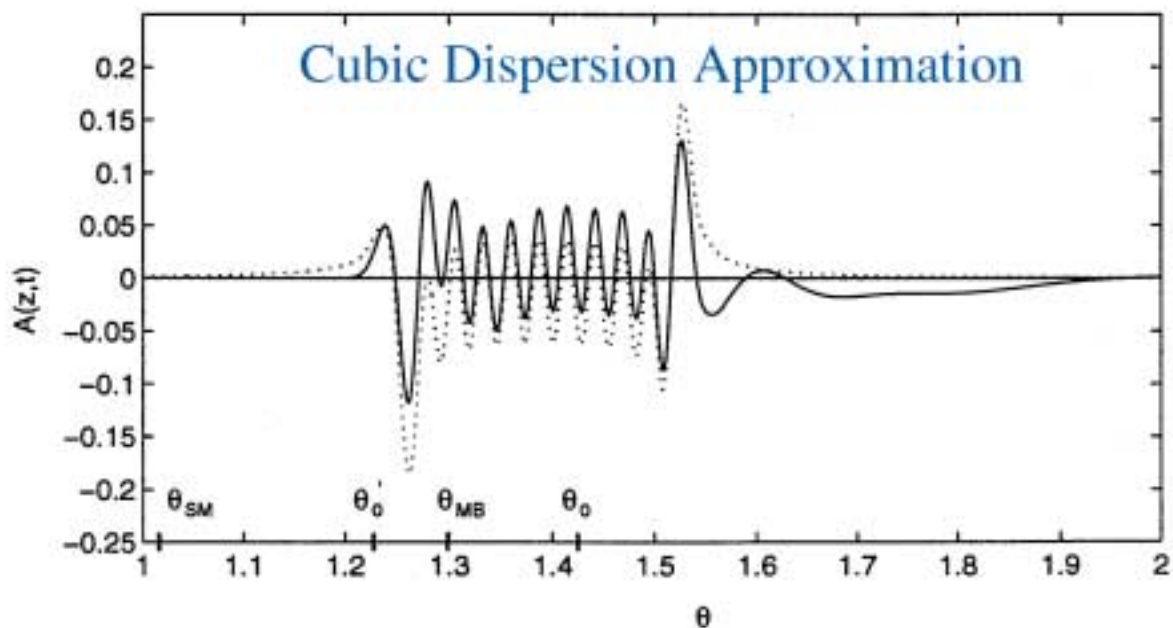
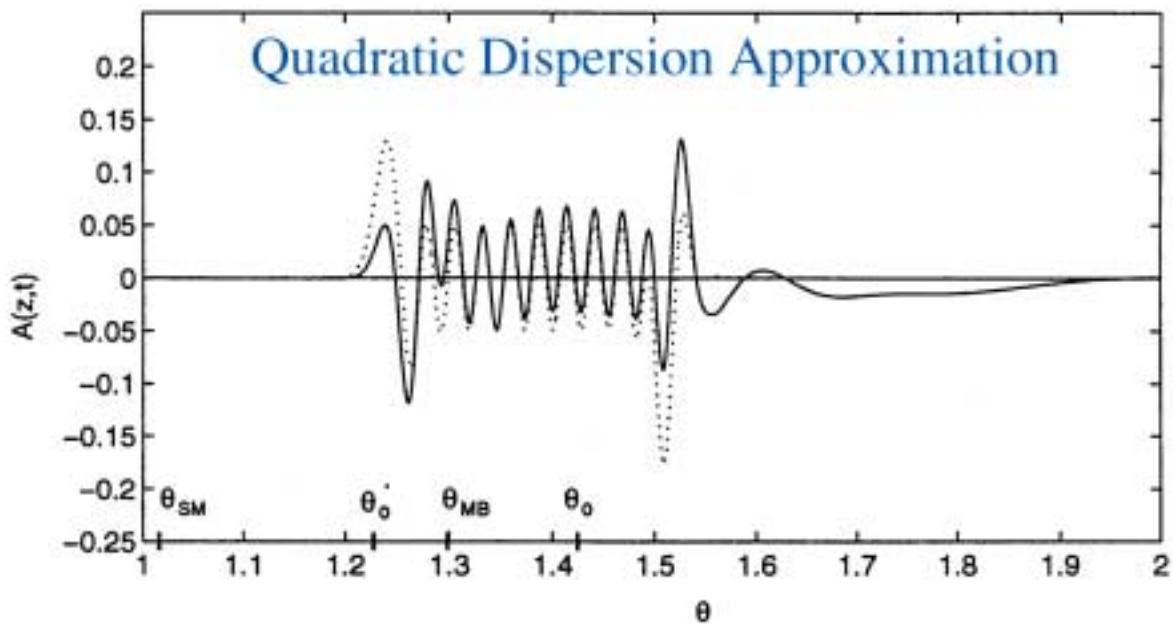
Propagated Single Cycle Pulse

$$1 < z/z_d < 20$$



Propagated Wave due to an Input 38.9fs Rectangular Envelope Pulse

$$z/z_d = 3$$



Higher-Order Dispersion Approximations

Anderson, Askne, & Lisak, Physical Review A 12, 1546 (1975): “the evolution of slowly varying wave pulses in strongly dispersive and absorptive media is studied by a recursive method. It is shown that the resulting envelope function may be obtained by including correction terms of arbitrary dispersive and absorptive orders.”

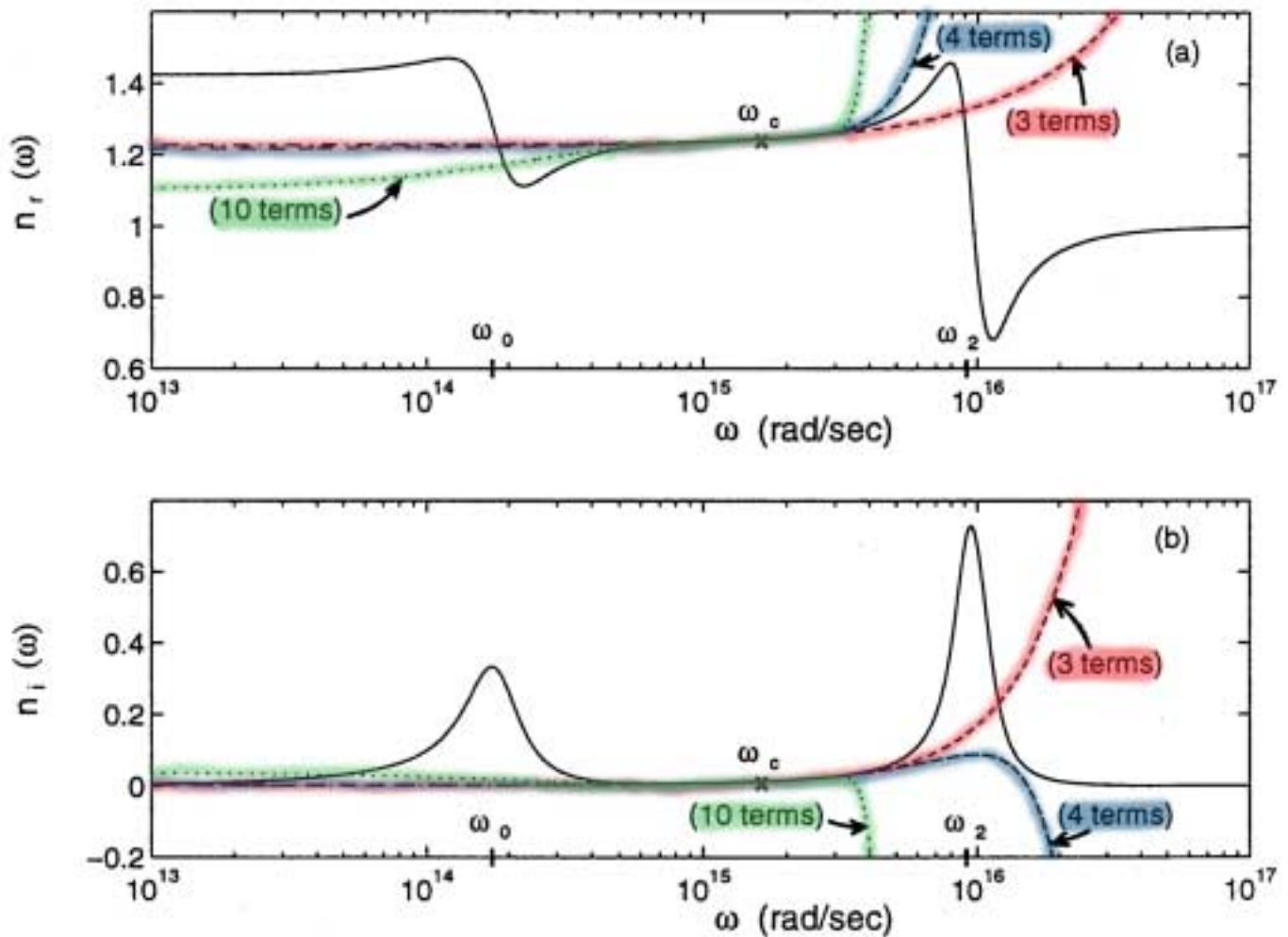
Butcher & Cotter, The Elements of Nonlinear Optics, ch. 2 (Cambridge, 1990): “to describe pulse propagation in dispersive media in general we must retain the second-order dispersion, and for ultrashort pulses or those with a wide frequency spectrum it may sometimes be necessary to also include higher-order terms.”

Akhamanov, Vysloukh, & Chirkin, Optics of femtosecond Laser Pulses, chs. 1-2 (American Institute of Physics, 1992): “one can analyze how the dispersion of a medium affects a propagating pulse for any higher-order approximation of the dispersion theory. Naturally, the higher-order approximations make the quantitative picture of dispersive spreading more precise although its basic features obtained for the second- and third-order approximations remain unchanged.”

Unfortunately, these assertions, although physically appealing, are not valid in the short pulse regime.

Xiao & Oughstun, Journal of the Optical Society of America B 16, 1773 (1999): “With the exception of a small neighborhood about some characteristic frequency of the initial pulse, the

inclusion of higher-order terms in the Taylor series approximation of the complex wavenumber in a causally dispersive, attenuative medium beyond the quadratic approximation is practically meaningless from both the physical and mathematical points of view.



Initial Conclusions

- *Any Study of the Velocity of an Ultrawideband Pulse in a Dispersive Material must give careful consideration to the Material Dispersion (including the Attenuation) over the Entire Frequency Domain.*
- *The Accuracy of the Group Velocity Approximation improves in the small propagation distance limit as $\Delta z \rightarrow 0$.*
- *Conclusions regarding Ultrawideband Pulse Dynamics (including any Pulse Velocity Measures) that are based upon the Quadratic or Higher-Order Dispersion Approximations should be viewed with Extreme Skepticism for Propagation Distances exceeding a single absorption depth in the dispersive material $\Delta z > z_d$, where $z_d = \alpha^{-1}(\omega_c)$ is evaluated at some characteristic frequency of the input pulse (e.g. the input pulse carrier frequency).*

A Brief Poetic Interlude

*There was a young chap named
Devaney
Whose arguments went faster than
electromagnetic energy
He published a paper in May
In an extremely noncausal way
With errata published the previous
February*

Slowly-Varying Envelopes, Ultrawideband Signals & Ultrashort Pulses

When is a pulsed field *slowly-varying* so that the group velocity approximation is applicable?

When is a signal *ultrawideband*?

When is a pulse *ultrashort*?

Notice that an ultrashort pulse must also be ultrawideband, but not vice-versa.

Replace the last two terms with the single designation of “*rapidly-varying*”. The relevant question is then: What marks the transition between slowly-varying and rapidly-varying?

Definition: A field is said to be *rapidly-varying* if any change in the field amplitude occurs on the order of or faster than the characteristic relaxation time of the dispersive material. If the field is not rapidly-varying, then it is said to be slowly-varying.

For a single resonance Lorentz model dielectric with damping constant δ (in radians/second), the associated relaxation time is $\tau_r \sim 1/\delta$. Precursor fields will then dominate the dynamical field evolution as the propagation distance Δz (typically) exceeds an absorption depth $z_d \equiv \alpha^{-1}(\omega_c)$ in the dispersive material, evaluated at some characteristic frequency ω_c of the pulse, if the inequality

$$\left| \frac{\partial(A/A_0)}{\partial t} \right| > \delta$$

is satisfied. The field is then said to be rapidly-varying.

If the opposite inequality $\left| \frac{\partial(A/A_0)}{\partial t} \right| < \delta$ is satisfied, then the field is said to be slowly-varying. The precursor fields will then have a negligible impact on the dynamical field evolution.

Asymptotic Description

Fourier-Laplace Integral Representation of the Propagated Plane Wave Pulse ($z \geq 0$)

$$A(z,t) = \frac{1}{2\pi} \Re \left\{ i \exp(-i\psi) \int_c \tilde{u}(\omega - \omega_c) \exp[(z/c)\phi(\omega, \theta)] d\omega \right\}$$

Complex Phase Function

$$\phi(\omega, \theta) = i(c/z) [\tilde{k}(\omega)z - \omega t] = i\omega[n(\omega) - \theta]$$

Dimensionless Space-Time Parameter $\theta = ct/z$.

Taylor Series Expansion about the Saddle Points of the Complex Phase Function

$$\phi'(\omega_{SP}, \theta) = 0$$

General Saddle Point Equation

$$\omega \frac{dn(\omega)}{d\omega} + n(\omega) = \theta$$

First-Order Saddle Point: $\phi' = 0$, $\phi'' \neq 0$

Second-Order Saddle Point: $\phi' = \phi'' = 0$, $\phi''' \neq 0$

etc...

Asymptotic Representation for a Multiple Resonance Lorentz Model Dielectric

$$A(z, t) \sim \underbrace{A_S(z, t)}_{\substack{\text{Sommerfeld} \\ \text{Precursor}}} + \underbrace{A_m(z, t)}_{\substack{\text{Middle} \\ \text{Precursors}}} + \underbrace{A_B(z, t)}_{\substack{\text{Brillouin} \\ \text{Precursor}}} + \underbrace{A_c(z, t)}_{\substack{\text{Pole} \\ \text{Contributions}}}$$

as $z \rightarrow \infty$.

Physical Significance of the Saddle Points

$$\frac{z}{c} \phi(\omega, \theta) = i \left(\tilde{k}(\omega) z - \omega t \right)$$

$$\begin{aligned} \therefore \frac{z}{c} \phi'(\omega, \theta) &= i \left(\frac{\partial \tilde{k}(\omega)}{\partial \omega} z - t \right) \\ &= 0 \quad \text{at the saddle points of } \phi \end{aligned}$$

$$\therefore \frac{z}{t} = \left(\frac{1}{\partial \tilde{k}(\omega) / \partial \omega} \right)_{\omega_{SP}} = v_g(\omega_{SP})$$

The Group Velocity is Real-Valued at the Saddle Points of the Complex Phase Function.

Power Series & Asymptotic Expansions

For a *Power Series Expansion* of a function $f(z)$

$$f(z) \cong \sum_{j=0}^N u_j(z)$$

the approximation to $f(z)$ at a fixed value of z improves as $N \rightarrow \infty$.

For an *Asymptotic Expansion* of a function $f(z)$

$$f(z) = S_N(z) + R_{N+1}(z)$$

where $S_N(z) = \sum_{j=0}^N a_j \psi_j(z)$ with $\{\psi_j(z)\}$ being an

asymptotic sequence of functions as $z \rightarrow \infty$, so

that $(\psi_{n+1}(z)/\psi_n(z)) \xrightarrow{z \rightarrow \infty} 0$, and where

$R_{N+1}(z) = O\{\psi_{N+1}(z)\}$ as $z \rightarrow \infty$ is the *Remainder*

Term after N terms, the approximation to $f(z)$ by

$S_N(z)$ improves for fixed N as $z \rightarrow \infty$. The first or

dominant term in the asymptotic expansion of

$f(z)$ gives the *Asymptotic Approximation* of $f(z)$.

N. H. Abel (1828): *“Divergent series are the invention of the devil, and it is a shame to base on them any demonstration whatsoever. By using them, one may draw any conclusion he pleases and that is why these series have produced so many fallacies and so many paradoxes...”*



Royal Palace, Oslo, Norway.

Single Resonance Lorentz Model Dielectric

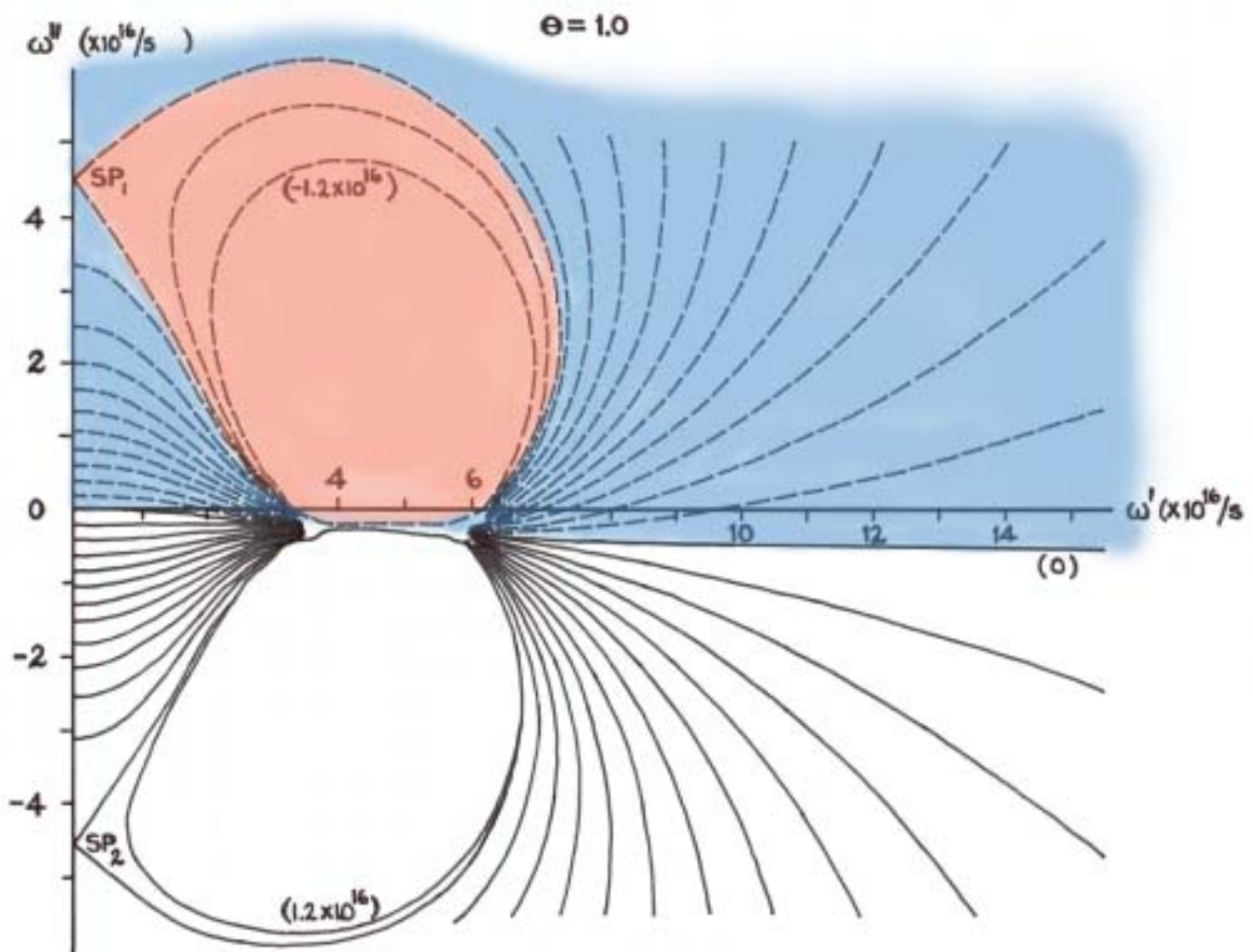
Oughstun & Sherman, *J. Opt. Soc. Am. B* **5**, 817-849 (1988)

Solhaug, Oughstun, Stamnes & Smith, *J. Eur. Opt. Soc. A, Pure & Applied Optics* **7**, 575-602 (1998)

$$\theta = 1.0$$

The pair of distant saddle points at infinity are dominant

$$X(\omega_{SP_d^\pm}, \theta = 1) = 0 > X(\omega_{SP_n^+}, \theta = 1)$$



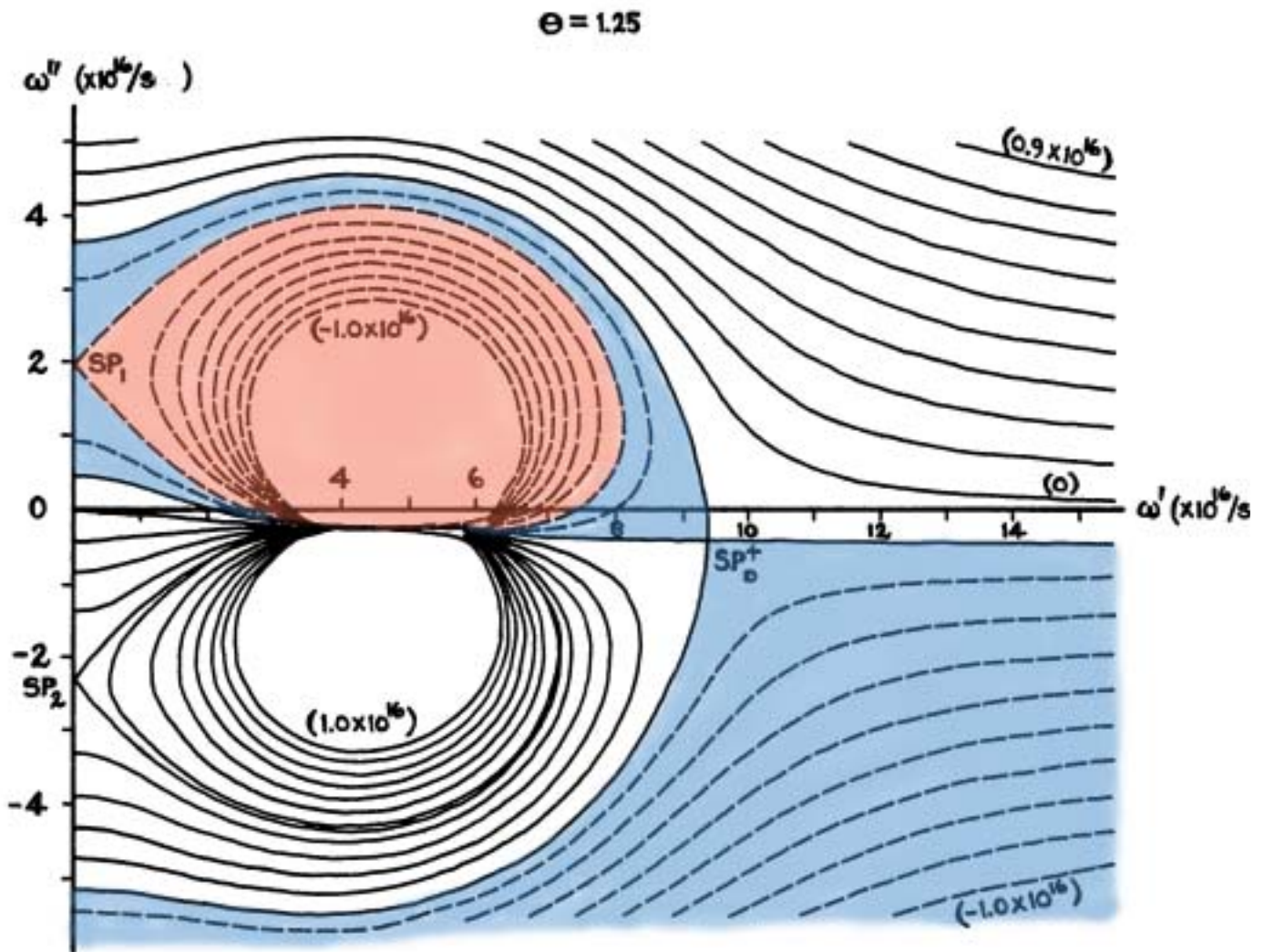
where

$$X(\omega, \theta) \equiv \Re\{\phi(\omega, \theta)\} .$$

$\theta = 1.25$

The pair of distant saddle points are the dominant saddle points

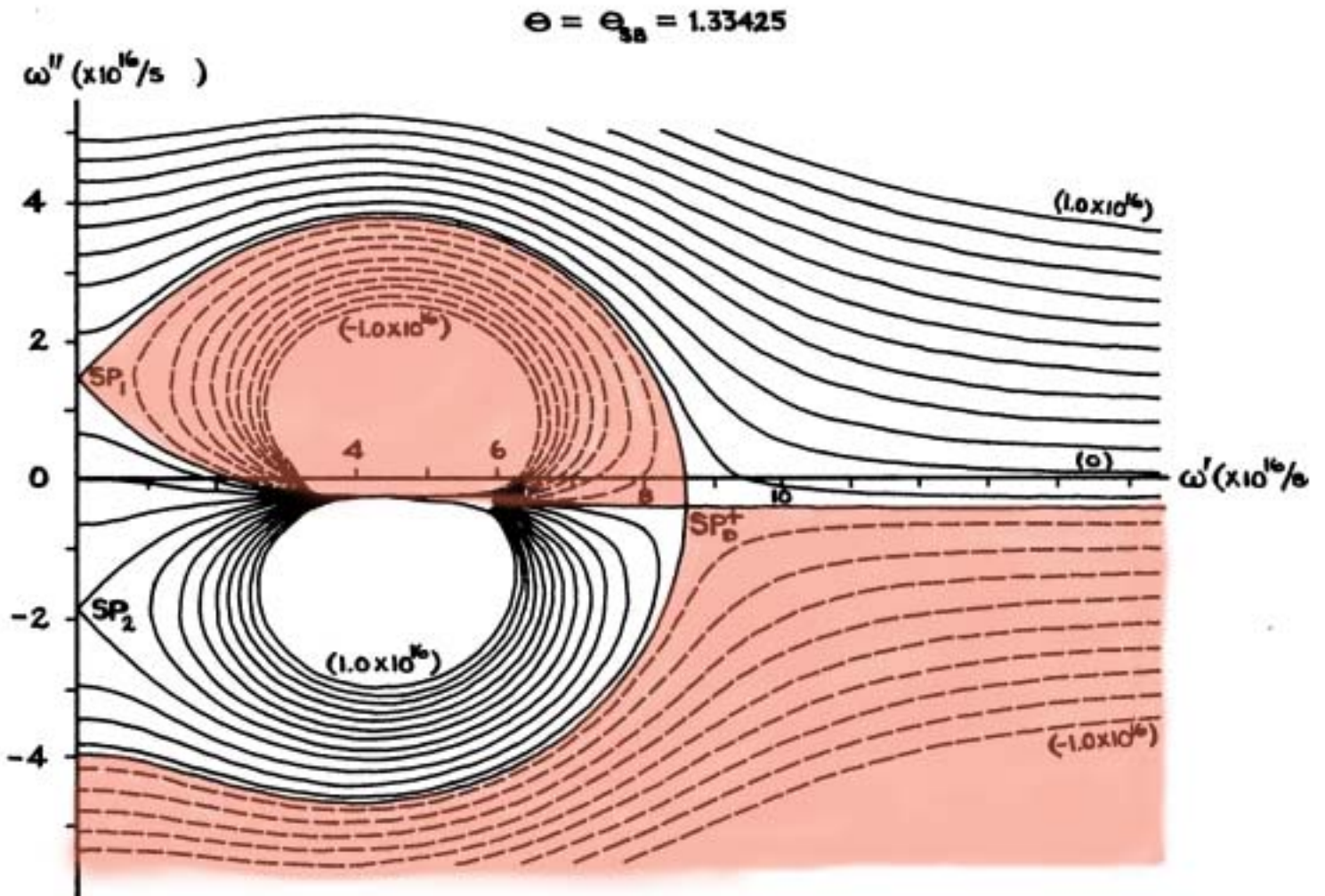
$$X(\omega_{SP_d^\pm}, \theta = 1.25) > X(\omega_{SP_n^+}, \theta = 1.25)$$



$$\theta = \theta_{SB} \approx 1.33425$$

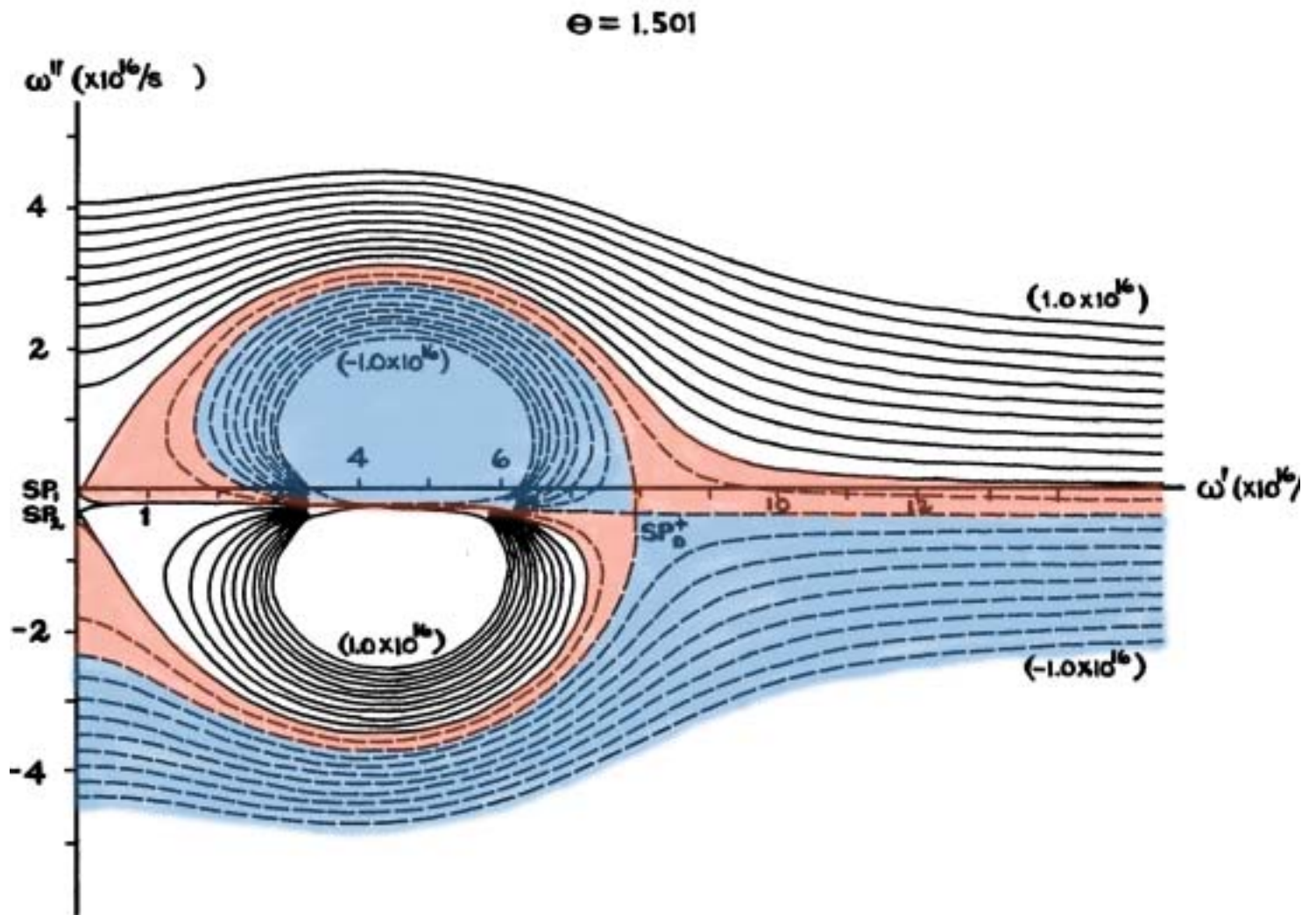
The upper near saddle point and the pair of distant saddle points are of equal dominance

$$X(\omega_{SP_d^\pm}, \theta_{SB}) = X(\omega_{SP_n^+}, \theta_{SB})$$



$\theta = 1.501$

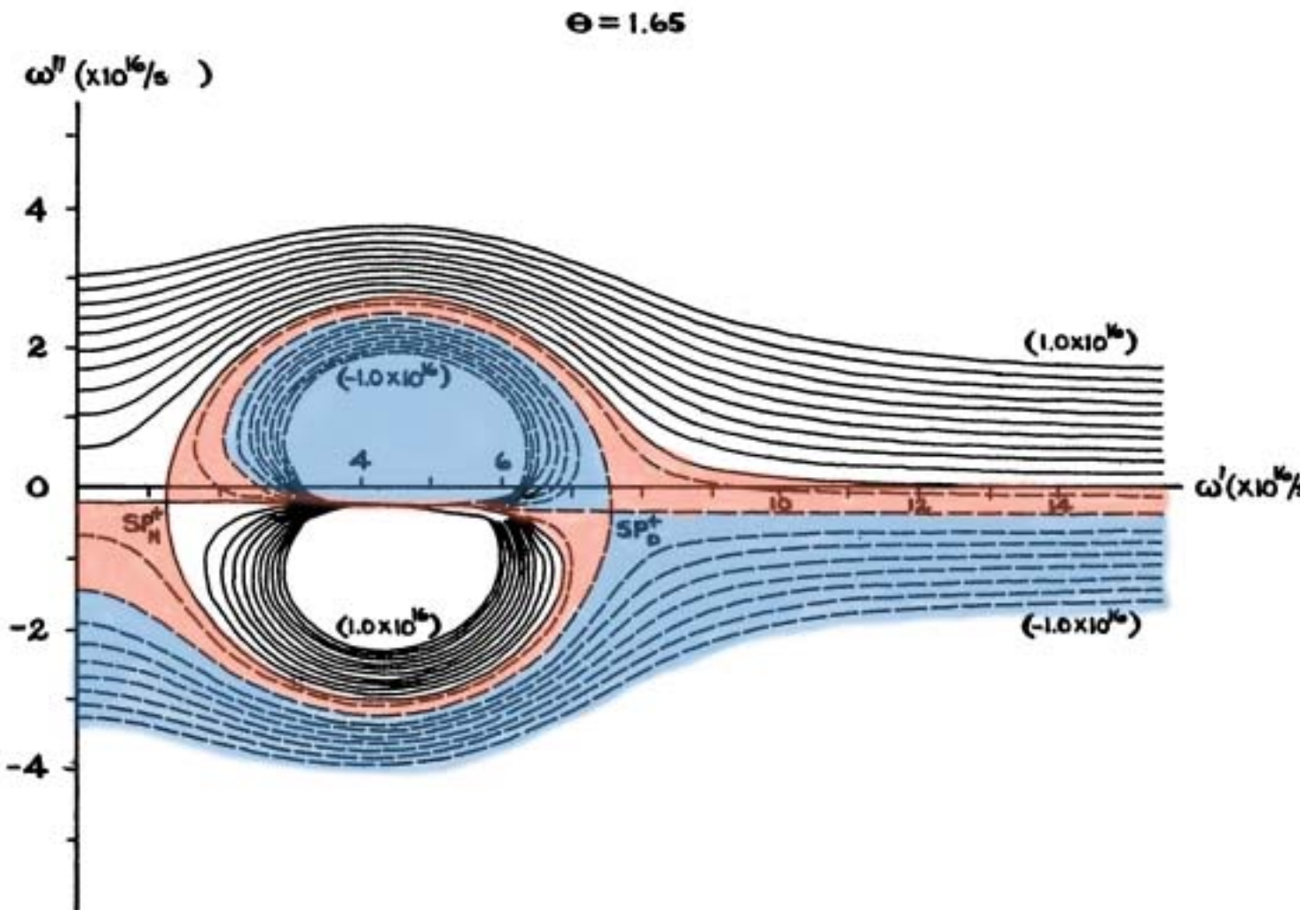
The upper near saddle point is the dominant saddle point and is just about to coalesce with the lower near saddle point, forming a second-order saddle point at $\theta = \theta_1 \approx 1.502$.



$$\theta = 1.65$$

The pair of near saddle points have moved off of the imaginary axis and into the lower half of the complex ω -plane and are the dominant saddle points and remain so for all $\theta > \theta_1$

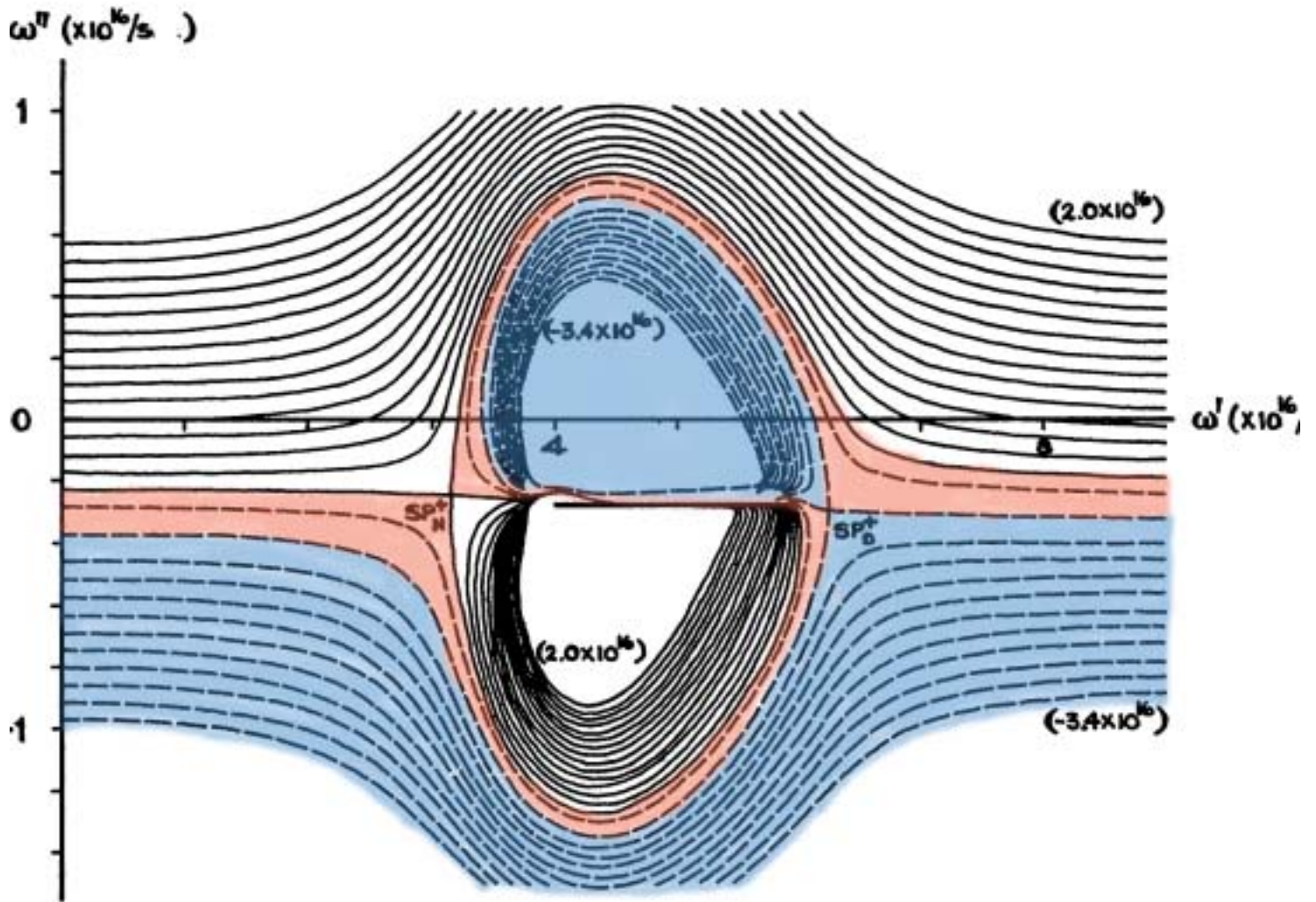
$$X(\omega_{SP_n^\pm}, \theta) > X(\omega_{SP_d^\pm}, \theta)$$



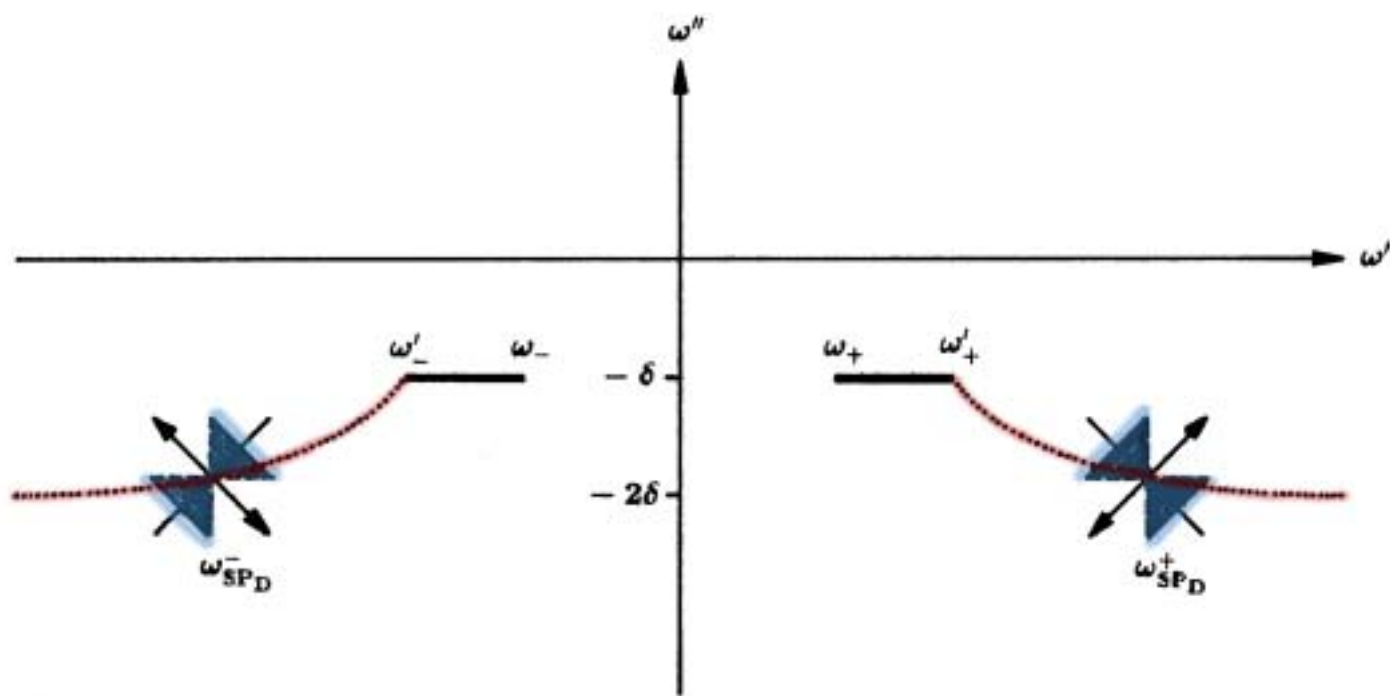
$\theta = 5.0$

As the space-time parameter $\theta \rightarrow \infty$, the near saddle points approach the inner branch points while the distant saddle points approach the outer branch points.

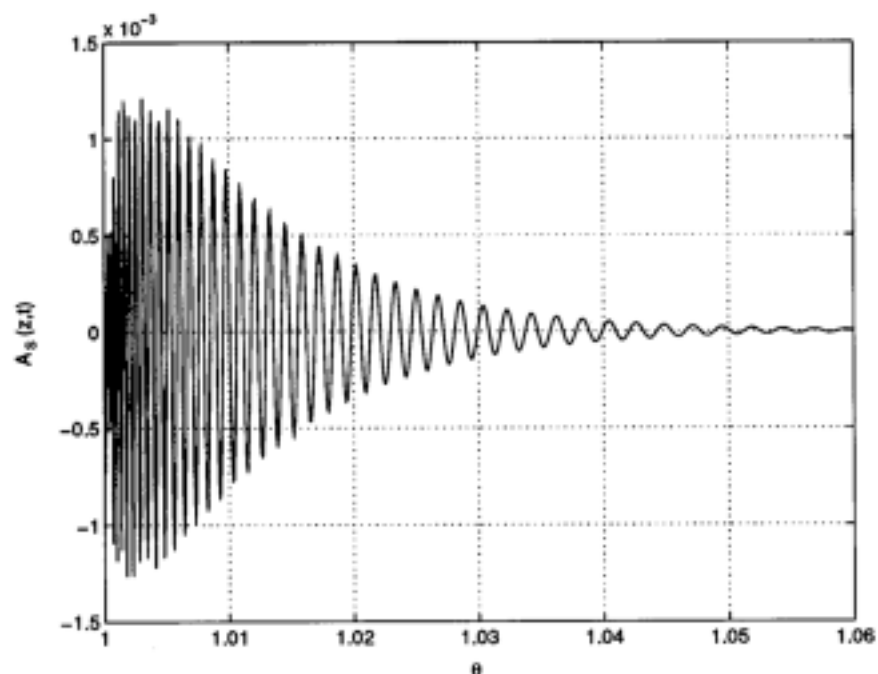
$\theta = 5.0$



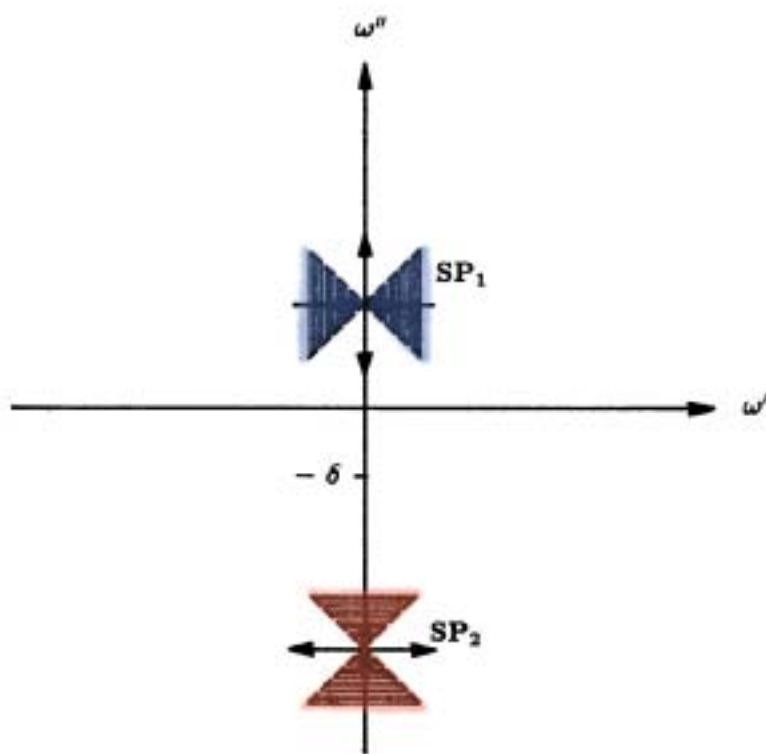
Distant Saddle Point Dynamics



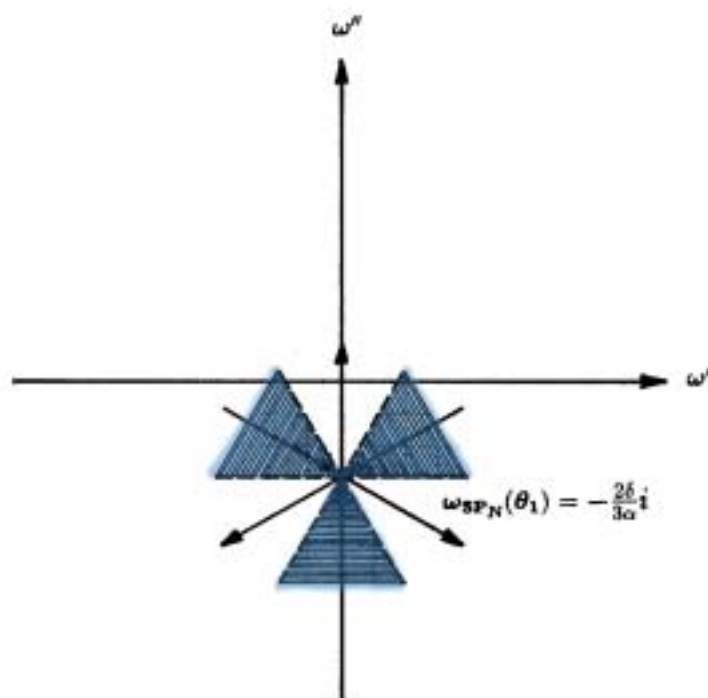
Sommerfeld Precursor Evolution



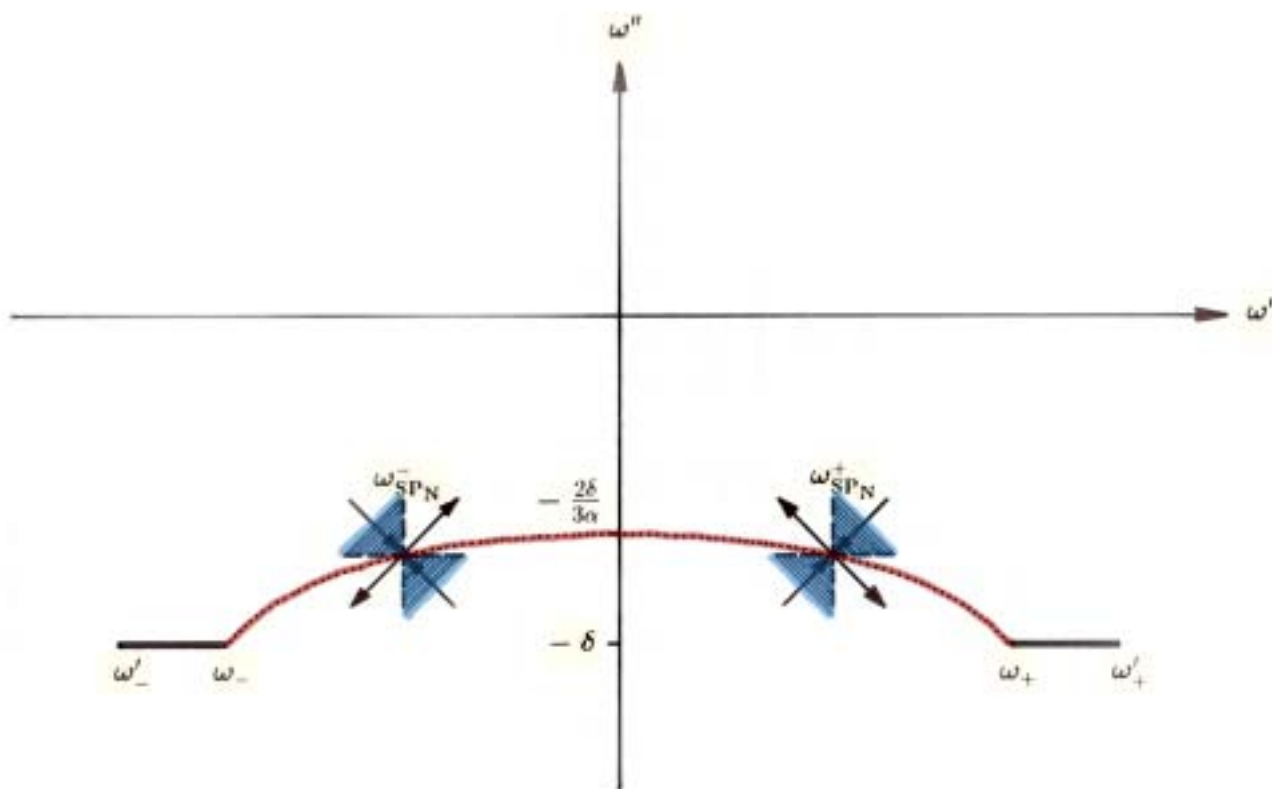
Near Saddle Point Dynamics ($1 \leq \theta < \theta_1$)



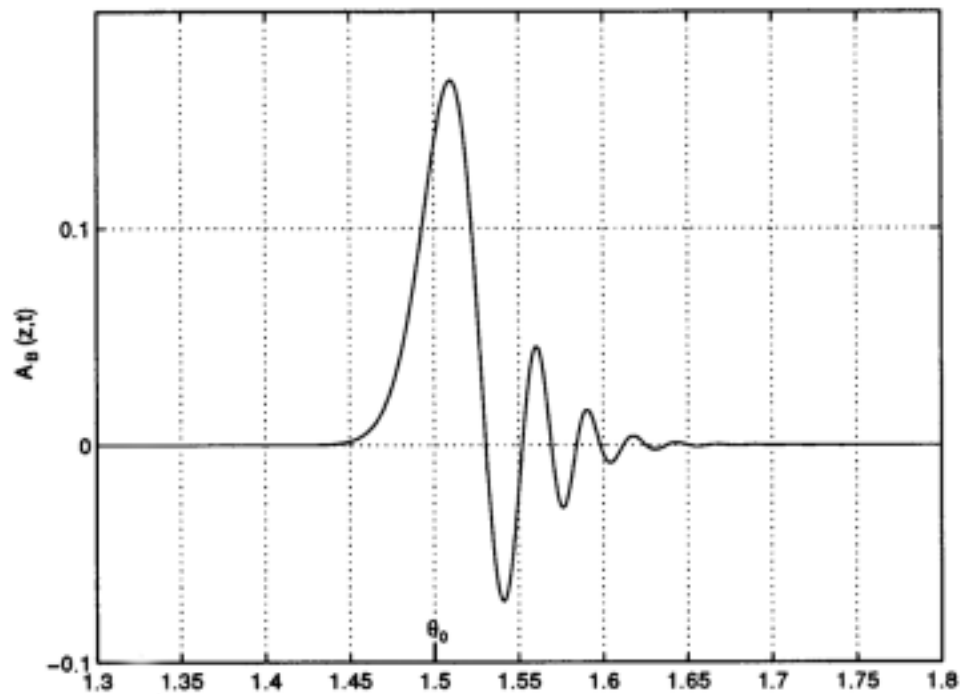
Near Saddle Point Dynamics ($\theta = \theta_1$)



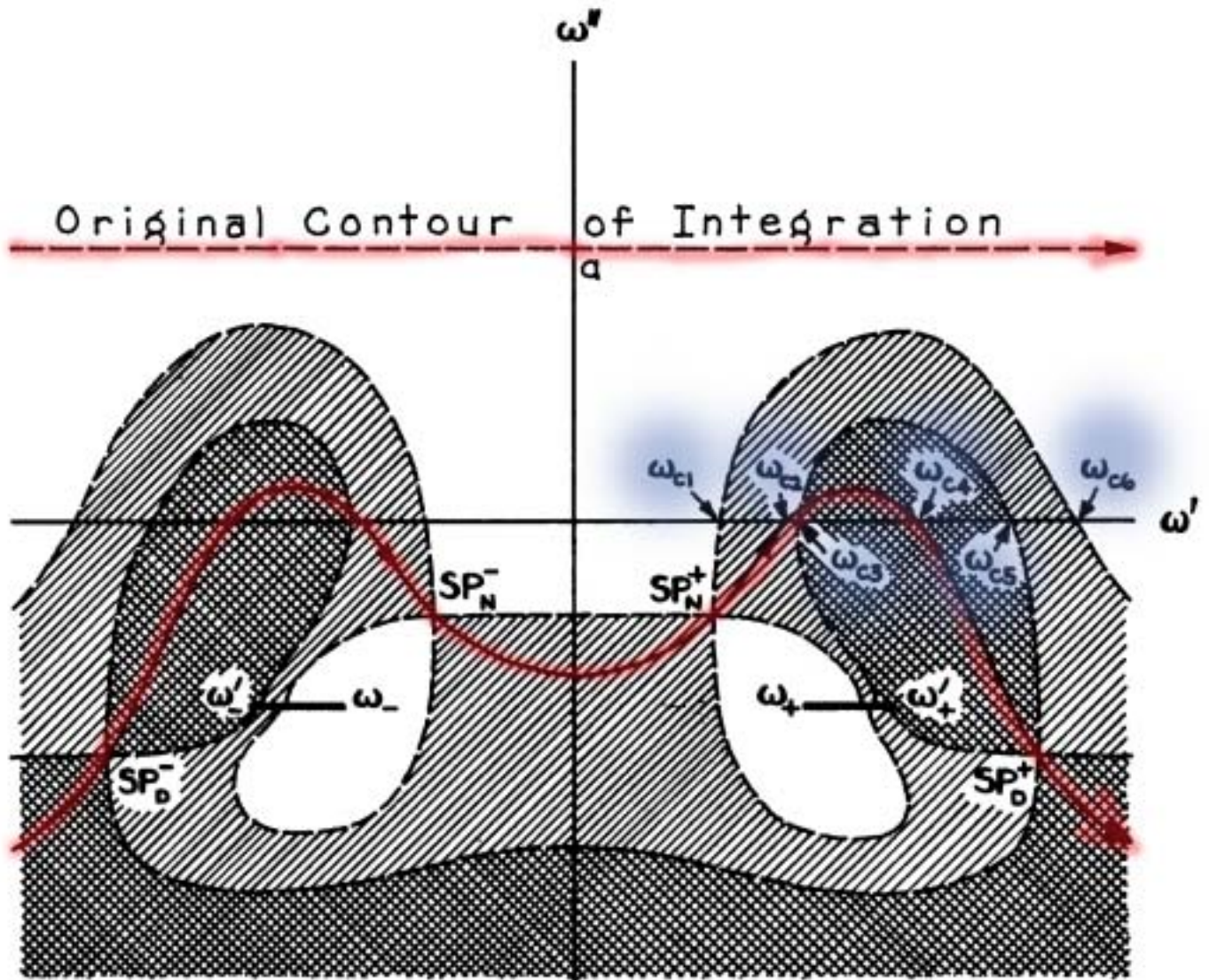
Near Saddle Point Dynamics ($\theta > \theta_1$)



Brillouin Precursor Evolution

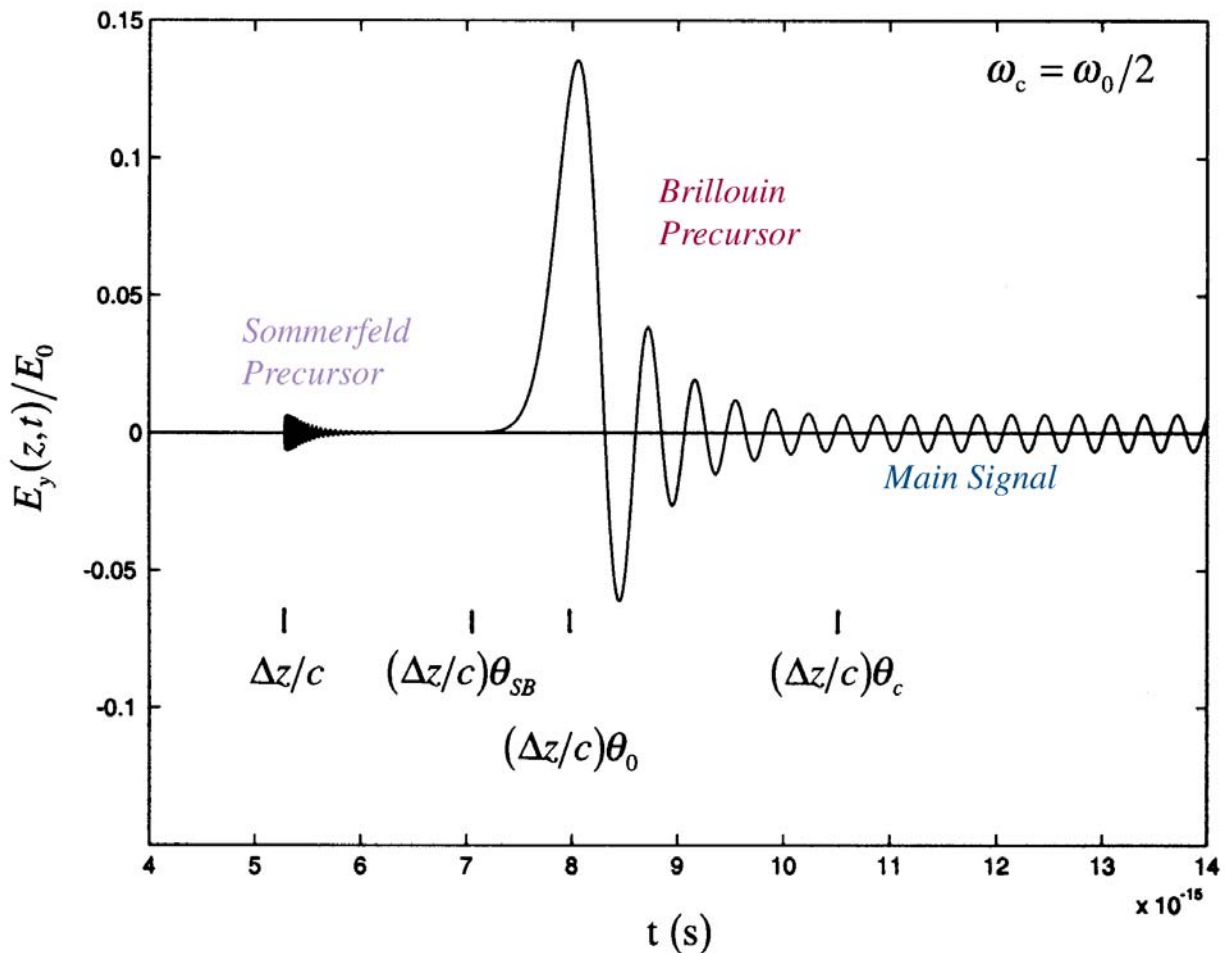


Pole Contribution & The Signal Arrival



Dispersive Signal Evolution (Oughstun & Sherman, *Electromagnetic Pulse Propagation in Causal Dielectrics*, Springer-Verlag, 1994).

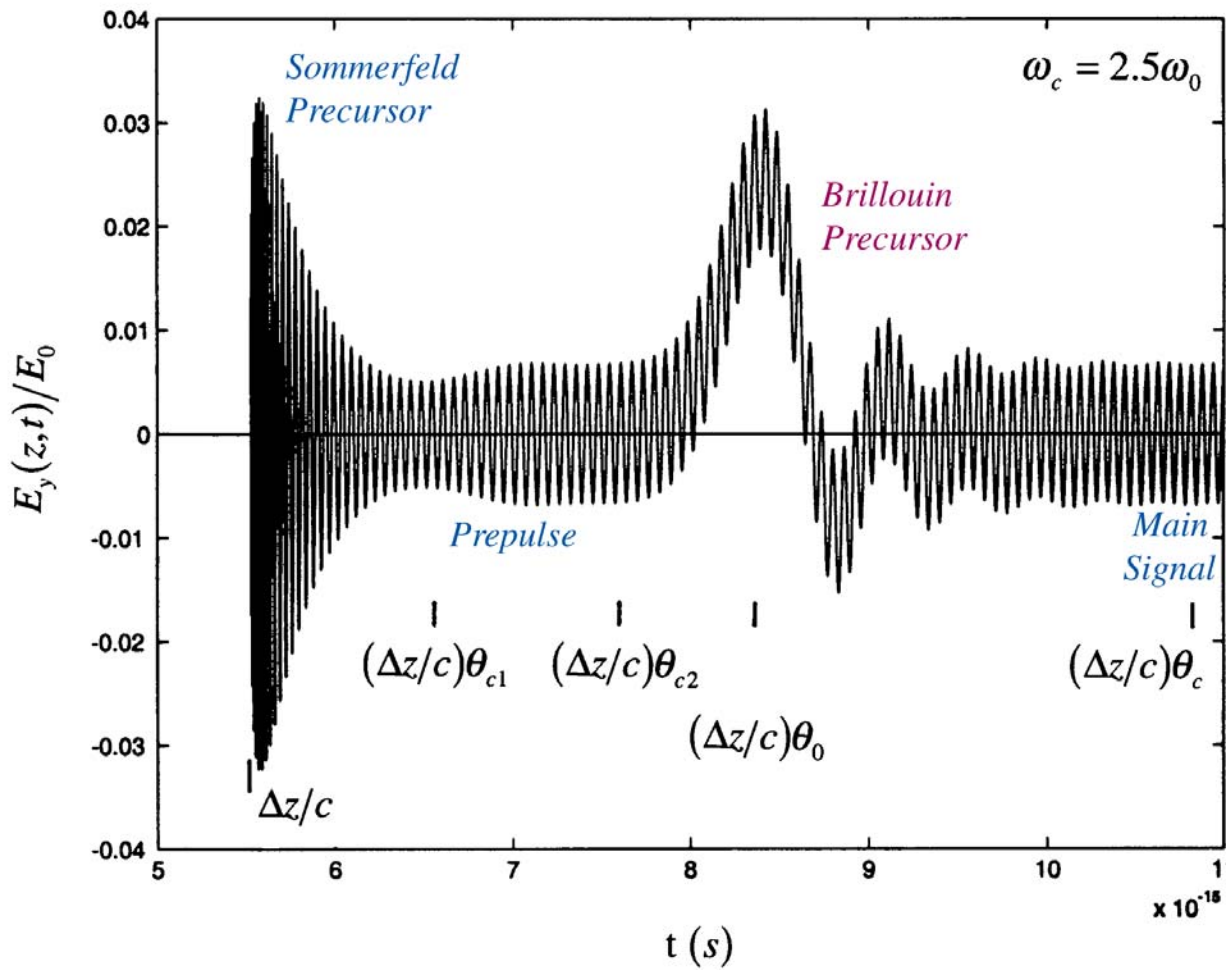
Case I $\omega_c < \omega_{SB}$ at 5 absorption depths into a single resonance Lorentz model dielectric



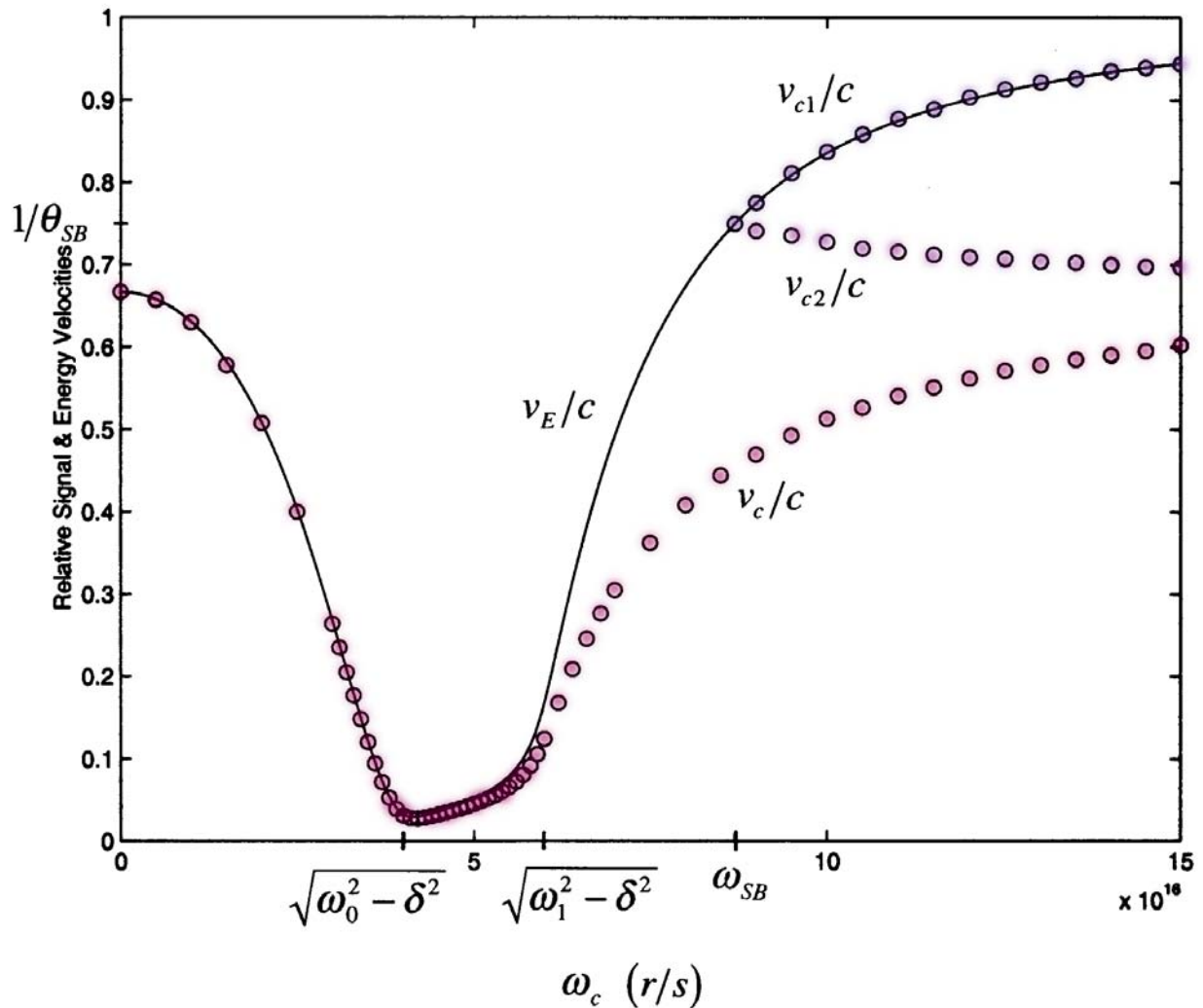
where

$$\omega_{SB} \approx \omega_0 \left(2 + b_0^2 / \omega_0^2 + 5\delta_0 / 3\omega_0^2 \right)^{1/2}$$

Case II $\omega_c > \omega_{SB}$ at 5 absorption depths into a single resonance Lorentz model dielectric

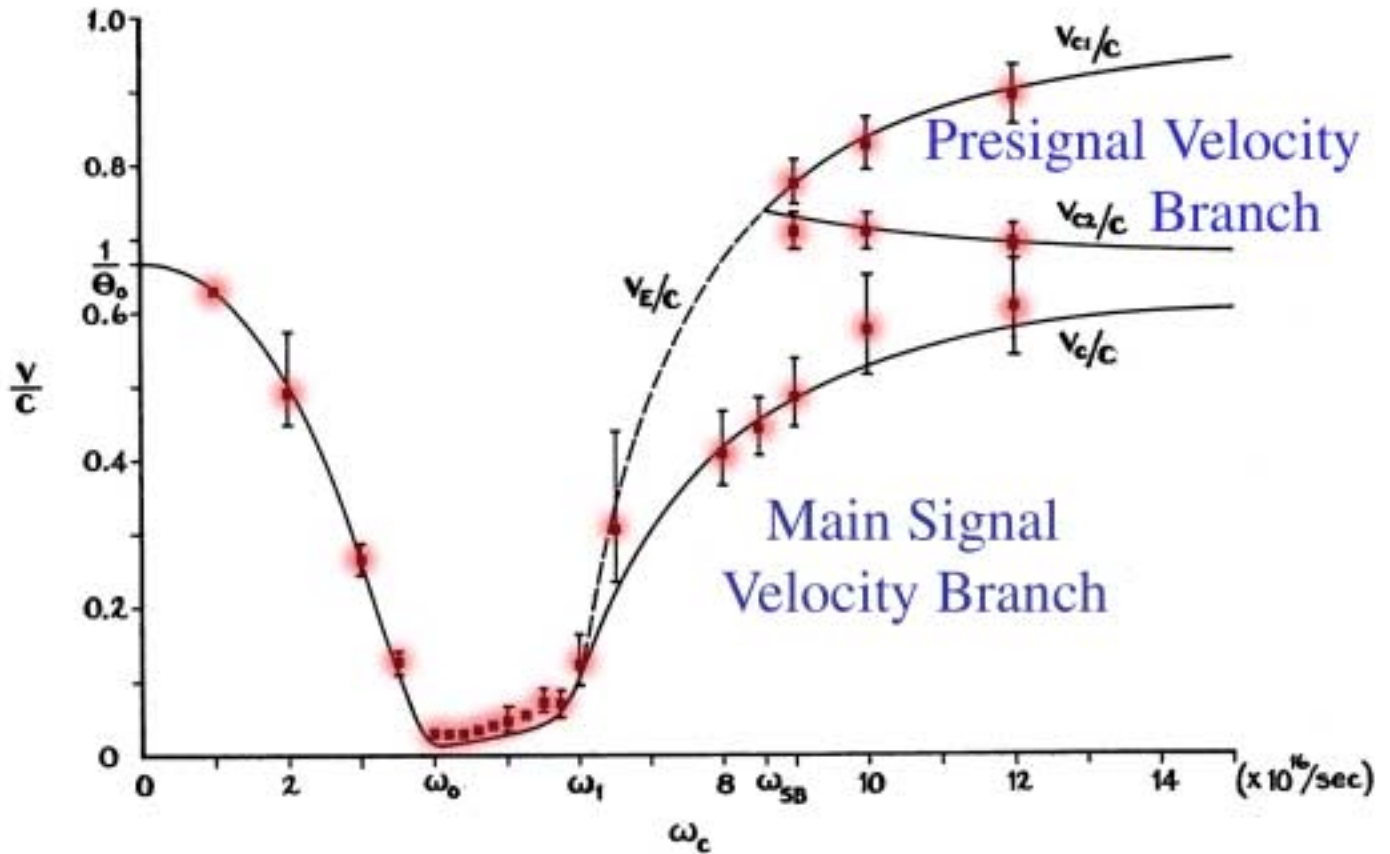


Signal & Energy Velocities in a Single Resonance Lorentz Model Dielectric



The signal velocity is the velocity at which information is transmitted through a dispersive material. It is always less than or equal to the speed of light c in vacuum and is bounded above by the energy transport velocity.

Signal & Energy Velocities



Oughstun, Wyns, & Foty, "Numerical Determination of the Signal Velocity in Dispersive Pulse Propagation," J. Opt. Soc. Am A 6, 1430 (1989).

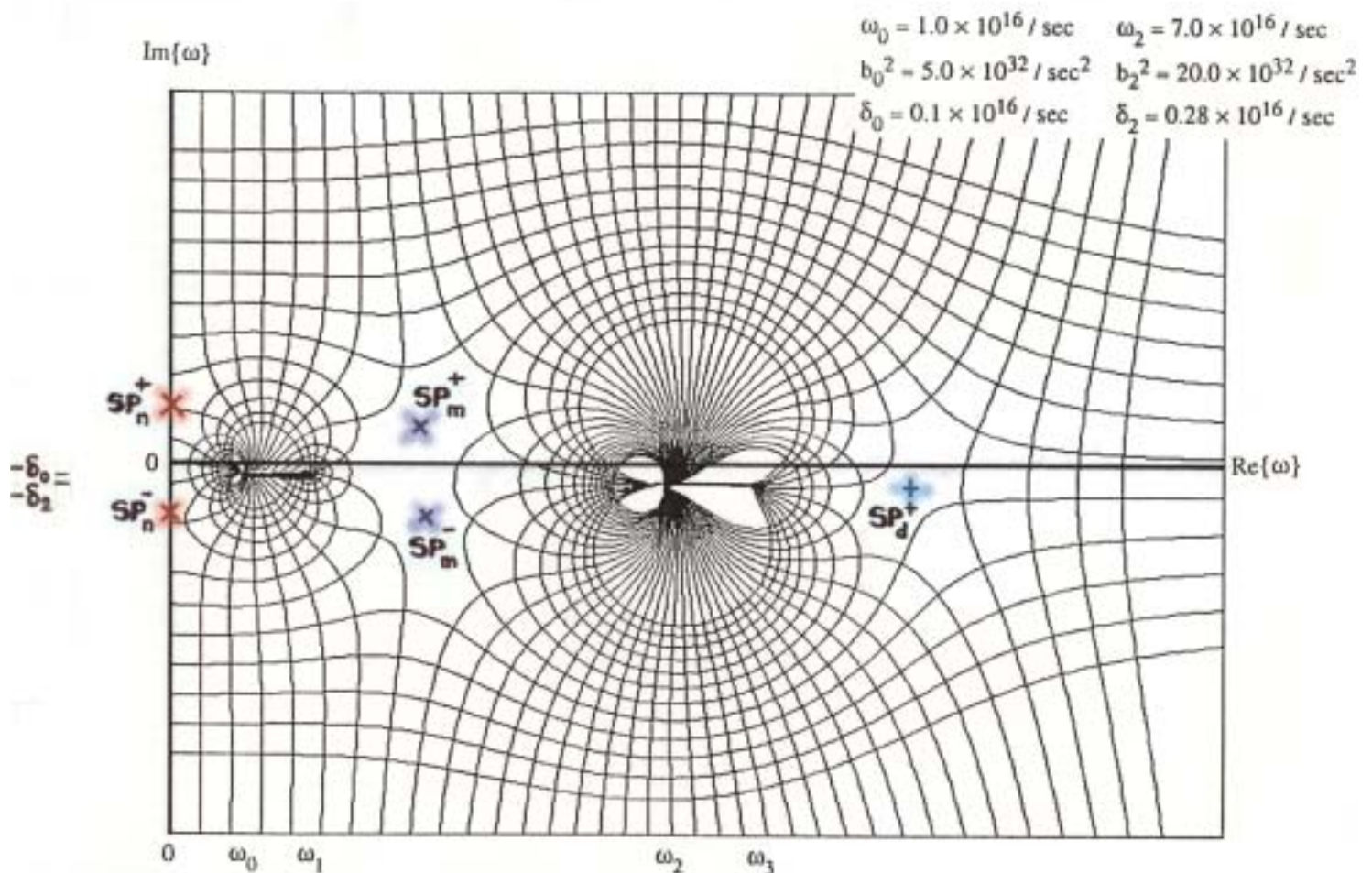
Sherman & Oughstun, "Energy-Velocity Description of Pulse Propagation in Absorbing, Dispersive Dielectrics," J. Opt. Soc. Am. B 12, 229 (1995).

Multiple Resonance Lorentz Model Dielectrics

Shen & Oughstun, *J. Opt. Soc. Am. B* 5, 2395-2398 (1988)

Laurens & Oughstun, *Ultra-Wideband, Short-Pulse Electromagnetics 4*, E. Heyman et al, eds., pp.243-264 (Plenum, New York, 1999)

Double Resonance Dielectric

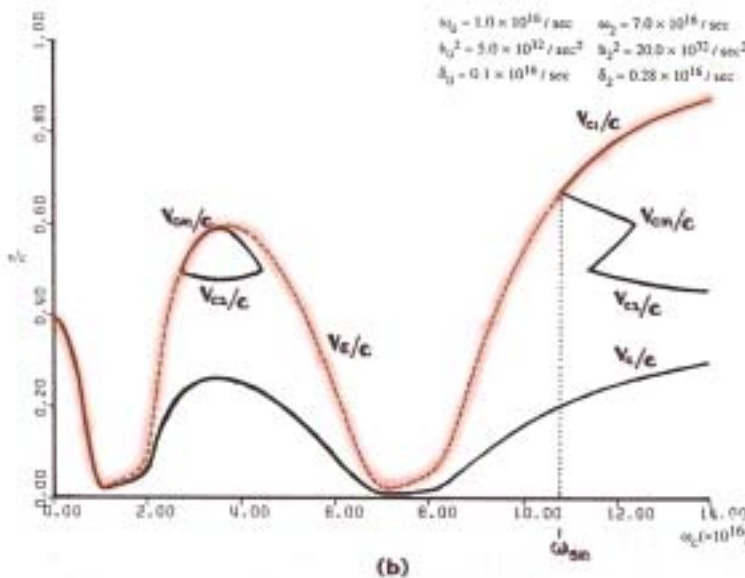
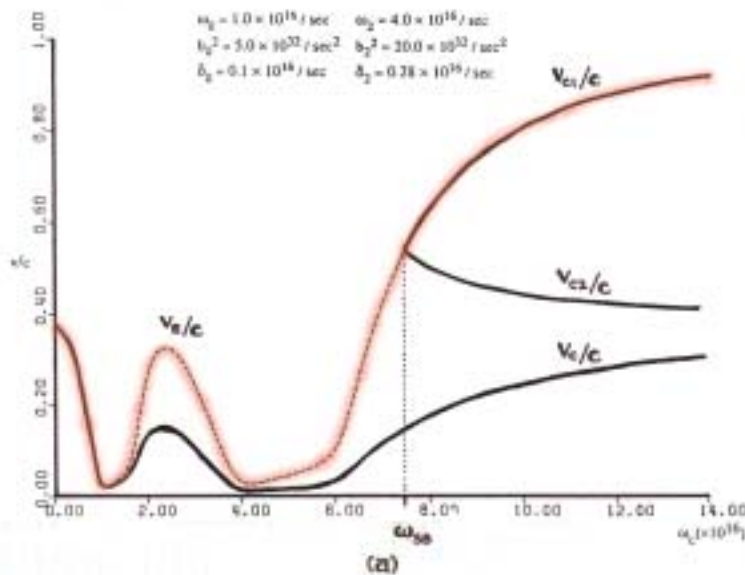


Each additional resonance line introduces two pairs of saddle points whose dynamical evolution in the complex ω -plane is bounded above by the nearest upper resonance structure. Whether or not these saddle points introduce a new precursor field is dependent upon the value of the local maximum in the energy velocity in that transmission band.

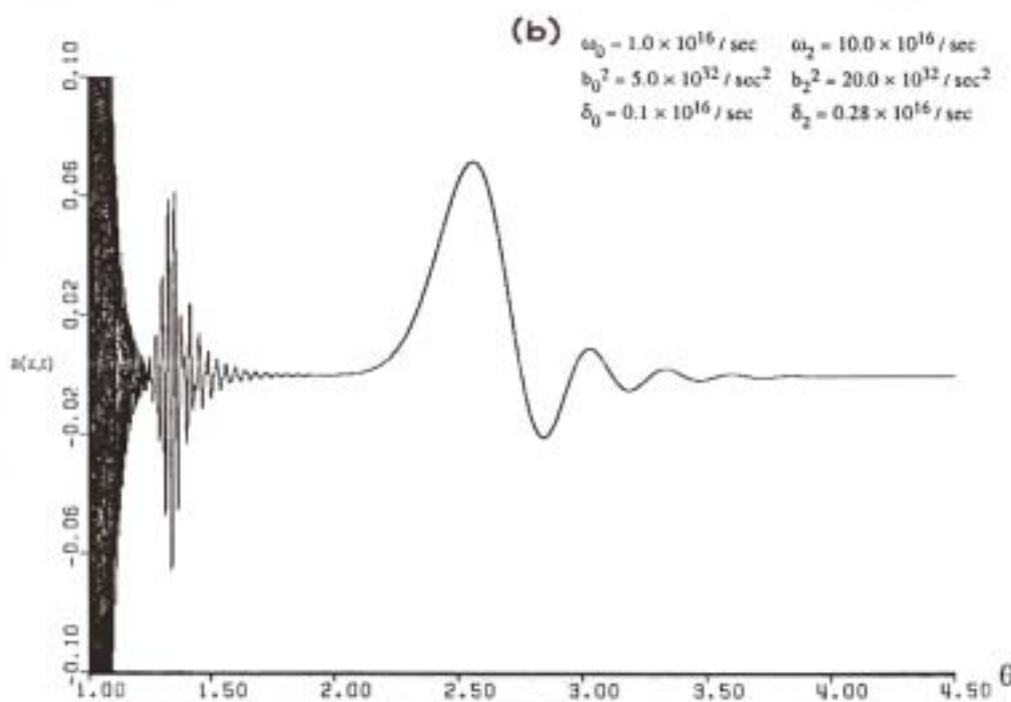
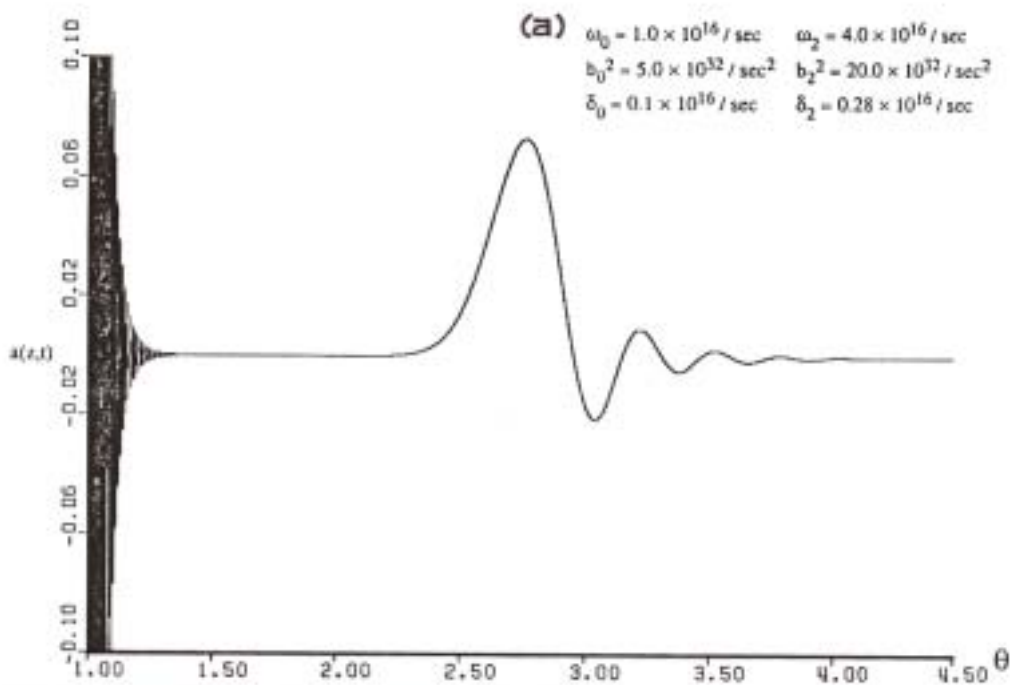
Theorem (Shen & Oughstun, 1988): *Let $\omega_j^{(\max)}$ denote the real frequency value in the j^{th} transmission band at which the energy velocity attains its' local maximum value $v_E(\omega_j^{(\max)})$ in that transmission band. If the inequality $v_E(\omega_j^{(\max)}) < v_E(0)$ is satisfied, where $v_E(0) = c/n(0) = c/\theta_0$, then the middle precursor field component $A_m^{(j)}(z, t)$ will be asymptotically negligible in comparison to the Sommerfeld and Brillouin precursors over the entire space-time evolution of the field. However, if the opposite inequality*

$$v_E(\omega_j^{(\max)}) > v_E(0)$$

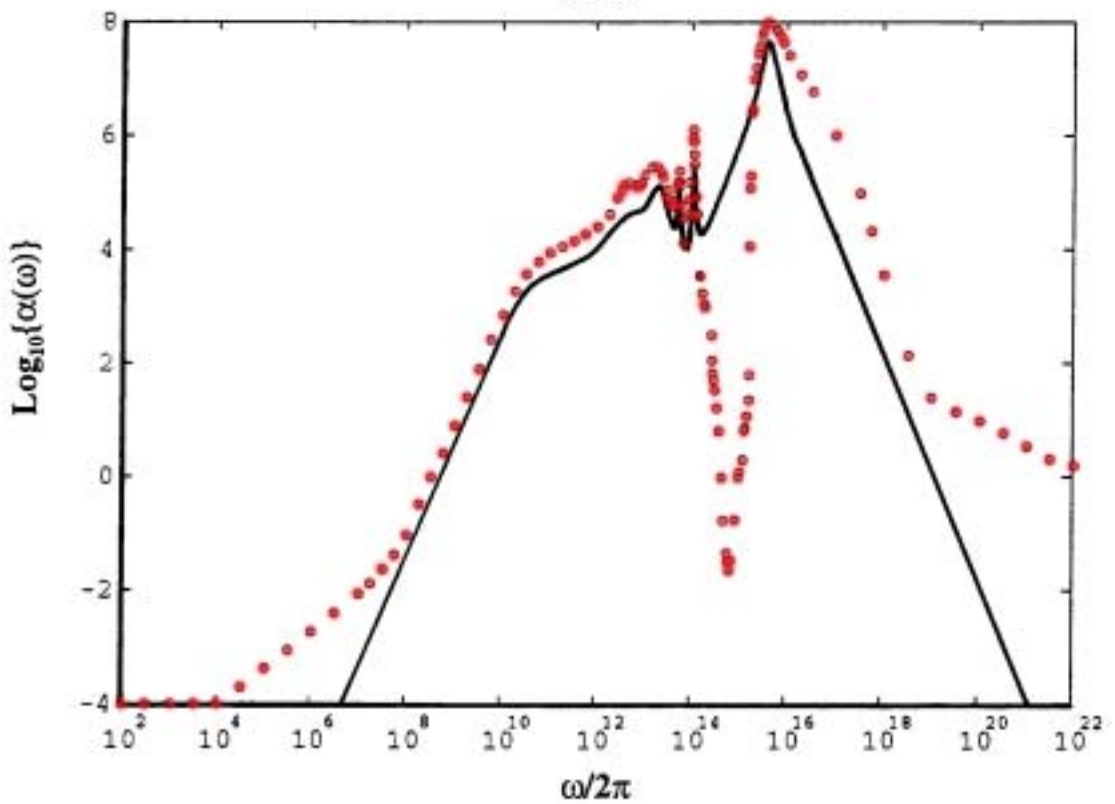
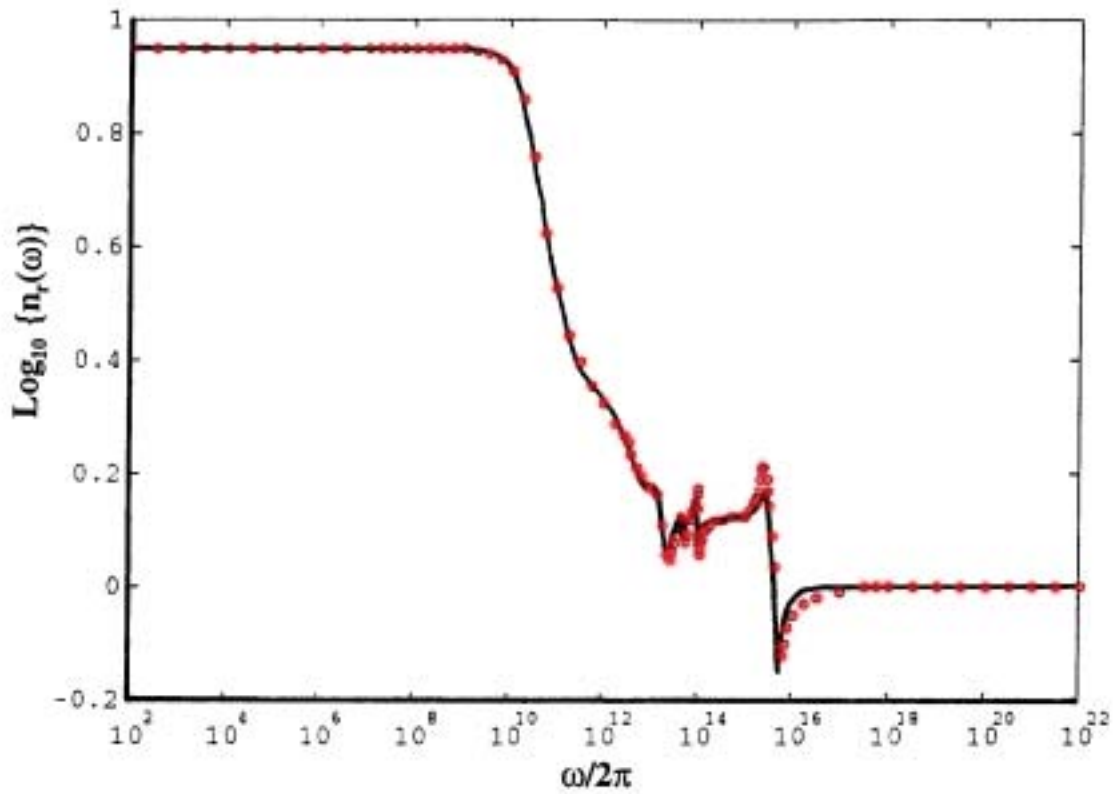
is satisfied, then the middle precursor field component $A_m^{(j)}(z,t)$ can become the asymptotically dominant contribution to the propagated field over some finite space-time interval in the field evolution.



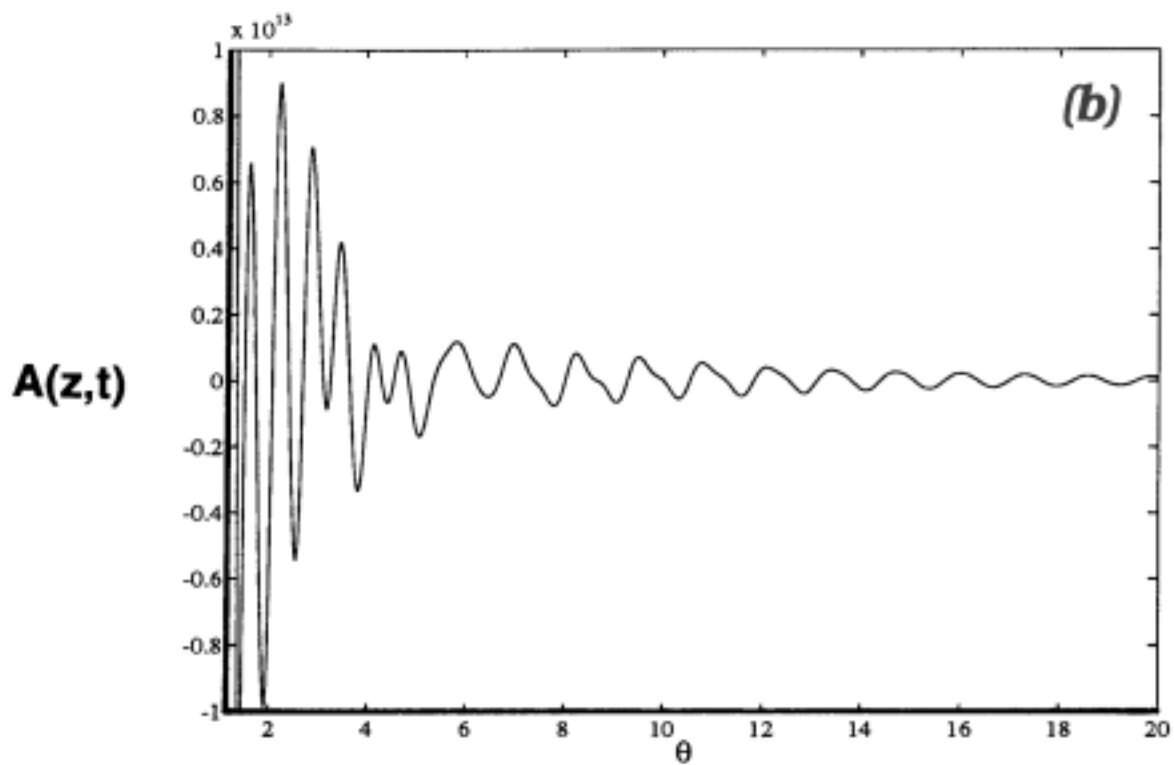
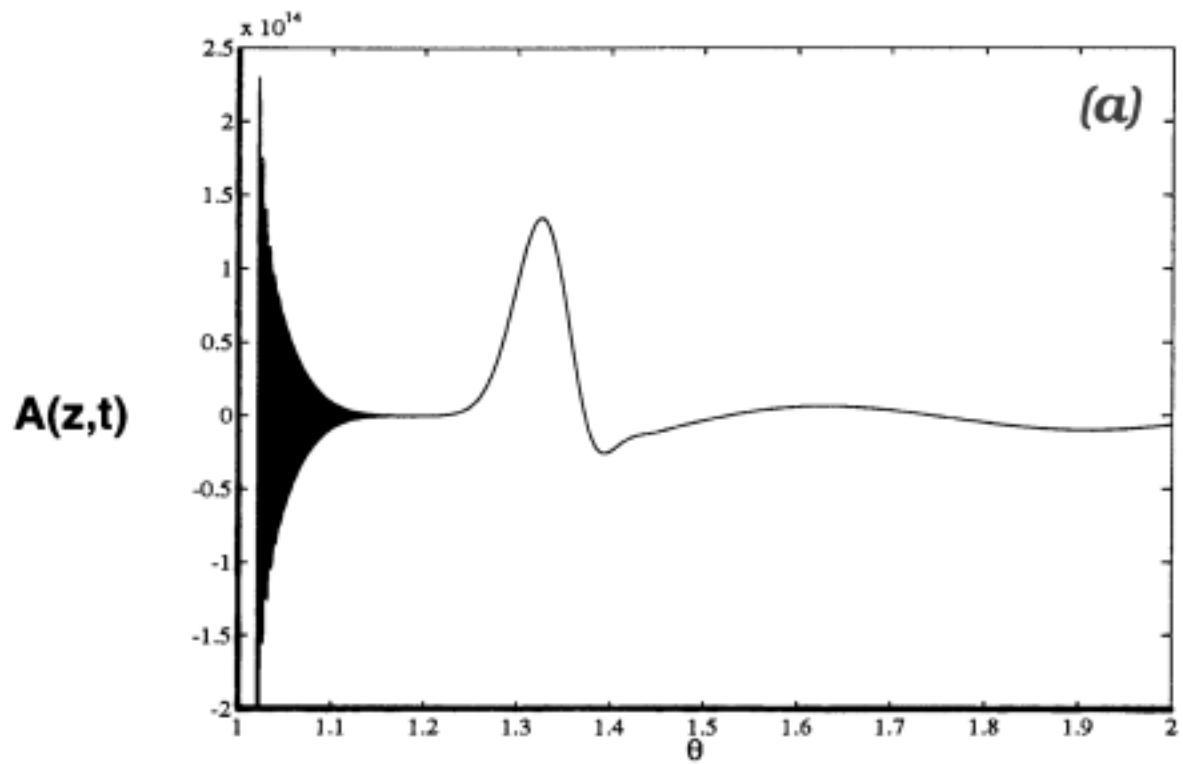
Impulse Response of a Double resonance Lorentz Model Dielectric (Shen & Oughstun 1988)



Triply-Distilled H₂O (*Laurens & Oughstun 1999*)



Impulse Response for Triply-Distilled H₂O



Uniform asymptotic description of ultrashort rectangular optical pulse propagation in a linear, causally dispersive medium

Kurt Edmund Oughstun*

Department of Computer Science and Electrical Engineering, University of Vermont, Burlington, Vermont 05405

George C. Sherman

Rocketdyne Division, MS FA40, Rockwell International Corporation, 6633 Canoga Avenue, Canoga Park, California 91303

(Received 10 October 1989)

The uniform asymptotic description of the propagation of an input rectangle-modulated harmonic signal of fixed angular frequency ω_c and initial pulse width T into the half-space $z > 0$ that is occupied by a single-resonance Lorentz medium is presented. The asymptotic description is developed by representing the input rectangular pulse as the difference between two Heaviside-unit-step-function-modulated signals that are separated in time by the initial pulse width T . This representation clearly shows that the resultant pulse distortion in the dispersive medium is primarily due to the Sommerfeld and Brillouin precursor fields that are associated with the leading and trailing edges of the input pulse. The dynamical pulse evolution with increasing propagation distance $z > 0$ is completely described for both long and very short initial pulse widths T . In both cases it is shown that the pulse distortion becomes severe when the propagation distance z is such that the precursor fields associated with the trailing edge of the pulse interfere with the precursor fields associated with the leading edge. Finally, the asymptotic theory clearly shows that the main body of the pulse propagates with the signal velocity in the dispersive medium.

I. INTRODUCTION

The classical theory of optical pulse propagation in a locally linear, homogeneous, isotropic, causally dispersive medium, as described by the Lorentz model, beginning with the seminal analysis of Sommerfeld¹ and Brillouin^{2,3} and continuing up to the modern asymptotic analysis of Oughstun and Sherman,⁴⁻⁶ has provided a complete, rigorous description of the dynamical field evolution for the two canonical problems of the input-unit-step-function-modulated signal of fixed carrier frequency ω_c and the input δ -function pulse. This analysis has focused on the complete precursor field evolution and the precise definition of the signal arrival and has led to a new physical description of dispersive pulse propagation⁷ in terms of the energy velocity and attenuation of time-harmonic waves that supplants the previous group-velocity description⁸⁻¹⁰ in the mature dispersion regime and reduces to it in the absence of absorption. The accuracy of this uniform asymptotic description in the mature dispersion regime has been completely verified through precise numerical simulations of both the Sommerfeld and Brillouin precursor field evolution¹¹ and the signal arrival¹² in a single-resonance Lorentz medium. The mature dispersion regime has been found¹² to include all propagation distances z that are greater than one absorption depth in the medium at the signal frequency. When this condition prevails, each quasimonochromatic component of the field propagates with its own characteristic velocity, which remains constant as the propagation continues. At each space-time point $\theta = ct/z$ the propagated field is then dominated by a single real frequency ω_E that is the

frequency of the time-harmonic field with the least attenuation that has an energy velocity^{13,14} equal to z/t , as described in Ref. 7.

The analysis of the present paper applies this modern asymptotic description to obtain a rigorous, uniformly valid description of rectangular pulse propagation in a single-resonance Lorentz medium in the mature dispersion regime. This approach does not rely upon any quasimonochromatic or slowly varying envelope approximation, as may be found in other descriptions,¹⁵⁻¹⁹ and so yields a canonical description of pulse dispersion phenomena that is completely valid for rapid rise-time pulses of arbitrary time duration. In addition, this approach does not depend upon any n th-order dispersion approximation that is central to other approaches,²⁰⁻²² so that it rigorously maintains the complete causality relations²³ that are critical to the proper analysis of linear dispersive pulse dynamics. It is only fair to point out that these other approaches are, in a broad sense, more general in that they are typically applicable to inhomogeneous media. However, what they gain in more general applicability they lose in complete rigor when considering the effects of dispersion on ultrashort pulse dynamics. For convenience, the notation employed in Refs. 5 and 6 is used throughout this paper.

The integral representation of the propagated plane-wave pulse in the half-space $z > 0$ is given by⁵

$$A(z, t) = \frac{1}{2\pi} \int_C \tilde{f}(\omega) e^{i(z/c)\theta(\omega, \theta)} d\omega, \quad (1.1)$$

where

$$\tilde{f}(\omega) = \int_{-\infty}^{\infty} f(t) e^{-i\omega t} dt \quad (1.2)$$

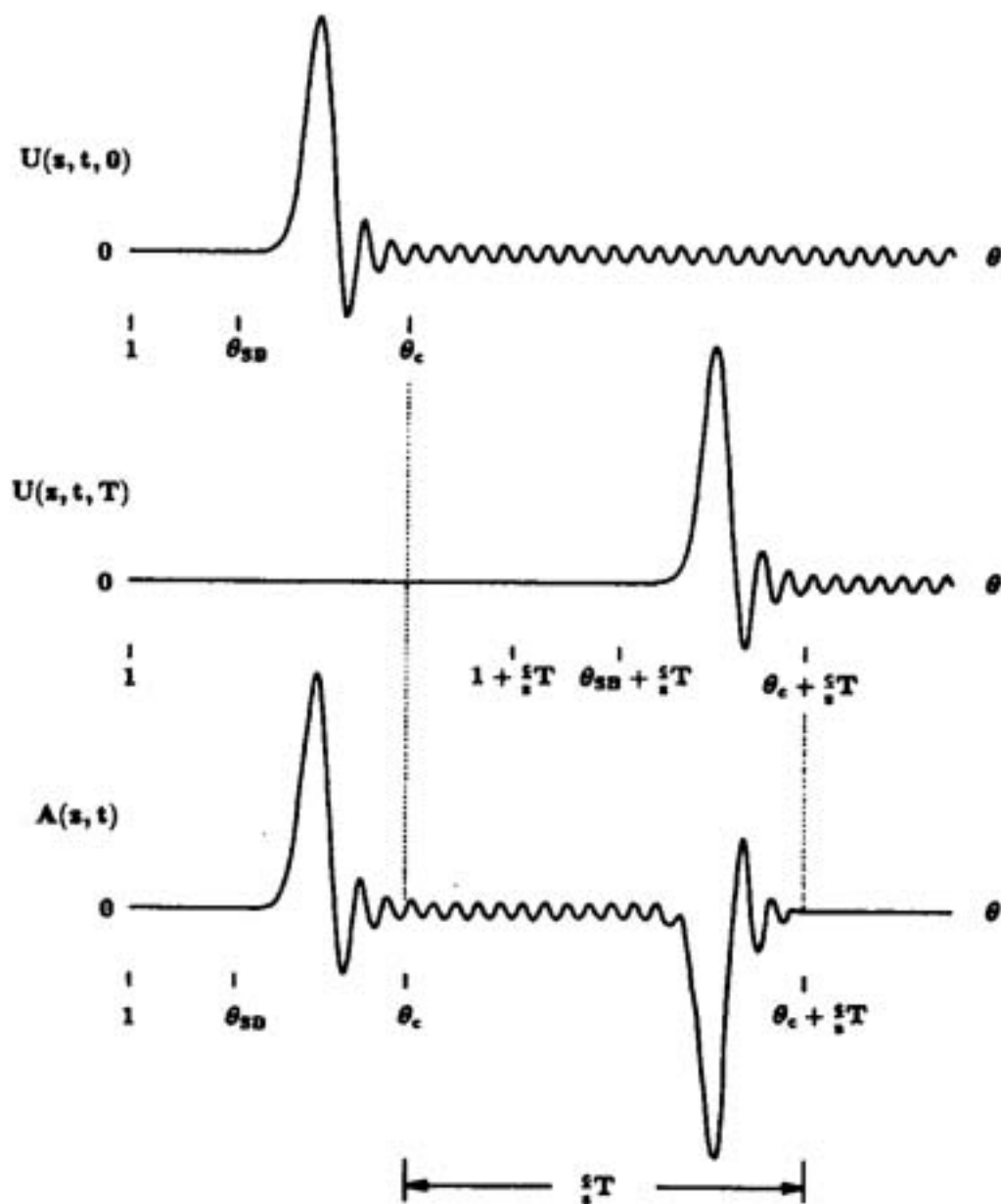


FIG. 12. Construction of the dynamical structure of the propagated field $A(z,t) = U(z,t,0) - U(z,t,T)$ in the below resonance signal frequency range $0 < \omega_c < \omega_0$ when $(c/z)T > \theta_c - 1$. When this situation prevails the interference between the precursor fields of the leading and trailing edges of the pulse is minimal and the resultant pulse distortion is also minimal.

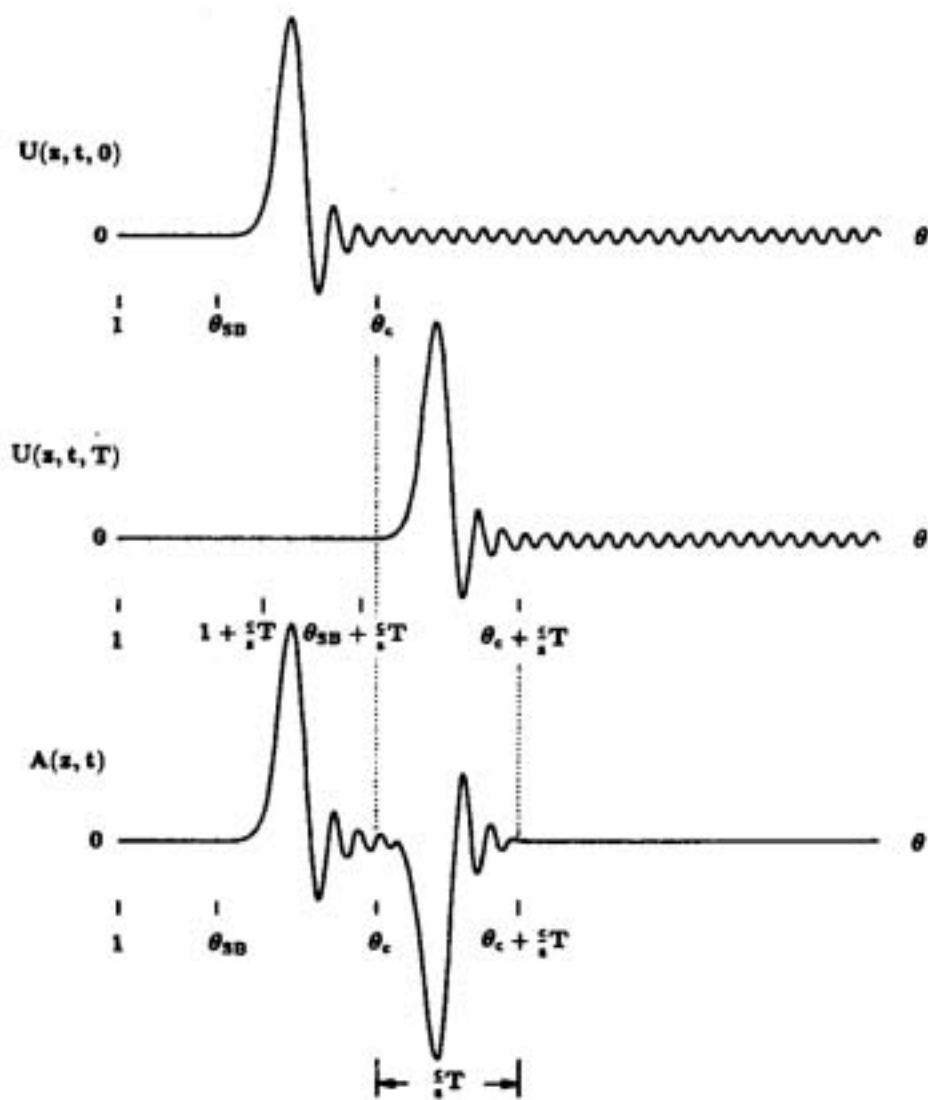


FIG. 13. Construction of the dynamical structure of the propagated field $A(z, t) = U(z, t, 0) - U(z, t, T)$ in the below resonance signal frequency range $0 < \omega_c < \omega_0$ when $\theta_c - 1 > (c/z)T > \theta_{SB} - 1$. When this situation prevails the interference between the precursor fields of the leading and trailing edges of the pulse is moderate and the resultant pulse distortion is also moderate.

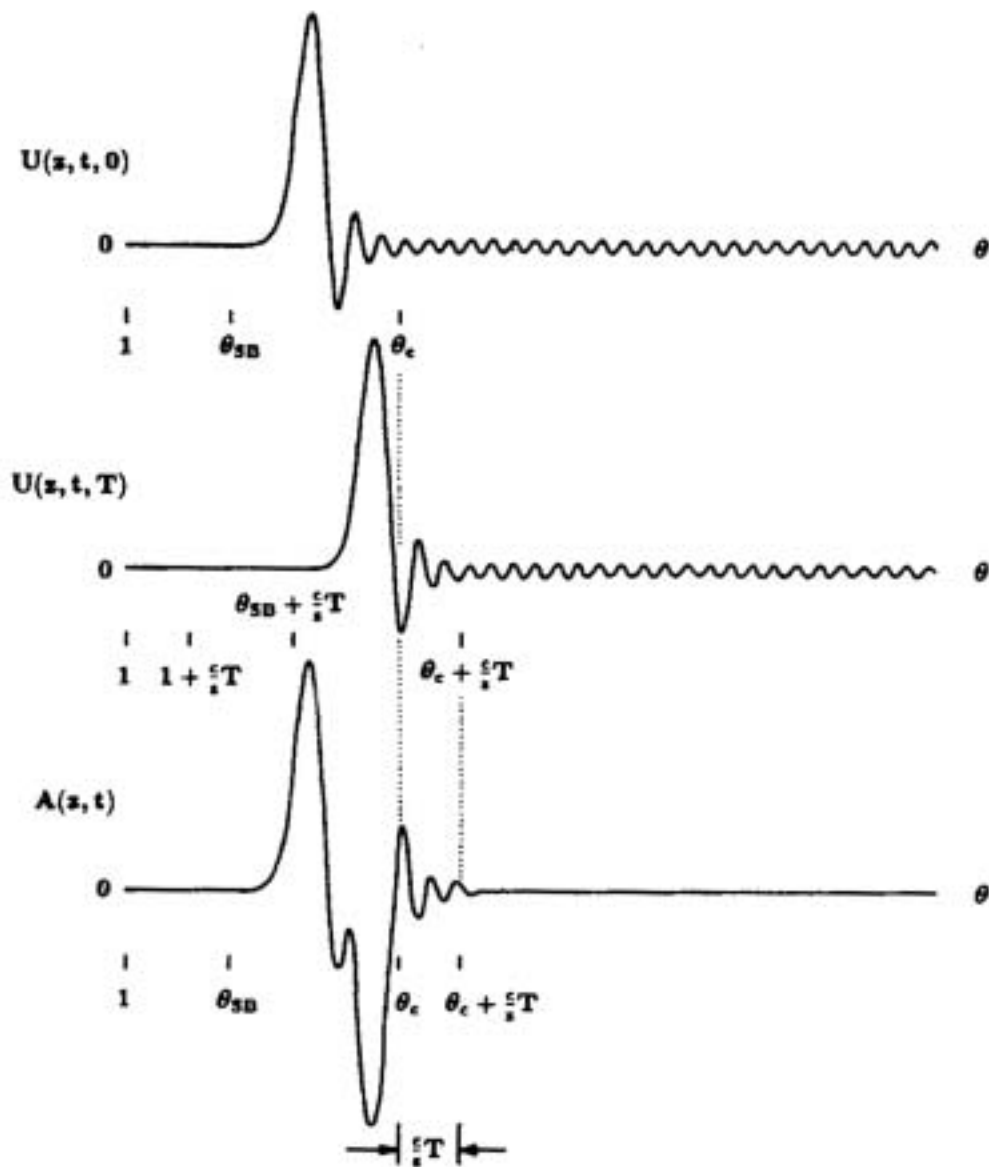


FIG. 14. Construction of the dynamical structure of the propagated field $A(z, t) = U(z, t, 0) - U(z, t, T)$ in the below resonance signal frequency range $0 < \omega_c < \omega_0$ when $(c/z)T \leq \theta_{SB} - 1$. When this situation prevails the interference between the precursor fields of the leading and trailing edges of the pulse is nearly complete and the resultant pulse distortion is severe.

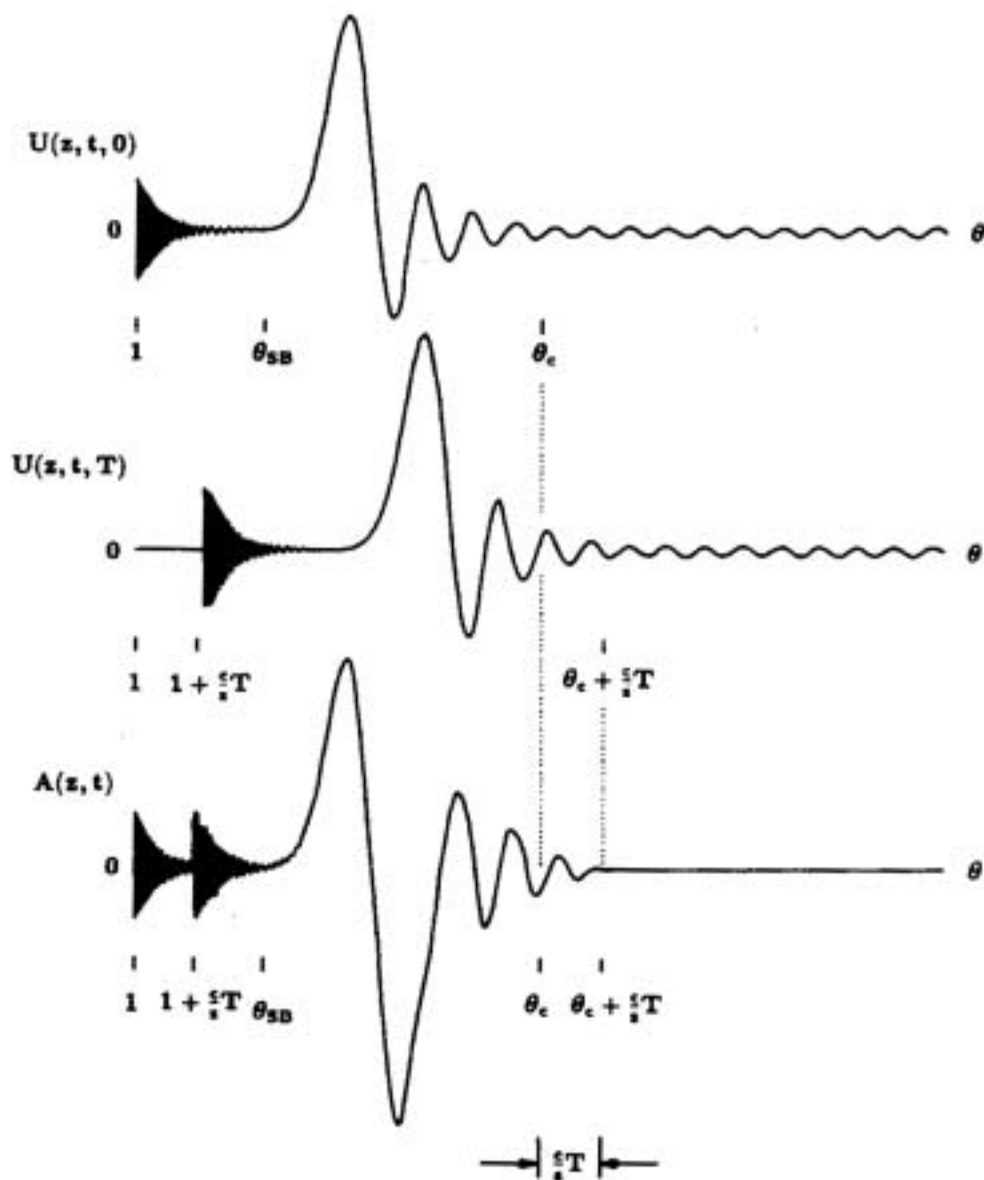


FIG. 15. Construction of the dynamical structure of the propagated field $A(z,t) = U(z,t,0) - U(z,t,T)$ for a near resonance signal frequency $\omega_c \in [\omega_0, \omega_1]$ when $(c/z)T \leq \theta_{SB} - 1$. When this situation prevails the interference between the precursor fields of the leading and trailing edges of the pulse is nearly complete and the resultant pulse distortion is severe.

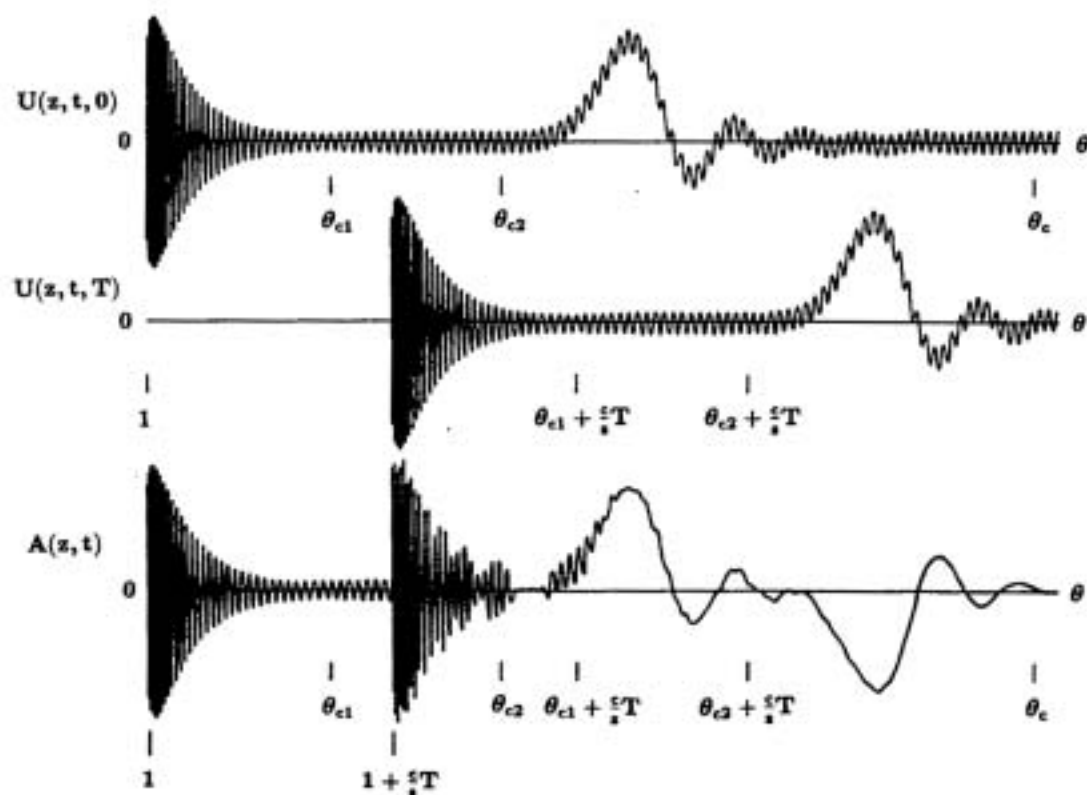


FIG. 16. Construction of the dynamical structure of the propagated field $A(z, t) = U(z, t, 0) - U(z, t, T)$ in the high signal frequency range $\omega_c > \omega_{yg} > \omega_0$ when $\theta_{c1} - 1 < (c/z)T < \theta_{c2} - 1$. When this situation prevails the interference between the precursor fields of the leading and trailing edges of the pulse is moderate to severe and the resultant pulse distortion is becoming severe.

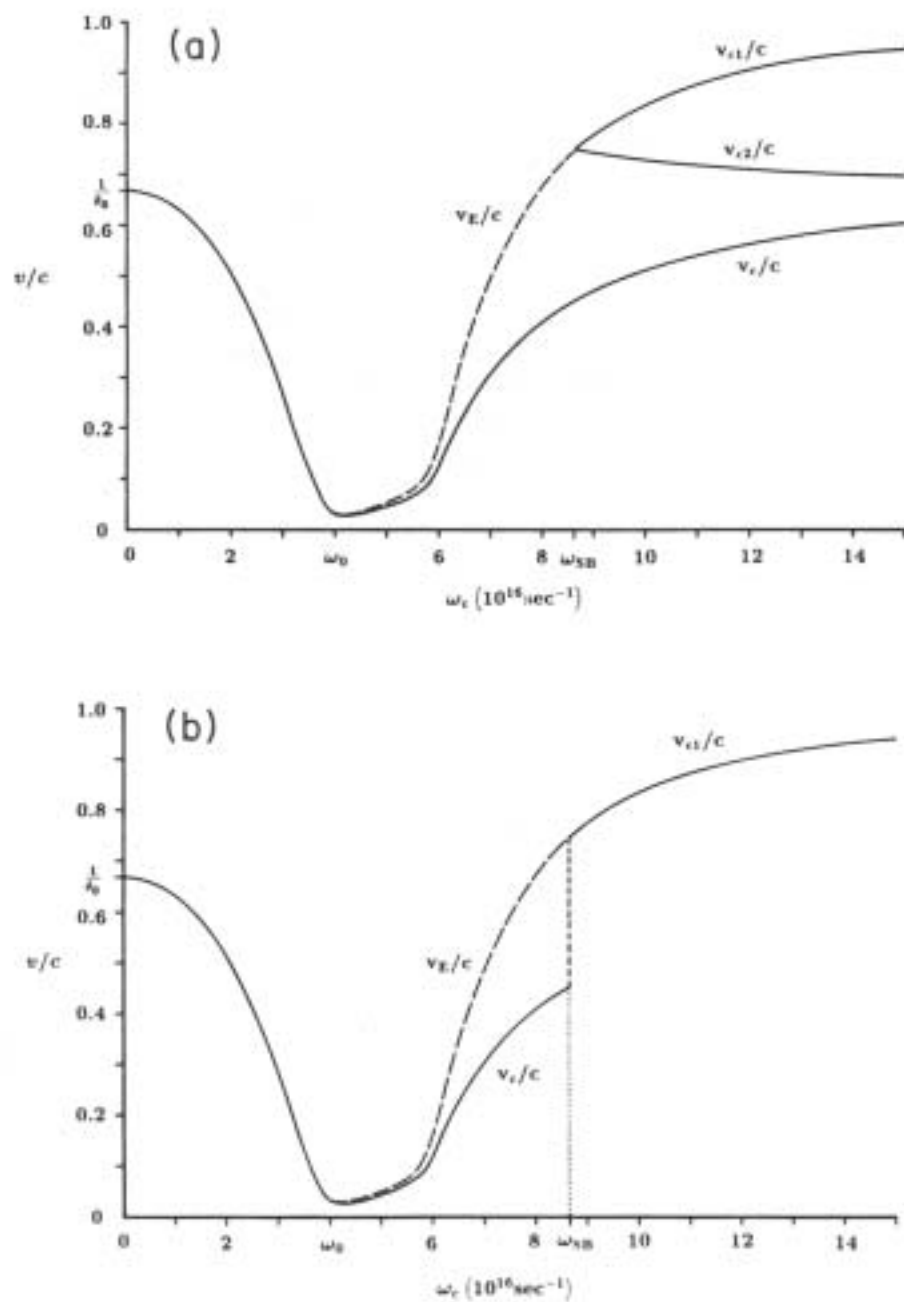


FIG. 11. Frequency dependence of (a) the main signal, anterior presignal, and posterior presignal velocities for a unit-step-function signal, and (b) the signal velocity for a rectangular pulse in a Lorentz medium with $\omega_0 = 4 \times 10^{16}/\text{sec}$, $b^2 = 20 \times 10^{12}/\text{sec}^2$, $\delta = 0.28 \times 10^{13}/\text{sec}$. The behavior of the energy-transport velocity for a strictly monochromatic field in the medium is indicated by the dashed curve in both figures.

Gaussian Pulse Propagation in a Dispersive, Absorbing Dielectric

Kurt E. Oughstun

College of Engineering & Mathematics, University of Vermont, Burlington, Vermont 05405

Constantinos M. Balicstis

Department of Computer Science & Electrical Engineering, University of Vermont, Burlington, Vermont 05405

(Received 28 March 1996)

The modified asymptotic description of dispersive Gaussian pulse propagation, which is uniformly valid in the initial pulse envelope width, is shown to reduce to the energy velocity description when the propagation distance becomes sufficiently large in a Lorentz model dielectric. This then resolves the apparent controversy between the modern asymptotic description upon which the energy velocity description is based and the classical group velocity description of Gaussian pulse propagation and related experimental results. [S0031-9007(96)01070-8]

PACS numbers: 42.25.Bs

The effects of frequency dispersion and absorption on the dynamical evolution of an electromagnetic pulse as it propagates through a homogeneous, isotropic, linear dielectric are properly described by asymptotic methods of analysis as originally investigated by Sommerfeld [1] and Brillouin [2] in 1914 using the method of steepest descents and improved upon and corrected by Oughstun and Sherman [3–5] using modern asymptotic expansion techniques [5]. This analysis clearly shows that after the pulse has propagated a sufficiently large distance into the medium its dynamics settle into a mature dispersion regime [5,6] in which the propagated field becomes locally quasimonochromatic with fixed local frequency, wavelength, and attenuation in each region of space that travels with its own characteristic velocity. The theory provides asymptotic expressions for the local wave properties at any given space-time point in the field domain. A physical explanation of these local wave properties was provided by Sherman and Oughstun [7] in 1981 with its entire proof just recently given [8]. In 1982, Chu and Wong [9] published experimental results for picosecond laser pulses propagating through thin samples of a linear dispersive dielectric whose peak absorption never exceeded 6 absorption lengths that were purported to disprove the energy velocity description while verifying the group velocity description. When combined with the Gaussian pulse results [10] of the modern asymptotic theory, the recently published modified asymptotic description [11,12] of Gaussian pulse propagation is found to provide the basis for a complete explanation of this apparent discrepancy.

Consider an input Gaussian envelope modulated harmonic wave of constant applied carrier frequency $\omega_c > 0$ and initial full pulse width $2T > 0$ that is centered about the time $t_0 > 0$ at the plane $z = 0$, given by

$$\begin{aligned} f(t) &= u(t) \sin(\omega_c t + \psi) \\ &= \exp\left\{-\left(\frac{t - t_0}{T}\right)^2\right\} \sin(\omega_c t + \psi), \end{aligned} \quad (1)$$

which is propagating in the positive z direction through a linear dielectric whose frequency dispersion is described by the single resonance Lorentz model with complex index of refraction

$$n(\omega) = \left(1 - \frac{b^2}{\omega^2 - \omega_0^2 + 2i\delta\omega}\right)^{1/2}, \quad (2)$$

which occupies the source-free half space $z \geq 0$. Here ω_0 is the undamped resonance frequency, b is the plasma frequency, and δ is the phenomenological damping constant of the dispersive, lossy dielectric. The integral representation of the propagated plane wave pulse in the half space $z \geq 0$ is given by

$$A(z, t) = \frac{1}{2\pi} \int_C \tilde{f}(\omega) \exp\left[\frac{z}{c} \phi(\omega, \theta)\right] d\omega, \quad (3)$$

where $\theta = ct/z$ is a dimensionless space-time parameter,

$$\phi(\omega, \theta) = i\omega[n(\omega) - \theta] \quad (4)$$

is the classical complex phase function, and where $\tilde{f}(\omega)$ is the temporal Fourier spectrum of the initial pulse $f(t) = A(0, t)$ at the input plane at $z = 0$. The spectral amplitude $\tilde{A}(z, \omega)$ of $A(z, t)$ satisfies the scalar Helmholtz equation $[\nabla^2 + \tilde{k}^2(\omega)]\tilde{A}(z, \omega) = 0$, with complex wave number $\tilde{k}(\omega) = \omega n(\omega)/c$.

From Eqs. (1) and (3), the classical integral representation of the propagated Gaussian envelope pulse is found as

$$A(z, t) = \frac{1}{2\pi} \mathfrak{N}\left\{i \int_C \tilde{u}(\omega - \omega_c) \exp\left[\frac{z}{c} \phi(\omega, \theta')\right] d\omega\right\}, \quad (5)$$

for $z \geq 0$, with the initial pulse spectrum

$$\tilde{u}(\omega) = \pi^{1/2} T \exp\left[-\frac{T^2}{4} \omega^2\right] \exp[-i(\omega_c t_0 + \psi)], \quad (6)$$

where $\theta' = \theta - ct_0/z$. The contour of integration C appearing here may be taken as any contour in the complex ω plane that is homotopic to the real frequency

axis. Since this spectrum is an entire function of ω , the propagated field has the asymptotic representation [10]

$$A(z, t) \sim A_S(z, t) + A_B(z, t), \quad (7)$$

as $z \rightarrow \infty$, with

$$A_j(z, t) = a_j \left(\frac{c}{2\pi z} \right)^{1/2} \mathfrak{N} \left\{ i \frac{\tilde{u}(\omega_{SP_j} - \omega_c)}{[-\phi^{(2)}(\omega_{SP_j}, \theta')]^{1/2}} \times \exp \left[\frac{z}{c} \phi(\omega_{SP_j}, \theta') \right] \right\} \quad (8)$$

for $j = S, B$. Here $a_S = 2$ and $\omega_{SP_j} = \omega_{SP_j}^+(\theta')$ denotes the distant first-order saddle point location of $\phi(\omega, \theta')$ in the right half of the complex ω plane for all $\theta' > 1$, while $a_B = 1$ for $1 < \theta' < \theta_1$ and $a_B = 2$ for $\theta_1 < \theta'$ where $\omega_{SP_B} = \omega_{SP_B}^+(\theta')$ denotes the near first-order saddle point location of $\phi(\omega, \theta')$ in the right half of the complex ω plane. Here $\theta_1 \equiv \theta_0 + 2\delta^2 b^2 / \theta_0 \omega_0^2 (3\omega_0^2 - 4\delta^2)$ denotes the space-time point at which the two near first-order saddle points coalesce into a single second-order saddle point, where $\theta_0 = n(0) = (1 + b^2/\omega_0^2)^{1/2}$ denotes the space-time point at which the upper near saddle point crosses the origin [3–5]. The nonuniform behavior exhibited in Eqs. (7) and (8) in any small neighborhood of the space-time point $\theta' = \theta_1$ may be corrected using uniform asymptotic expansion techniques [4,5]. The asymptotic contribution due to the near saddle points is referred to as a generalized Brillouin precursor field, while that due to the distant saddle points is referred to as a generalized Sommerfeld precursor field [10,11].

Because of the initial Gaussian envelope spectrum (6), the asymptotic description of each pulse component $A_S(z, t)$ and $A_B(z, t)$ contains a Gaussian amplitude factor of the form $\exp\{-(T/2)^2[\mathfrak{N}(\omega_{SP_j}) - \omega_c]^2\}$, $j = S, B$. In addition, each pulse component contains an exponential attenuation factor that is given by the product of the propagation distance z with the attenuation that is characteristic of the real phase behavior $\mathfrak{N}\{\phi(\omega_{SP_j})\}$ at the relevant saddle point, and the instantaneous oscillation frequency of each pulse component in the mature dispersion regime is approximately given by $\mathfrak{N}\{\omega_{SP_j}\}$ in the ultrashort pulse limit as $T \rightarrow 0$. Consequently, for a below resonance carrier frequency $\omega_c \in (0, \omega_0)$ the instantaneous oscillation frequency of the generalized Brillouin precursor $A_B(z, t)$ crosses ω_c as it chirps upward towards ω_0 , while for an above resonance carrier frequency $\omega_c \in (\omega_1, \infty)$ the instantaneous oscillation frequency of the generalized Sommerfeld precursor $A_S(z, t)$ crosses ω_c as it chirps downwards towards ω_1 , in each case the Gaussian amplitude factor peaking to unity when $\mathfrak{N}\{\omega_{SP_j}(\theta')\} = \omega_c$. For an intra-absorption band carrier frequency $\omega_c \in (\omega_0, \omega_1)$ the carrier frequency is never attained by either pulse component.

If the input signal frequency ω_c is within the absorption band of the medium, so that $\omega_0 \leq \omega_c \leq \omega_1$, then both pulse components $A_S(z, t)$ and $A_B(z, t)$ will be present in roughly equal proportion; the Brillouin precursor component $A_B(z, t)$ becomes more pronounced as ω_c is

decreased from ω_1 to ω_0 and dominates the propagated field evolution as ω_c is decreased below the medium resonance frequency, whereas the Sommerfeld precursor component $A_S(z, t)$ becomes more pronounced as ω_c is increased from ω_0 to ω_1 and dominates the propagated field evolution as ω_c is increased above ω_1 . The numerically determined dynamical field evolution, due to an input ultrashort Gaussian pulse with initial pulse width $2T = 0.2$ fsec and carrier frequency $\omega_c = 5.75 \times 10^{16} \text{ sec}^{-1}$ that is near the upper end of the absorption band of a single resonance Lorentz medium with parameters $\omega_0 = 4 \times 10^{16} \text{ sec}^{-1}$, $b^2 = 20 \times 10^{32} \text{ sec}^{-2}$, and $\delta = 0.28 \times 10^{16} \text{ sec}^{-1}$, is illustrated in Fig. 1. This case is of particular interest since the group velocity at this signal frequency is very nearly equal to the speed of light c in vacuum. The generalized Sommerfeld precursor pulse component is seen to first emerge in the propagated field structure as the propagation distance increases into the mature dispersion regime, its peak amplitude propagating with a velocity just below c ; notice that the smallest propagation distance considered is nearly 21 absorption depths into the medium at this intra-absorption band carrier frequency. As the propagation distance increases, the generalized Brillouin precursor pulse component emerges, its peak amplitude propagating with a velocity that approaches the value $c/\theta_0 = c/n(0)$ from above. The propagated field due to an input ultrashort Gaussian pulse then separates into two distinct pulse components that propagate with different peak velocities, the faster pulse component being the high-frequency generalized Sommerfeld precursor whose instantaneous oscillation frequency $\omega_s(\theta)$ chirps downward towards ω_1 , followed by the slower, low-frequency generalized Brillouin precursor whose instantaneous oscillation frequency $\omega_B(\theta)$ chirps upward towards ω_0 . Each feature of this dynamical field evolution is properly described by the energy velocity description of Refs. [7,8].

As the initial pulse width $2T$ is increased, the asymptotic approximation (7) and (8) of the propagated field evolution remains qualitatively correct, while its quantitative accuracy decreases at a fixed propagation distance. This asymptotic description will remain quantitatively accurate as the pulse width is increased provided that the propagation distance is allowed to increase, in keeping with the definition of an asymptotic expansion in Poincaré's sense [13] as $z \rightarrow \infty$. However, since the medium is attenuative, the usefulness of this description decreases as $2T$ increases, since the important features of the field evolution (particularly when compared to experimental observations) are typically observed at some fixed observation distance in the medium.

The classical integral representation (5) with the spectrum (6) may be rearranged so as to yield the modified integral representation [12]

$$A(z, t) = \frac{1}{2\pi} \mathfrak{N} \left\{ i \int_C \tilde{U}_M \exp \left[\frac{z}{c} \Phi_M(\omega, \theta') \right] d\omega \right\} \quad (9)$$

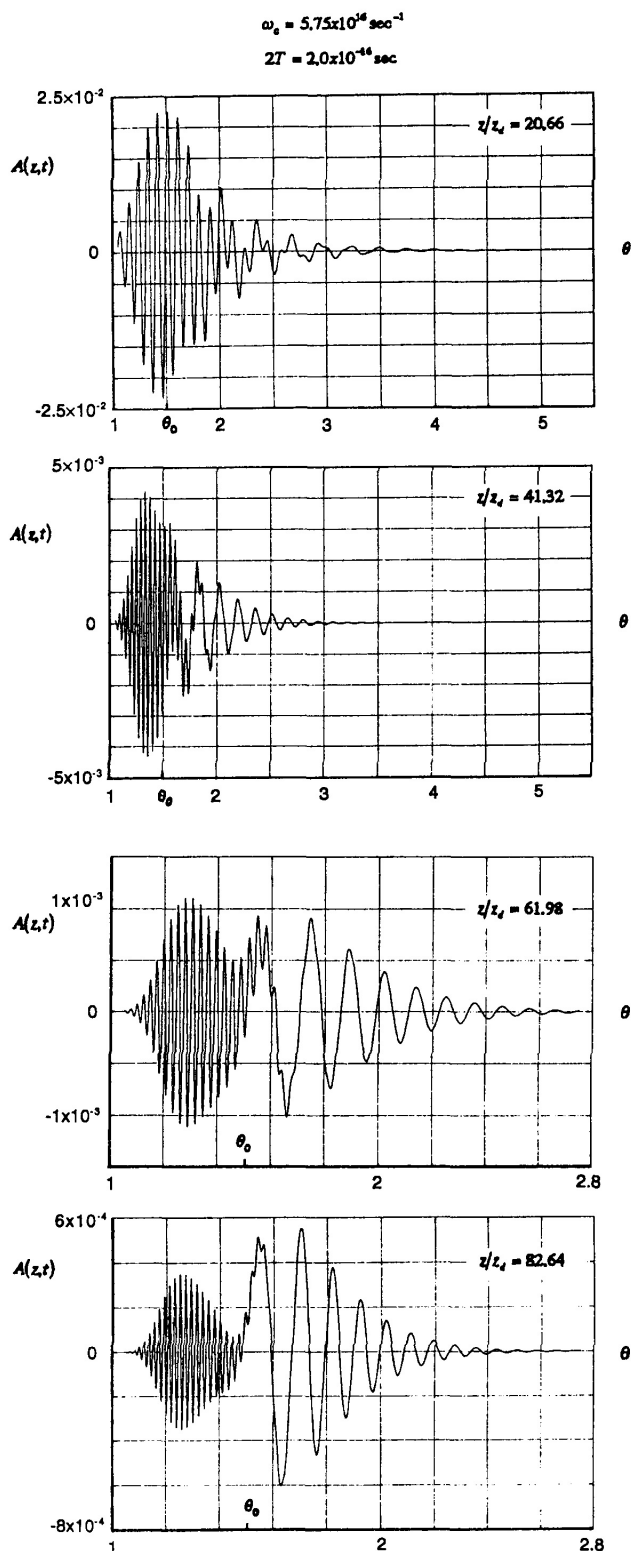


FIG. 1. Numerically determined dynamical field evolution of an input 0.2 fsec Gaussian pulse with intra-absorption band carrier frequency $\omega_c = 5.75 \times 10^{16} \text{ sec}^{-1}$ in a single resonance Lorentz model dielectric.

for all $z \geq 0$, where the modified spectral amplitude function

$$\tilde{U}_M = \pi^{1/2} T \exp[-i(\omega_c t_0 + \psi)] \quad (10)$$

is independent of the angular frequency ω , and where

$$\Phi_M(\omega, \theta') = \phi(\omega, \theta') - \frac{cT^2}{4z} (\omega - \omega_c)^2 \quad (11)$$

is the modified complex phase function. In the ultrashort pulse limit, as $2T \rightarrow 0$, the modified phase function reduces to the classical phase function $\phi(\omega, \theta')$ and the asymptotic behavior of (9) is determined by the behavior about the saddle points of $\phi(\omega, \theta')$, as in Eqs. (7) and (8). Hence, if the classical asymptotic description given in Eqs. (7) and (8) is valid (to some specific degree of accuracy) for some given input pulse width $2T$ at a given propagation distance z , then this description will remain equally valid (to that same degree of accuracy) as the initial pulse width is increased provided that z is also increased in such a manner that the ratio T^2/z remains fixed.

The saddle point dynamics of the modified phase function are now dependent upon both the initial pulse width and the propagation distance, as well as upon the dimensionless space-time parameter θ' . These saddle points are found [12] to remain isolated from each other for all θ' when $T \neq 0$ and are each of first order. Only two of these saddle points are found [12] to contribute to the asymptotic behavior of the modified integral representation (9) as $z \rightarrow \infty$, so that the propagated field has the same asymptotic representation given in Eq. (7) with

$$A_j(z, t) = \left(\frac{c}{2\pi z}\right)^{1/2} \Re \left\{ i \frac{\tilde{U}_M}{[-\Phi_M^{(2)}(\omega_j, \theta')]^{1/2}} \times \exp\left[\frac{z}{c} \Phi_M(\omega_j, \theta')\right] \right\} \quad (12)$$

for $j = S, B$. Here ω_j denotes the modified distant ($j = S$) and near ($j = B$) saddle-point locations in the right half of the complex ω plane whose dynamics are described in Ref. [12]. Each pulse component $A_j(z, t)$, $j = S, B$, contains a Gaussian amplitude factor, the peak amplitude point of each pulse component propagating at the classical group velocity evaluated at the instantaneous oscillation frequency of the field at the space-time point.

The dispersive action of the same Lorentz model dielectric on an input 5 fsec Gaussian pulse, whose carrier frequency $\omega_c = 5.625 \times 10^{16} \text{ sec}^{-1}$ is just below the upper end of the medium absorption band, produces a superluminal velocity of the peak in the envelope of the propagated field at a sufficiently small propagation distance, as indicated in Fig. 2 by data point 1. The envelope peak in the propagated field at this propagation distance (19.96 absorption depths at ω_c) has the associated instantaneous frequency $\omega_{ps} \cong 5.71 \times 10^{16} \text{ sec}^{-1}$, and it propagates with the classical group velocity $v_{ps} = v_g(\omega_{ps}) \cong 1.16c$. This same envelope peak slows down to a subluminal velocity as the propagation distance increases (data point 2) because the instantaneous oscillation frequency of this peak amplitude point increases as the propagation distance increases. The envelope peak in the propagated field at this propagation distance (49.91 absorption depths at ω_c)

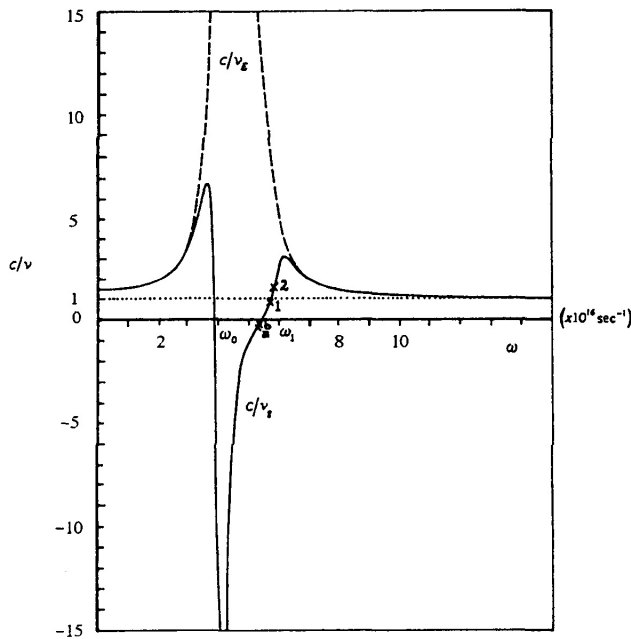


FIG. 2. Inverse relative velocity of propagation of the peak amplitude point of the propagated field due to an input Gaussian pulse (data points 1,2 and a, b). The solid curve describes the frequency dependence of the inverse relative group velocity $c/v_g(\omega_{pk})$ evaluated at the instantaneous oscillation frequency ω_{pk} of the peak amplitude point of the propagated pulse component $A_k(z, t)$, while the dashed curve in the figure describes the frequency dependence of the inverse relative energy velocity $c/v_E(\omega_{pk})$ of a monochromatic field of angular frequency ω_{pk} .

has shifted to the higher instantaneous oscillation frequency $\omega_{ps} \cong 5.83 \times 10^{16} \text{ sec}^{-1}$, and it now propagates with the classical group velocity $v_{ps} = v_g(\omega_{ps}) \cong 0.65c$. Thus, as the propagation distance increases, the instantaneous oscillation frequency evolves out of the absorption band and the pulse dynamics evolve toward the energy velocity description which is valid in the mature dispersion regime.

Negative velocity motions of the amplitude peak are obtained from the modified asymptotic description [12] for an input 10 fsec Gaussian pulse with applied carrier frequency $\omega_c = 5.25 \times 10^{16} \text{ sec}^{-1}$, as indicated by data points a and b in Fig. 2. At the smallest propagation distance considered (58.05 absorption depths at ω_c) the envelope peak of the propagated pulse has the associated instantaneous oscillation frequency $\omega_{ps} \cong 5.29 \times 10^{16} \text{ sec}^{-1} > \omega_c$ and propagates with the classical group velocity $v_{ps} = v_g(\omega_{ps}) \cong -2.86c$. As the propagation distance is increased to 145.13 absorption depths, the instantaneous oscillation frequency at the envelope peak has shifted to the higher frequency value $\omega_{ps} \cong 5.35 \times 10^{16} \text{ sec}^{-1}$ and the envelope peak now propagates with the classical group velocity $v_{ps} = v_g(\omega_{ps}) \cong -4.45c$. The modified asymptotic description then shows that, as the propagation distance increases, the low-frequency components that are present in the input pulse spectrum are attenuated at a larger rate than are the high-frequency

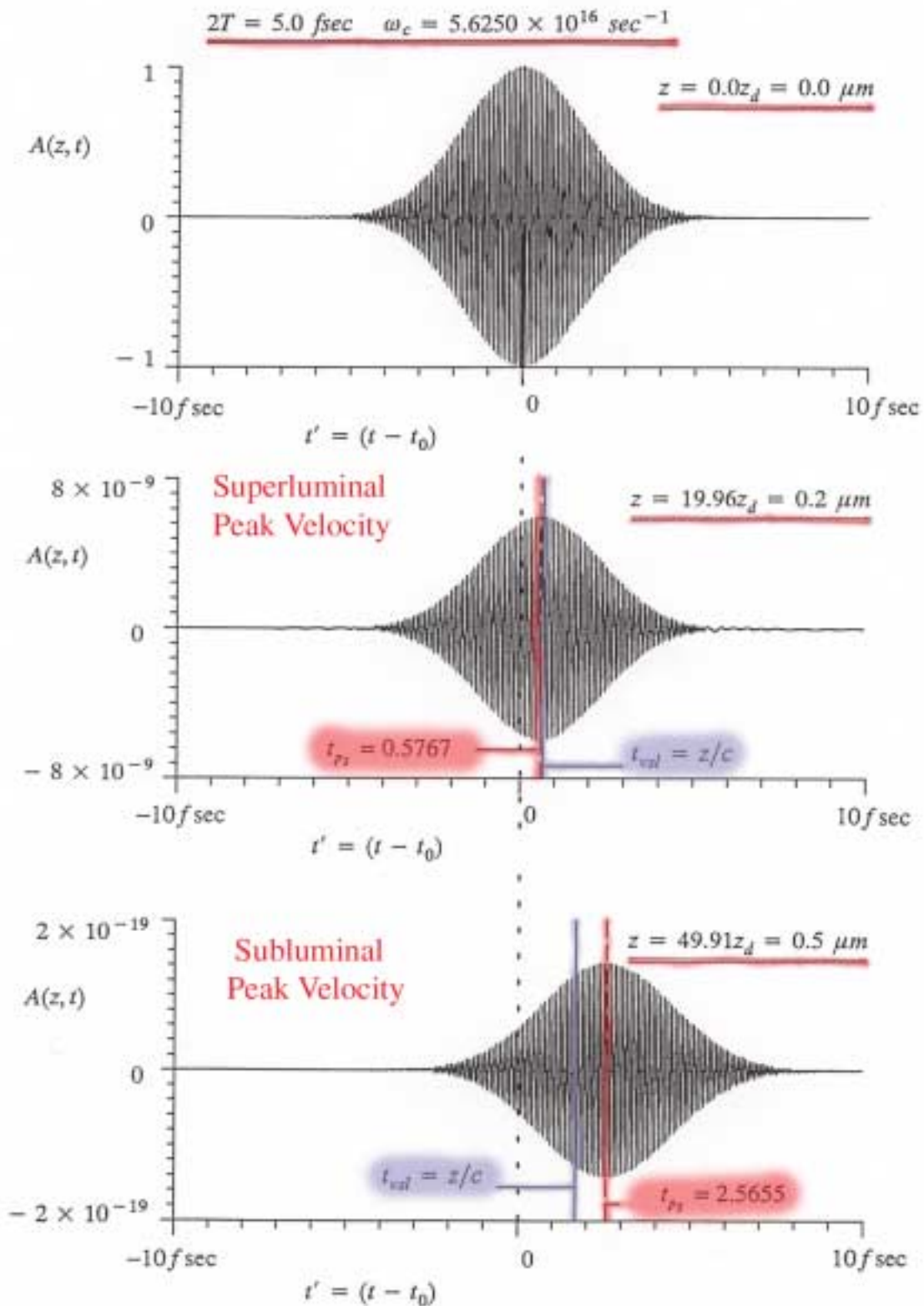
components, so that the propagated pulse spectrum becomes dominated by an increasingly higher frequency component, and the peak in the envelope of the propagated pulse propagates with the group velocity at this frequency value. Again, as the propagation distance increases into the mature dispersion regime, the pulse dynamics evolve toward the energy velocity description; however, the overall field amplitude also rapidly attenuates to zero in this case.

Because of the small propagation distance of at most 6 absorption depths in their laboratory arrangement, the experimental results of Chu and Wong [9] are restricted to the small propagation distance limit below the mature dispersion regime. The modified asymptotic description [12] bridges the gap between these two regimes, being in agreement with the experiment results [9] at small propagation distances, while reducing to the classical asymptotic description at sufficiently large propagation distances in the dispersive, lossy medium. Moreover, the modified asymptotic description provides, for the first time, a mathematically rigorous derivation of the correct group velocity description of Gaussian pulse propagation in a dispersive, lossy medium and clearly shows how that description evolves into the energy velocity description as the propagation distance increases into the mature dispersion regime.

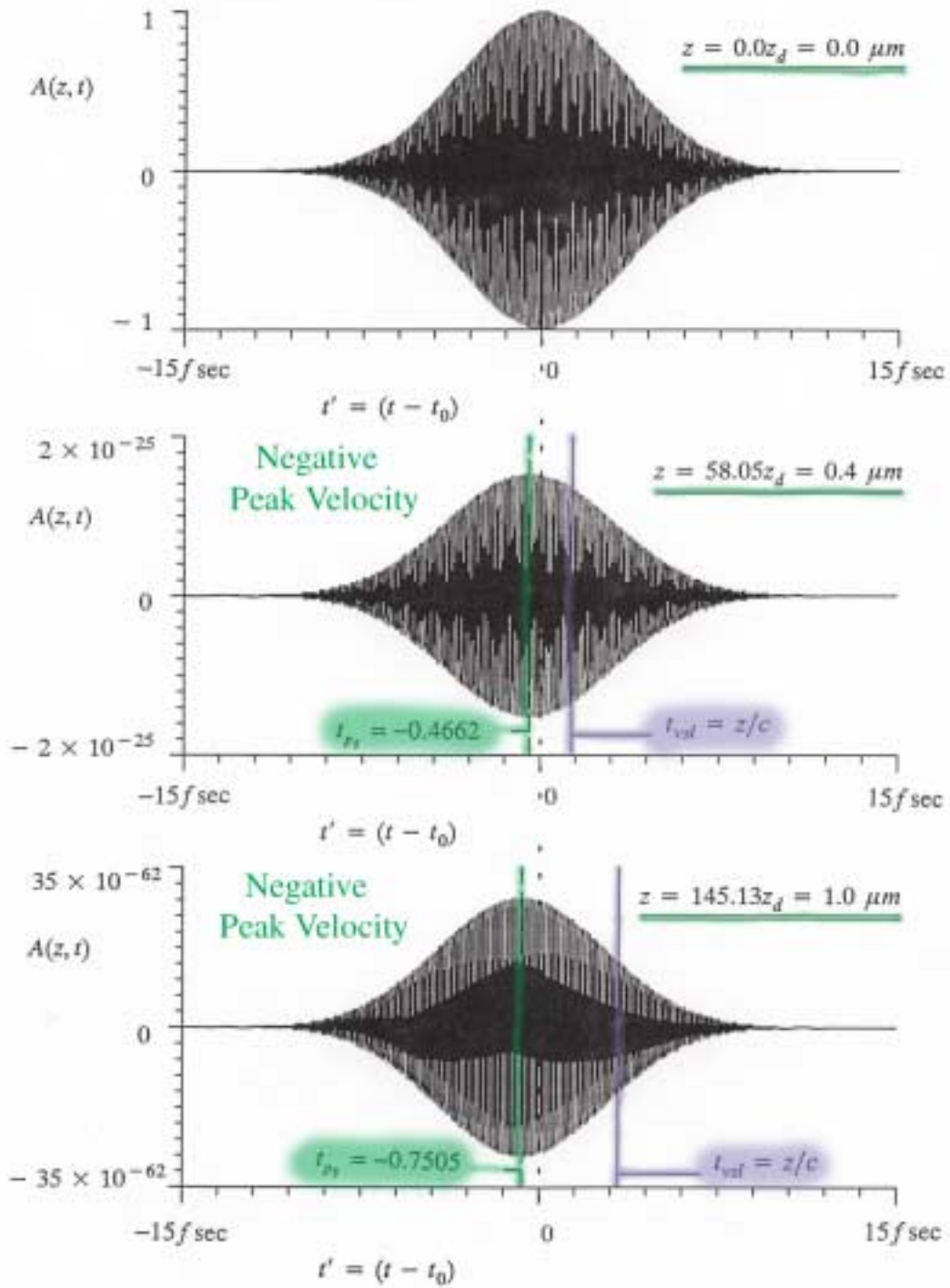
This research has been supported by United States Air Force Office of Scientific Research Grant No. F49620-94-1-0430.

- [1] A. Sommerfeld, *Ann. Phys.* **44**, 177–202 (1914).
- [2] L. Brillouin, *Ann. Phys.* **44**, 203–240 (1914).
- [3] K.E. Oughstun and G.C. Sherman, *J. Opt. Soc. Am. B* **5**, 817–849 (1988).
- [4] K.E. Oughstun and G.C. Sherman, *J. Opt. Soc. Am. A* **6**, 1394–1420 (1989).
- [5] K.E. Oughstun and G.C. Sherman, *Electromagnetic Pulse Propagation in Causal Dielectrics* (Springer-Verlag, Berlin, 1994).
- [6] B.R. Baldock and T. Bridgeman, *Mathematical Theory of Wave Motion* (Halsted, New York, 1981), Chap. 5.
- [7] G.C. Sherman and K.E. Oughstun, *Phys. Rev. Lett.* **47**, 1451–1454 (1981).
- [8] G.C. Sherman and K.E. Oughstun, *J. Opt. Soc. Am. B* **12**, 229–247 (1995).
- [9] S. Chu and S. Wong, *Phys. Rev. Lett.* **48**, 738–741 (1982). See also A. Katz and R.R. Alfano, *Phys. Rev. Lett.* **49**, 1292 (1982); S. Chu and S. Wong, *Phys. Rev. Lett.* **49**, 1293 (1982).
- [10] K.E. Oughstun and J.E.K. Laurens, *Radio Sci.* **26**, 245–253 (1991).
- [11] C.M. Balictsis and K.E. Oughstun, *Phys. Rev. E* **47**, 3645–3669 (1993).
- [12] C.M. Balictsis and K.E. Oughstun, *Phys. Rev. E* (to be published).
- [13] E.T. Copson, *Asymptotic Expansions* (Cambridge Univ. Press, Cambridge, 1971), Chap. 2.

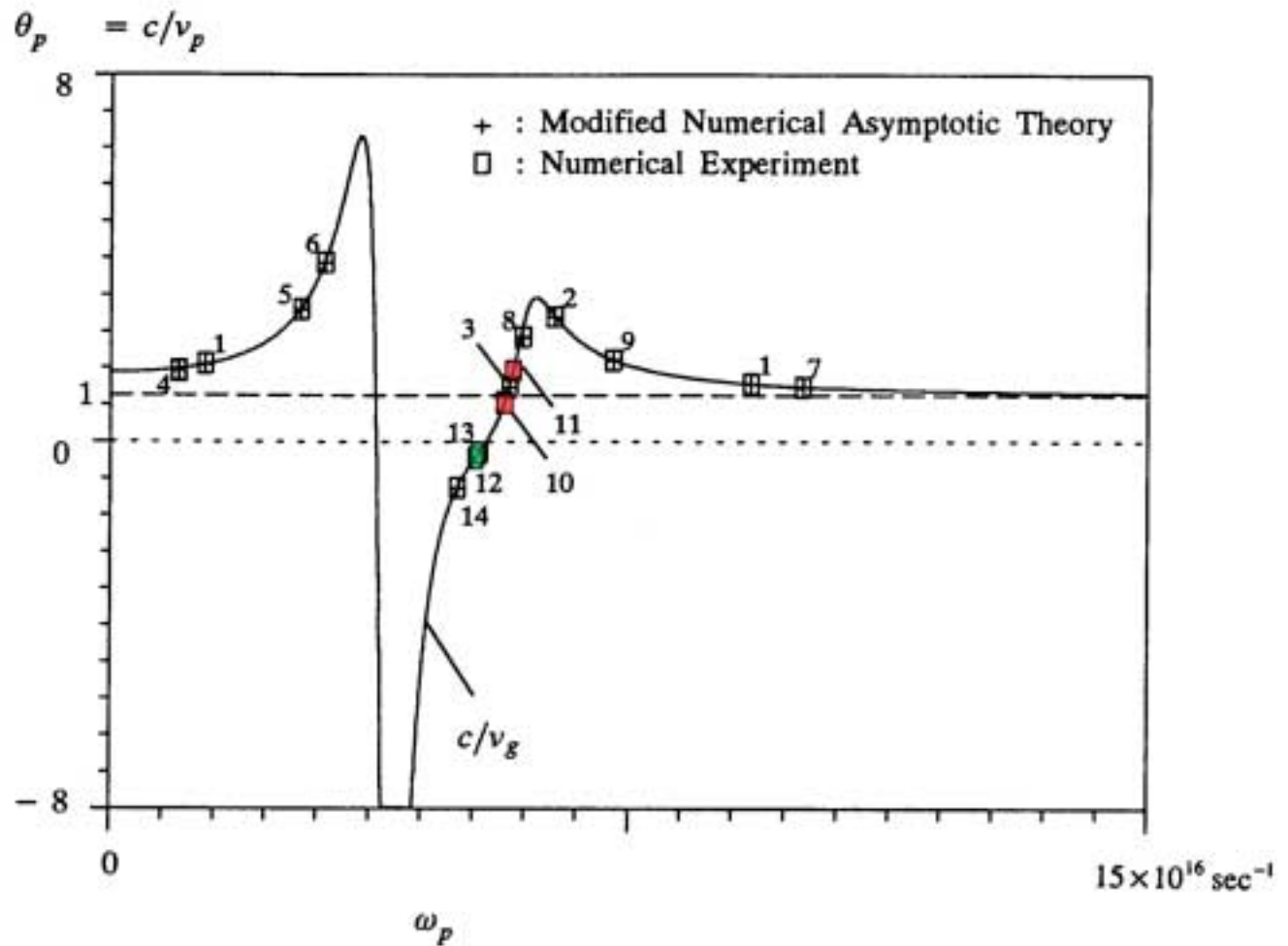
Ultrashort Gaussian Pulse Propagation



$$2T = 10.0 \text{ fsec} \quad \omega_c = 5.250 \times 10^{16} \text{ sec}^{-1}$$



Peak Velocity Behavior



As the Propagation Distance Increases, the Pulse Dynamics Evolve into that described by the Energy Velocity Description.

Oughstun & Balitsis, Phys. Rev. Lett. 77, 2210 (1996).

Balitsis & Oughstun, Phys. Rev. E 55, 1910 (1997).

OPTICS

Light faster than light?

Rolf Landauer

A rotating lighthouse beacon impinges on a distant wall. The resulting spot can move along the wall faster than the velocity of light. That is not a violation of relativity; one spot is not the source of the next spot. Measurements by Steinberg, Kwiat and Chiao¹ of pulse propagation through an optical film, which reflects most of the incident light, show that the few transmitted photons arrive earlier than the velocity of light would allow, based on the simplest notions of their time of impingement on the filter. But as in the case of the moving beacon, that velocity is presumed not to represent the retardation between a cause and its effect.

The filter consists of a periodic array of layers of material with alternately high and low refractive index. In the wavelength range from 600 to 800 nanometers, the reflections arising at the successive interfaces reinforce constructively, reflecting about 99 per cent of the incident light. The electromagnetic wave decays exponentially through the thickness of the filter.

Such evanescent waves where the decay is associated with reflections, not absorption, also occur in total internal reflection, when a wave is incident obliquely on an optically less dense medium. Evanescent waves are found in waveguides below their cut-off frequency. The reflection of most of the incident photons, and the accompanying exponential decay, are reminiscent of quantum mechanical tunneling, when a particle is incident on a barrier that classically would cause the particle to be turned around. If the barrier is thin enough, quantum

mechanics allows some chance of transmission. The analogy goes beyond that sketched here; quantum tunneling and electromagnetic evanescent waves are described by closely related equations.

The time associated with quantum barrier penetration has been discussed for over six decades, particularly within the past decade. Many of these analyses follow a wave packet through the barrier, comparing the time of an emerging peak to the arrival time of an incident peak. It can be argued that quantum mechanics does not conserve peaks; an emerging peak is not necessarily related to the incident peak in a causative physical way. To make this convincing, a particular wave packet and barrier have been described² in which the incident peak arrives at the barrier after the transmitted peak has already left the far side of the barrier. In that particular example the small departing peak clearly arises from the front end of the incident packet.

The use of an auxiliary degree of freedom, coupled to the tunneling process and used as a clock, represents an alternative theoretical and experimental approach³. When incoming peaks cannot be simply physically identified with emerging peaks, then there is no reason to expect the time measured by a clock to agree with that found by following peaks.

Steinberg and co-workers¹ use an ingenious two-photon interference method for measuring the delay (see figure). Two-photon interference methods⁴ do not, as the name suggests, cause one photon to interfere with an independently generated one, but instead cause one history for the set of two photons to interfere with another history. Typically the two photons involved are generated together, and

are essentially clones. If the two photons arrive simultaneously, with two different paths, at the half-silvered mirror, then the history in which both are reflected, and the history where both are transmitted, can be shown to interfere destructively. Thus, if two photons arrive simultaneously within the time resolution of the detectors, but not close enough in time to cause the destructive interference just mentioned, we are more likely to detect coincident arrival. This provides a delicate tool for measuring the relative timing for the arrival of two photons. Insertion of the filter causes a change in delay, which can be measured by introducing a compensating change in the length of the alternative vacuum path. Despite the emphasis Steinberg and collaborators place on the quantum nature of this experiment, that seems to be an incidental aspect. If, instead of single photons, we had used large pulses and measured relative arrival times through nonlinear optic effects, we could have measured the same delay.

In their principal result, a delay corresponding to a velocity of $1.7c$ (where c is the speed of light) is measured. Such superluminal velocities have also been measured in experiments on microwaves^{5,6}, although there the more complex geometry leads to difficulties in interpretation. The measured delay in the new work agrees with predictions for the delay of the transmitted peak, relative to the incident one.

Wave propagation is more complex than geometrical optics. We cannot easily assign a portion of the incident wave to each portion of the transmitted wave. Therefore, this experiment is not a demonstration of a real physical velocity exceeding c . We can seek an easy explanation by assuming that the whole

transmitted wave comes from the front end of the much larger incident wave. Nevertheless, this experiment underlines work that remains to be done. Could the experimental details be modified so that the light pulse emerges from the evanescent region before the incident peak has even reached that region? Measurements of an interaction time of a transmitted photon with its evanescent region, via a physical clock, are needed.

But even at a fundamental theoretical level, the easy explanation suggested is unsatisfying. Are we quite sure that if we signal with photon polarization, and if we are willing to lose most of the photons in an evanescent region, that we have no chance of a rare superluminal signal propagation? Our understanding of this is not all that it deserves to be, although it does seem unlikely that the well accepted light velocity barrier will crumble.

Rolf Landauer is at the IBM T. J. Watson Research Center, PO Box 218, Yorktown Heights, New York 10598, USA.

1. Steinberg, A, Kwiat, P. G., & Chiao, R., *Phys. Rev. Lett.*, **71**, 708-711 (1993).
2. Landauer, R. & Martin, Th., *Solid State Commun.* **84**, 115-117 (1992).
3. Landauer, R., *Nature* **341**, 567-568 (1989).
4. Greenberger, D. M., Horne, M. A., & Zeilinger, A., *Phys. Today* **46**, 22-29 (Aug 1993).
5. Enders, A. & Nimitz, G., *Phys. Rev. B* **47**, 9605 (1992).
6. Ranfagni, A., Fabeni, P., Pazzi, G. P., & Mugnai, D., *Phys. Rev. E* **48**, 1453-1460 (1993).

The Pulse Centrovelocity & Superluminal Pulse Velocities

(Peatross, Glasgow & Ware, *Phys. Rev. Lett.* **84**, 2370-2373, 2000)

The *pulse centrovelocity* is determined from the temporal centroid of the Poynting vector for a plane wave pulse propagating in the $+z$ -direction

$$\langle t \rangle_z \equiv \frac{\hat{\mathbf{z}} \cdot \int_{-\infty}^{\infty} t \mathbf{S}(z, t) dt}{\hat{\mathbf{z}} \cdot \int_{-\infty}^{\infty} \mathbf{S}(z, t) dt}$$

as

$$v_{\text{centro}} = \frac{z - z_0}{\langle t \rangle_z - \langle t \rangle_{z_0}}$$

where $\langle t \rangle_{z_0}$ denotes the temporal centroid of the initial pulse at $z = z_0$. By the Parseval-Plancherel theorem

$$\langle t \rangle_z = T \left\{ \tilde{E}(z, \omega) \right\} = -i \frac{\hat{\mathbf{z}} \cdot \int_{-\infty}^{\infty} \frac{\partial \tilde{\mathbf{E}}(z, \omega)}{\partial \omega} \times \tilde{\mathbf{H}}(z, \omega) d\omega}{\hat{\mathbf{z}} \cdot \int_{-\infty}^{\infty} \tilde{\mathbf{S}}(z, \omega) d\omega}$$

Energy Centroid Time Delay

$$\begin{aligned}\Delta t &= \langle t \rangle_z - \langle t \rangle_{z_0} \\ &= G_z + R_{z_0} = G_{z_0} + R_z\end{aligned}$$

Group Delay Energy Centroid

$$G_z = \left\langle \frac{\partial \beta(\omega)}{\partial \omega} \Delta z \right\rangle = \Delta z \frac{\int_{-\infty}^{\infty} \tilde{S}(z, \omega) \frac{\partial \beta(\omega)}{\partial \omega} d\omega}{\int_{-\infty}^{\infty} \tilde{S}(z, \omega) d\omega}$$

Pulse Reshaping Delay

$$R_{z_0} = T \left\{ \underbrace{\tilde{E}(z_0, \omega) e^{-\alpha(\omega)\Delta z}}_{\text{Dispersively Attenuated Initial Pulse Spectrum}} \right\} - T \left\{ \underbrace{\tilde{E}(z_0, \omega)}_{\text{Time of the Initial Centroid}} \right\}$$

According to Peatross, Glasgow & Ware (*Phys. Rev. Lett.* **84**, 2370-2373, 2000), this “result provides a context wherein group velocity is always meaningful even for broad band pulses and when the group velocity is superluminal or negative. The result imposes superluminality on sharply defined pulses.”

Not True for the Delta Function Pulse.

Sherman & Oughstun, Phys. Rev. Lett. 47, 1451-1454, (1981)

Oughstun & Sherman, J. Opt. Soc. Am. B 5, 817-849 (1988)

Sherman & Oughstun, J. Opt. Soc. Am. B 12, 229-247 (1995)

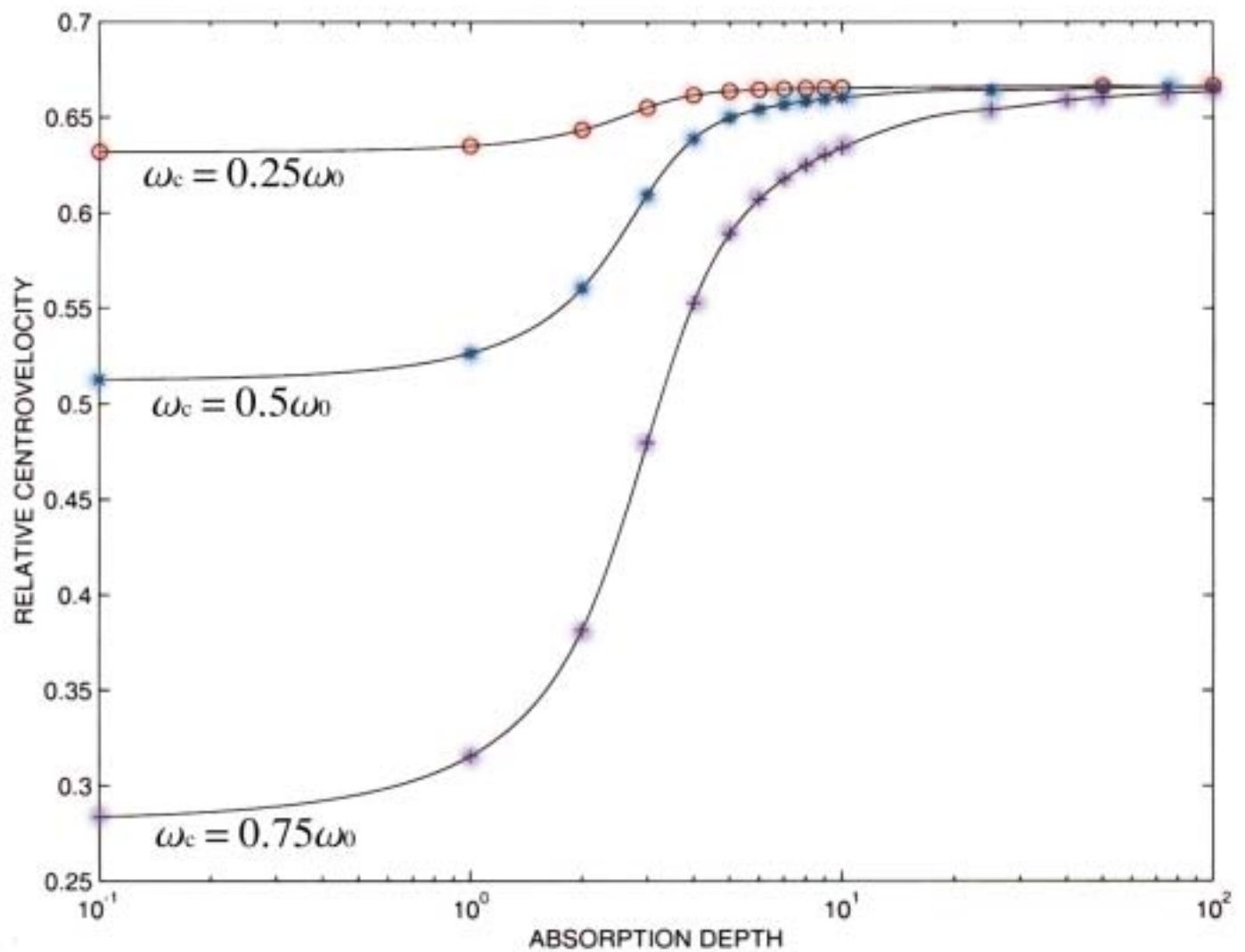
Not True for the Heaviside Step-Function Envelope Pulse.

Oughstun & Sherman, J. Opt. Soc. Am. B 5, 817-849 (1988)

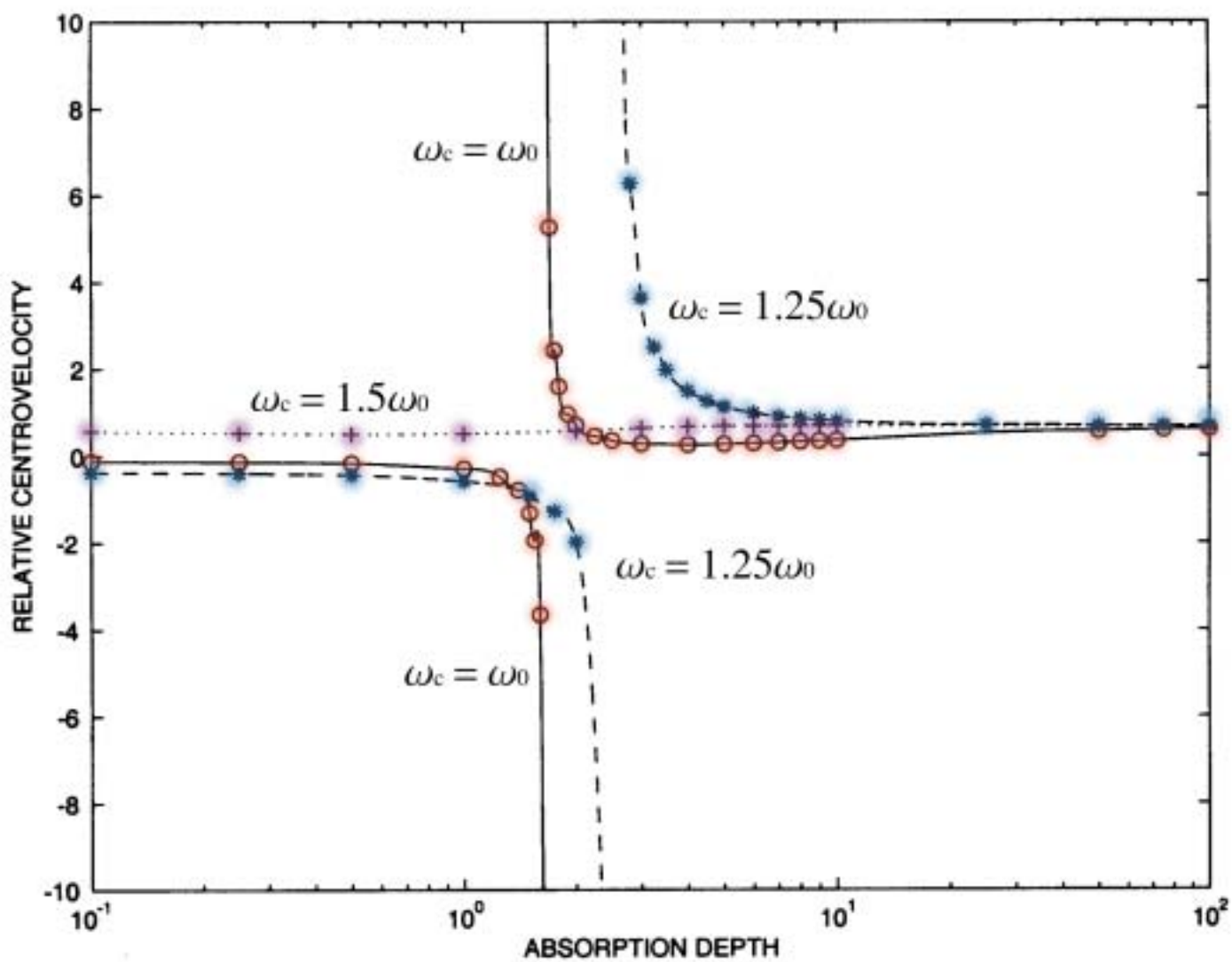
Not True for the Rectangular Envelope Pulse of Arbitrarily Short (or Long) Pulse Duration $T > 0$.

Oughstun & Sherman, Phys. Rev. A 41, 6090-6113, (1990)

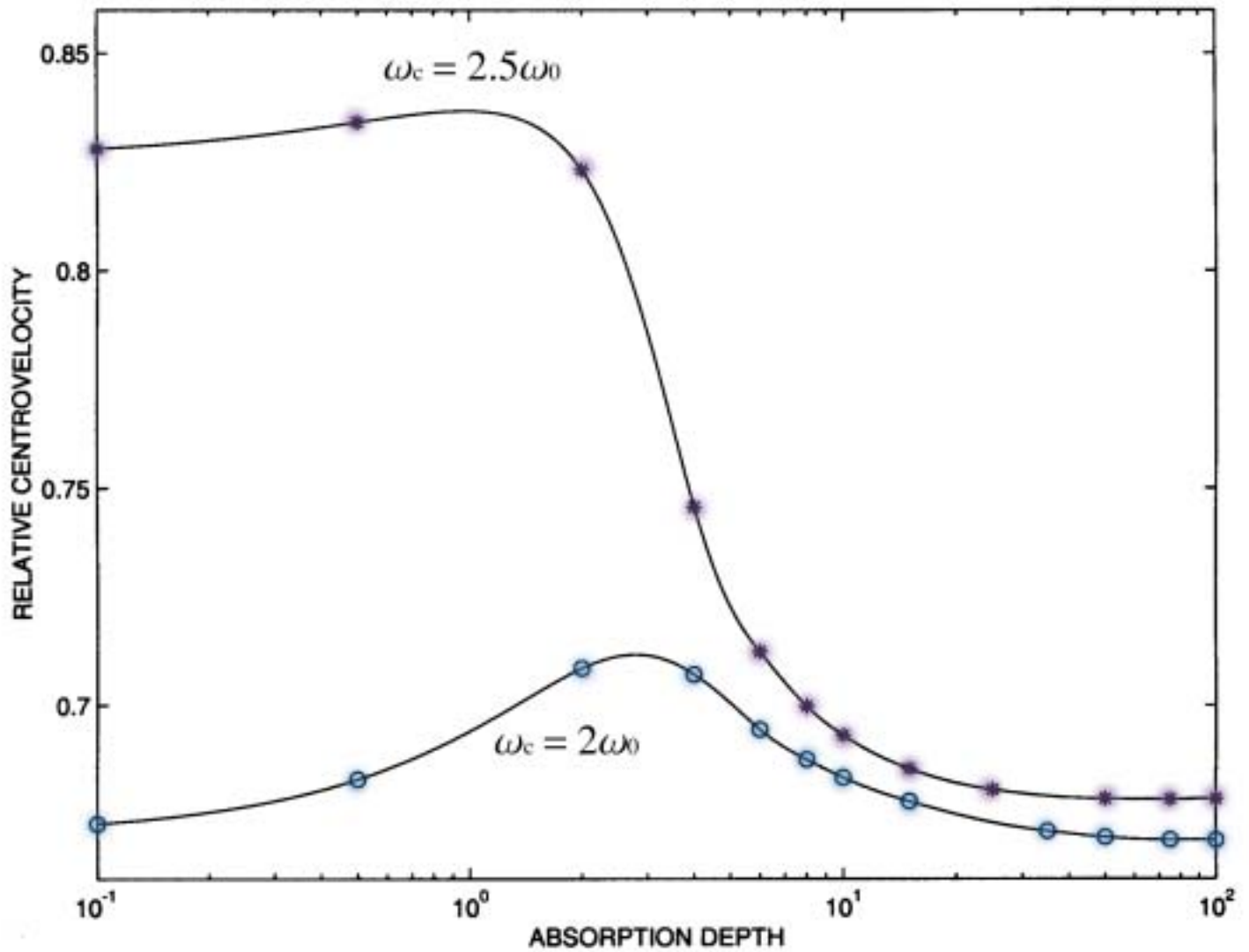
Ten Cycle Rectangular Envelope Pulse Below Resonance Carrier Frequency



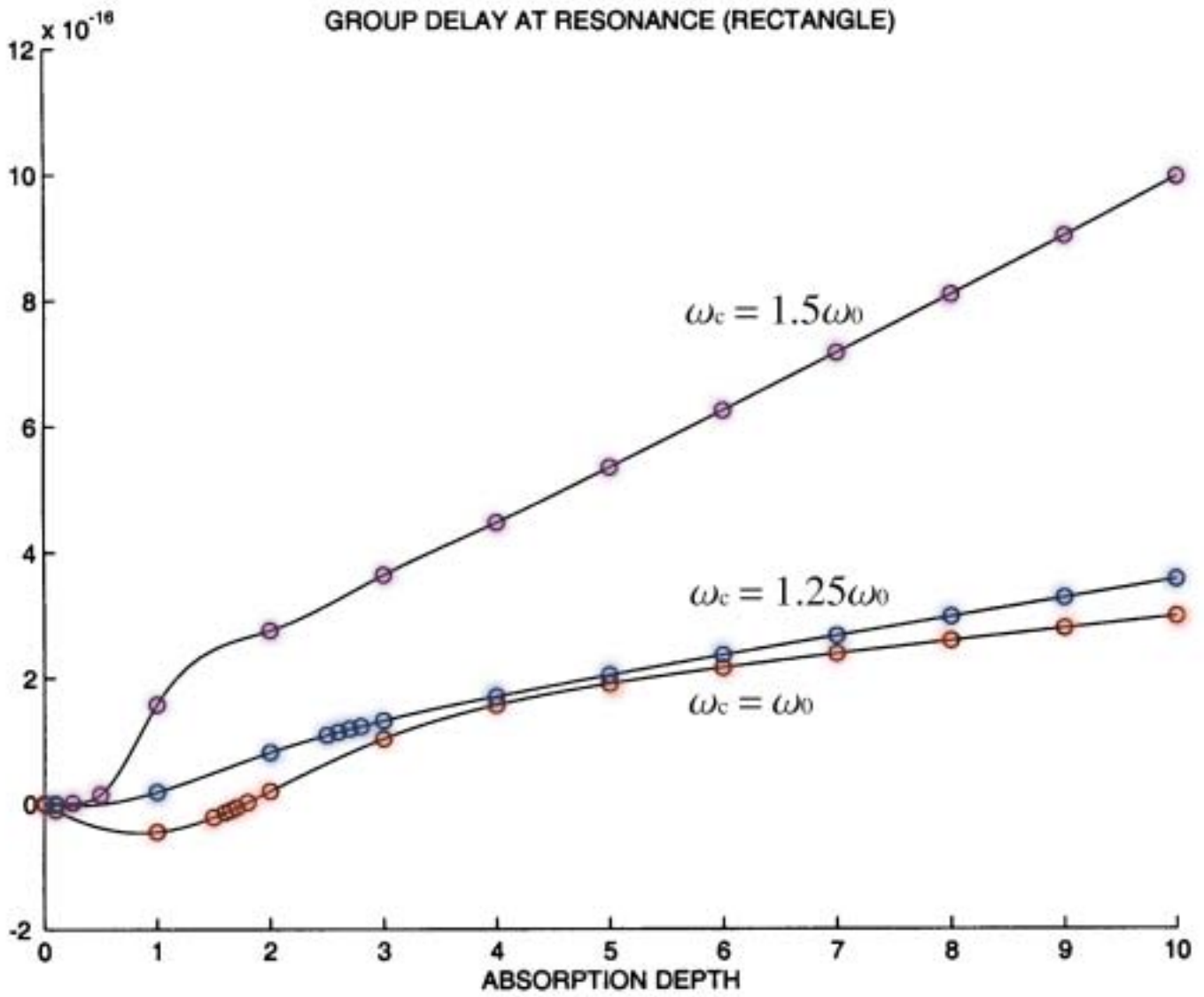
Ten Cycle Rectangular Envelope Pulse Intra-Absorption Band Carrier Frequency



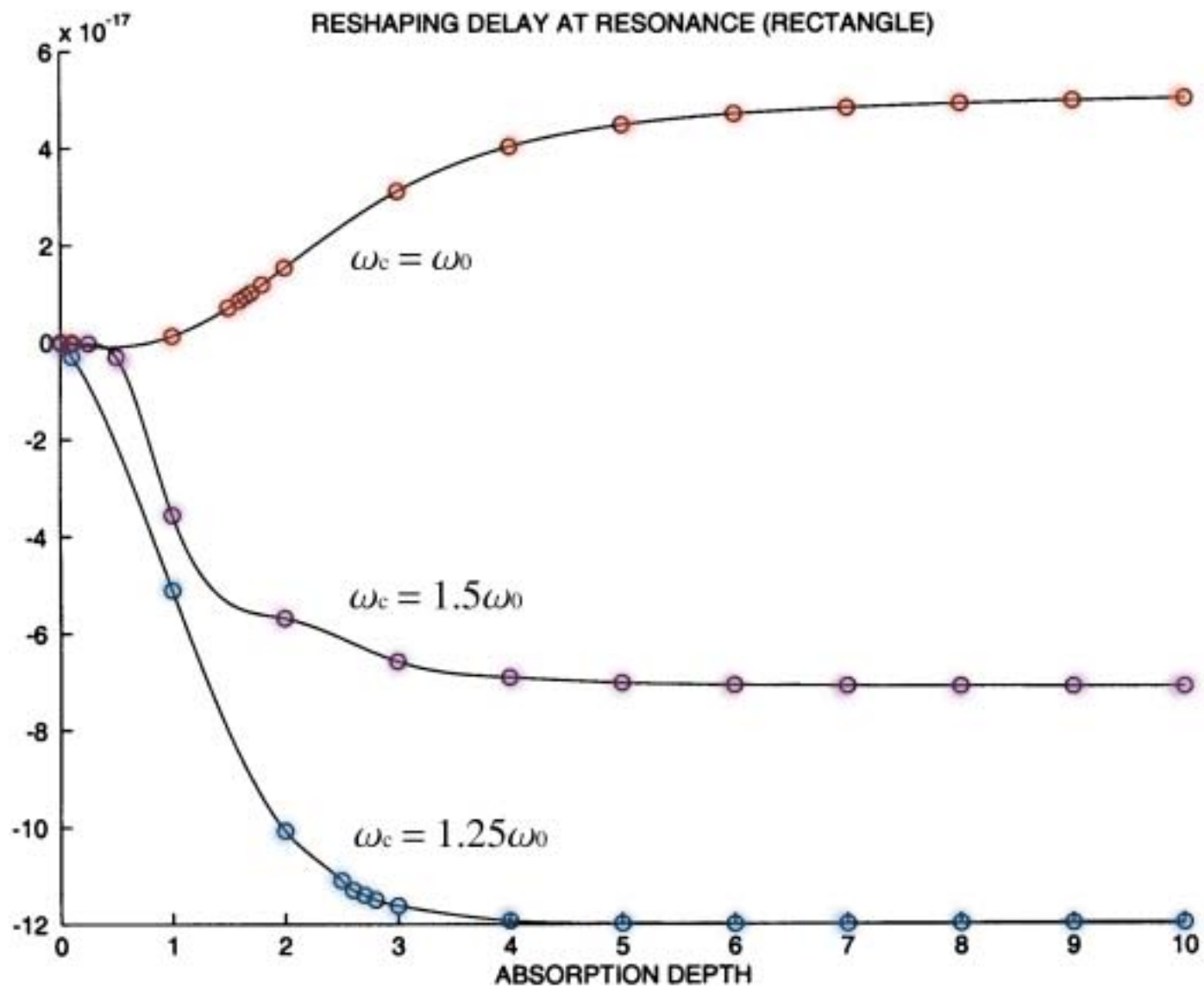
Ten Cycle Rectangular Envelope Pulse Above Absorption Band Carrier Frequency



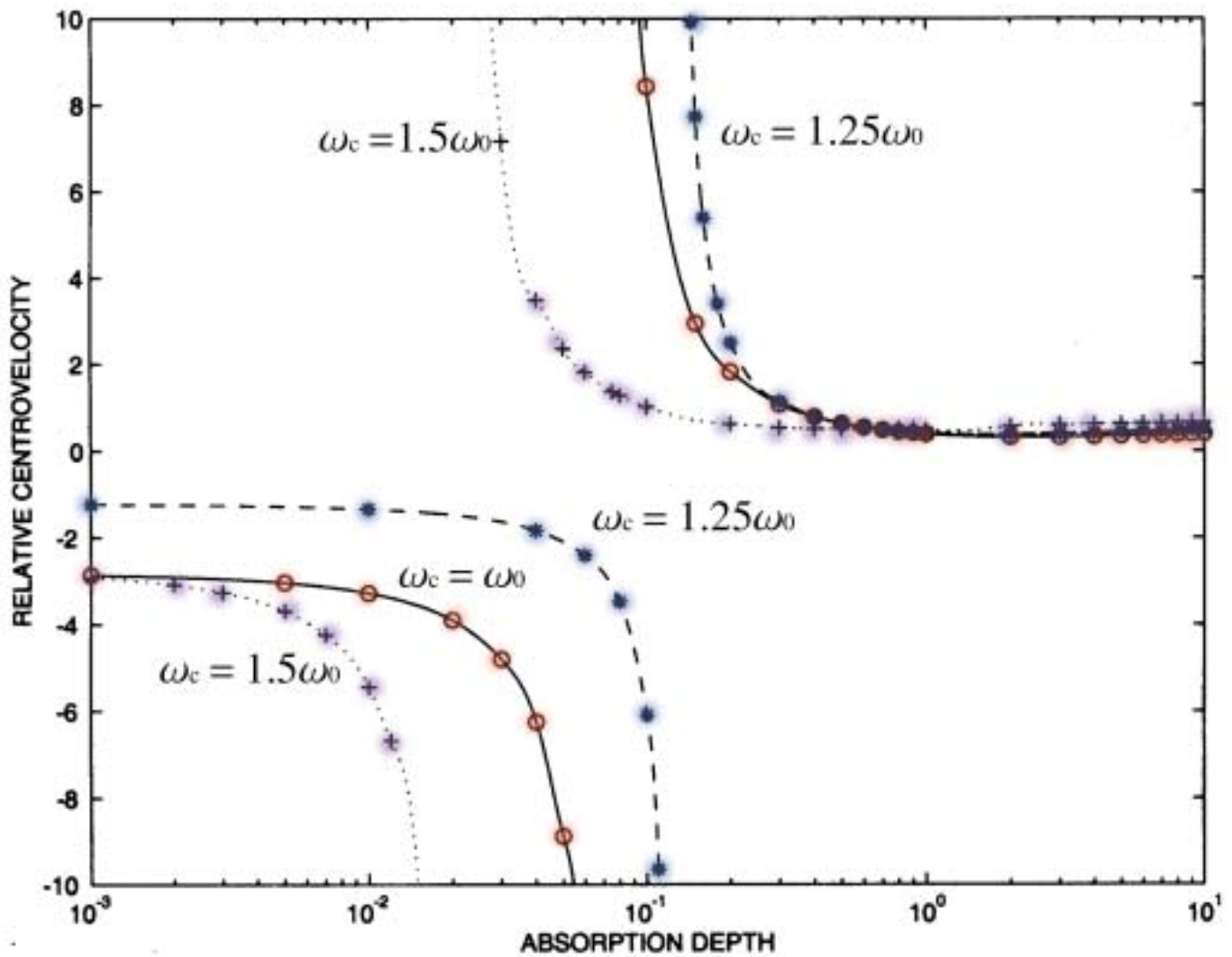
GROUP DELAY AT RESONANCE (RECTANGLE)



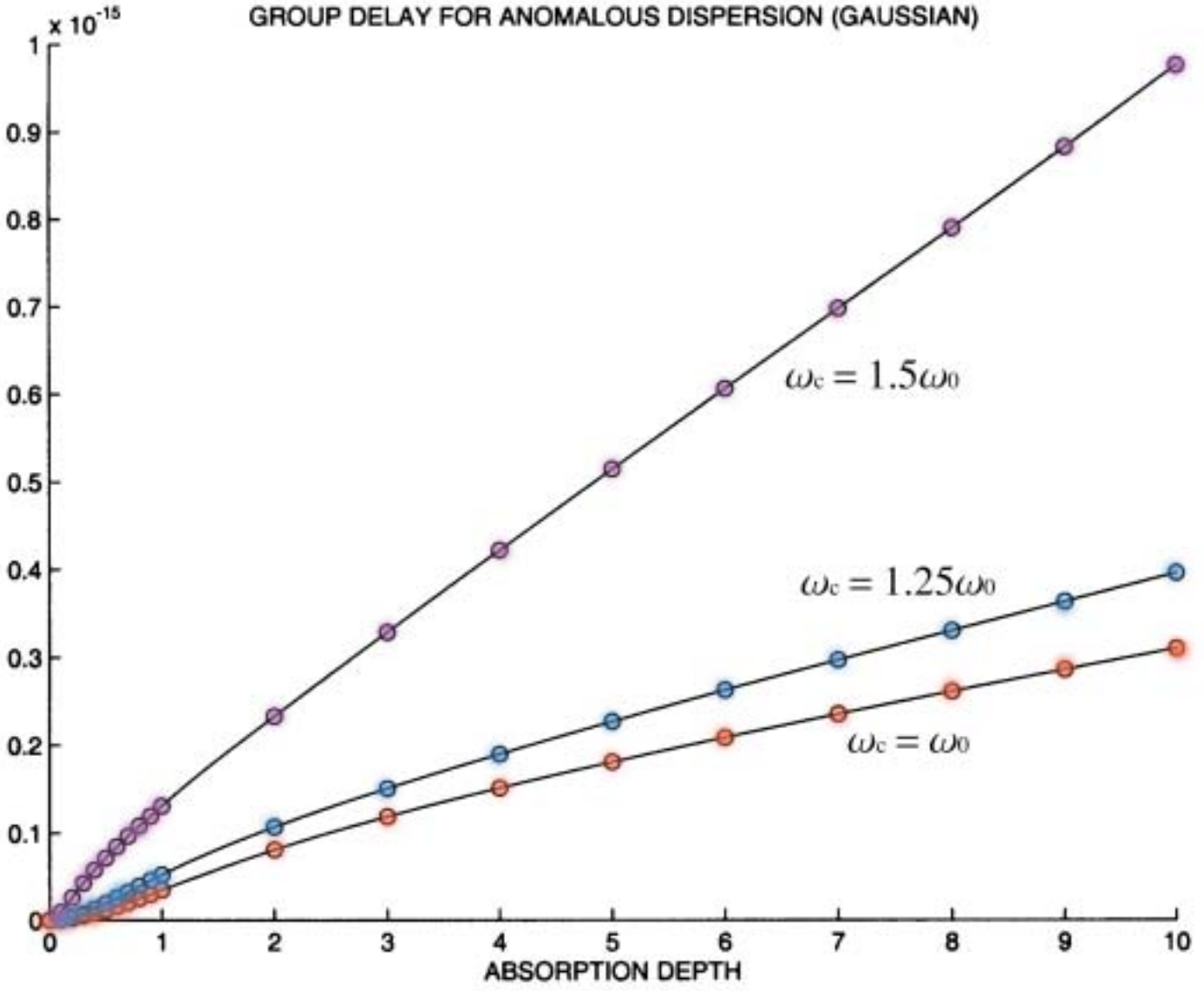
RESHAPING DELAY AT RESONANCE (RECTANGLE)



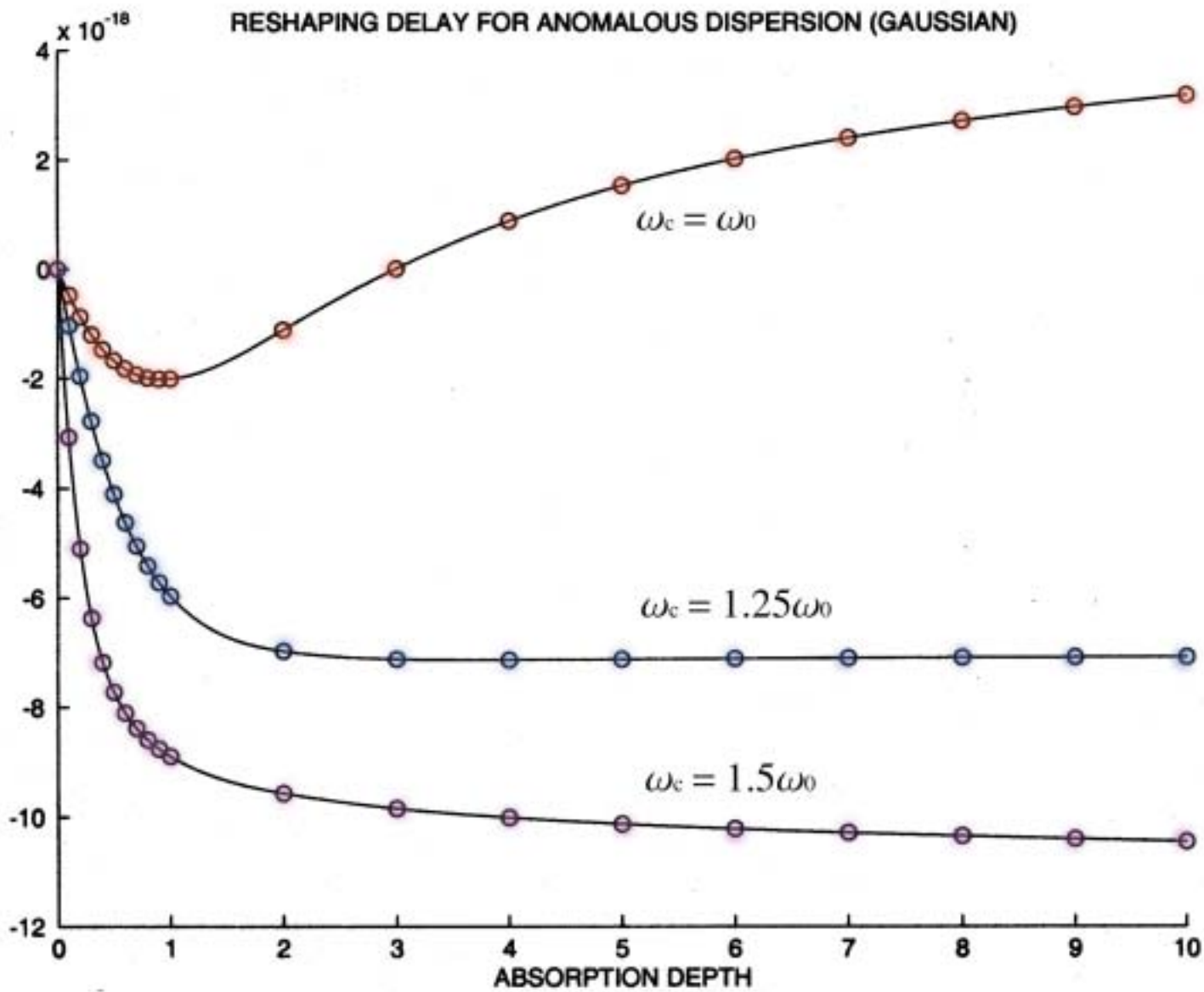
Single Cycle Gaussian Envelope Pulse Intra-Absorption Band Carrier Frequency



GROUP DELAY FOR ANOMALOUS DISPERSION (GAUSSIAN)



RESHAPING DELAY FOR ANOMALOUS DISPERSION (GAUSSIAN)



Conclusions

- Superluminal peak velocities in causally dispersive materials can occur momentarily (fleetingly) for sufficiently small propagation distances in the immature dispersion regime due to pulse envelope reshaping. For input signals that vanish for $t < t_0$, such superluminal behavior only occurs after the passage of the luminal wavefront; i.e. for $t > t_0 + \Delta z/c$.
- As the propagation distance increases into the mature dispersion regime, the pulse centroid velocity for an input rapidly-varying pulse becomes subluminal and approaches the velocity of the dominant precursor field.
- As tempting as it may seem, pulse reshaping does not imply either superluminal energy or superluminal information transfer.
- Gaussian Pulses are the Ultimate Wizard's Magic Wand.